RMIT UNIVERSITY

Development of Brown Coal Fly Ash Geopolymer Concrete

A thesis submitted in fulfilment of the requirements for the degree of Doctor of Philosophy

Rahmat Dirgantara
BEngSc(Civil), MEngSc(Melb)

Civil and Infrastructure Engineering
School of Engineering
RMIT University

August 2016

DECLARATION

I certify that except where due acknowledgement has been made, the work is that of the author alone; the work has not been submitted previously, in whole or in part, to qualify for any other academic award; the content of the thesis is the result of work which has been carried out since the official commencement date of the approved research program; any editorial work, paid or unpaid, carried out by a third party is acknowledged; and, ethics procedures and guidelines have been followed.

Rahmat Dirgantara

August 2016

ACKNOWLEDGEMENTS

I would like to express my deepest gratitude and respect to my supervisor, Dr. David Law and A/Prof Tom Molyneaux. The discussions always broaden my horizon, being taught and guided by someone who has the wisdom, knowledge and experiences will lead my steps in the future. Their thought and support throughout this study has been invaluable.

A special thanks to Direktorat Jenderal Pendidikan Tinggi (Ditjen Dikti), Ministry of Education, Republic of Indonesia for the scholarship to undertake this study in the earlier stage, Ketua and my colleagues in the Department of Civil Engineering, STTH Medan, Sumatera Utara, Indonesia for allowing me to further my study.

Finally, I would like to thank Pavel, Erick, Kevin, Bao, Kee Kong, Ramesh, Shamir and Saravanan for their support in the Civil engineering laboratory, and Chemical engineering laboratory staffs Cameron, Sandro and Muthu. I would also like to thank Philip Francis and his team for their assistance in the scanning electron microscopy and EDAX analysis.

I would like to acknowledge the support provided by Brown Coal Innovation Australia (BCIA) Top Up Scholarship for this research. Many thanks to Loy Yang (AGL), Yallourn (Energy Australia) and Hazelwood (GDF-SUEZ Australian Energy), and PQ Australia for supplying the materials for this research. My dear friends Arie Wardhono, Fifi, Farhad and other research students in the postgraduate study room no 24, for your companions. Without you all, the whole experience will be bland and not enjoyable.

Dedication

To my soul mate my wife Epita Sarah Pane
This journey and thesis would have been remained a dream without your love and support. May Allah give you heaven.

To my toddler Jacob
Allah sent you as I am starting this research. You are an angel that inspires me;
to my children Rizqi, Risyad and Ezra
Thank you for being my wonderful children. Without it this thesis is nothing. Hope you all could reach your highest dream.

To my Ibu and Ayah
I know it is your prayer that allowed me to go this far.
May Allah reward and bless you.

To Abmar's Buk Kul, Wakde, Pakde Yan, Nitsa, Tita and Om Win
Thank you for the remote support and encouragement.

TABLE OF CONTENTS

Page

LIST OF TABLES

Page

LIST OF FIGURES

Page

ABSTRACT

Substitution of Portland cement by pozzolanic material (PM) or supplementary cementing materials (SCM) is potentially the most effective way of decreasing both energy consumption and the production of greenhouse gases from Ordinary Portland (OP) cement production. One of the most common waste materials used at present is Pulverised Fly Ash (PFA) from coal fired power stations. This by-product can be interground, blended with the cement or substituted for cement. The levels of substitution can be from 20 to 70% of the OP cement or even a 100% replacement in geopolymer concretes.

ASTM C618 defines fly ash into 2 classes, class F is produced from burning anthracite and bituminous coals and class C fly ash from lignite and sub-bituminous coals. In Australia only, lignite is referred to as brown coal and categorized as neither class F nor class C due to the high sulphur content. In geopolymer concrete, the silicate materials in the fly ash binder react with the alkaline activator and become soluble reactants which form geopolymer paste that binds the aggregates and other unreacted materials together. Geopolymer concretes based on class F and class C fly ash have been found to give similar strength to both OP and blended cements concretes. However, to date little research has been undertaken on the feasibility of using brown coal fly ash as a binder. At present there is also no commercial use of the material in the construction industry with the majority of the material being sent to landfill.

This research investigated the possibility of using brown coal fly ash as a binder to produce geopolymer concrete, specifically Australia - Victoria - La Trobe Valley brown coal fly ash. The research comprised: a review of brown coal, class C and F fly ashes and their geopolymerization mechanisms; production of brown coal fly ash geopolymer mortar and optimization of the mix design to produce geopolymer concrete; evaluation of the reaction kinetics, microstructural development of geopolymeric formulations, and mechanical durability characteristics of geopolymer concrete.

The initial research investigated brown coal fly ash geopolymer mortar using fly ash from three power plants: Loy Yang, Yallourn and Hazelwood. The Loy Yang brown coal fly ash geopolymer mortar displayed compressive strengths compatible with the production of geopolymer concrete with acceptable strength for use in the construction industry. However, the geopolymer mortar specimens from Hazelwood and Yallourn brown coal fly ash gave results that indicated they were are not feasible to use for geopolymer concrete due to their inherent chemical composition.

Based on the optimal mortar composition the production and properties of geopolymer concrete produced from Loy Yang brown coal fly ash was investigated. The results showed that concrete with a compressive strength over 40 MPa could be produced, though the alkali modulus and SiO_2/Al_2O_3 ratio were significantly more restrained that those previously reported for class F based geopolymer concrete. In addition to the compressive strengths, the FTIR and zeta potential data showed that the Loy Yang brown coal fly ash has properties feasible for the manufacture of a geopolymer concrete that could be used as a construction material. However, variability in the performance between batches of the Loy Yang brown coal fly ash and incomplete geopolymerization of large scale specimens under elevated temperature curing conditions were observed. The microscopy and porosity data showed that the geopolymer produced had a large number of pores in the macropore region together with a large number of interconnected pores and an inhomogeneous structure. This was reflected in the durability analysis, resistivity, UPV, carbonation, chloride diffusion, air permeability and sorptivity data which all gave results indicative of poor quality concrete. These results coupled with the variability in the chemical composition within the ash and the high sulphur content raise concerns over the consistency of the concrete produced and the long term performance. Overall, the research provides a fundamental understanding of the geopolymerization mechanism for Loy Yang brown coal fly ash geopolymer mortar and concrete and presents an opportunity for potentially diverting a waste stream into a useful material.

LIST OF PUBLICATIONS

Content from the thesis has been published in the following papers:

Dirgantara, R., D. Law, T. Molyneaux and D. Kong (2013), “Brown coal fly ash geopolymer mortar”, Proceedings of the 22nd Australian Conference on the Mechanics of Structures and Materials, ACMSM 22, Sydney, Australia, 11-14 December 2012, CRC Press/Belkema, pp. 1119-1122.

Law, D. W., T. K. Molyneaux, A. Wardhono, R. Dirgantara and D. Kong (2013), “The Use Brown Coal Fly Ash To Make Geopolymer Concrete”, Proceeding ACCTA 2013, International Conference on Advances in cement and Concrete Technology in Africa, Johannesburg, South Africa, 28-30 January 2013, pp.603-610.

Dirgantara, R., D. Law and T. Molyneaux (2013), “Brown Coal Fly Ash Geopolymer Concrete”, Proceeding of the Concrete 2013: 26th Biennial National Conference of the Concrete Institute of Australia, Gold Coast, Australia, 16-18 October 2013.

Law, D. W., T. K. Molyneaux and R. Dirgantara (2013), “Properties of Brown Coal Fly Ash Geopolymers Mortar”, Proceeding of the Concrete 2013: 26th Biennial National Conference of the Concrete Institute of Australia, Gold Coast, Australia, 16-18 October 2013.

Dirgantara, R., D. W. Law and T. K. Molyneaux (2014), "COMPRESSIVE STRENGTH VARIABILITY OF BROWN COAL FLY ASH GEOPOLYMER CONCRETE." Proceeding of the 5th International Conference Non-Traditional Cement & Concrete, NTCC V, Brno, Czech Republic, 16-19 June 2014, pp. 33-36.

Dirgantara, R., D. W. Law and T. K. Molyneaux (2014), "COMPRESSIVE STRENGTH VARIABILITY OF BROWN COAL FLY ASH GEOPOLYMER CONCRETE." IJRET: International Journal of Research in Engineering and Technology 03, Special Issue 13, pp. 165-169.

Dirgantara, R and D. Law (2013), “Effects of Elevated Temperature Curing of Brown Coal Fly Ash Geopolymer”, The 24nd Australian Conference on the Mechanics of Structures and Materials, Perth, Australia, 2016 (paper accepted).

CHAPTER 1

INTRODUCTION

1.1. Background

The use of Portland cement as the main binder material in concrete raises a number of environmental concerns due to the energy consumption and the emission of CO_2. It is estimated that one tonne of cement releases between 0.7 to 1 tonnes of CO_2, and that cement production contributed to 7% of worldwide greenhouse gas emission in 2004 (Davidovits 1994a, Naik 2008, Meyer 2009). Other concerns have also highlighted the use of coal as a primary energy source and the release of fly ash as a by-product, some of which becomes environmental waste (Naik and Singh 1993, Manz 1997, ADAA 2007, Malhotra 2008, Keyte 2009). Fly ash can be used as a replacement material for cement, with the use of class F fly ash as a partial replacement for cement well established (Oscar 1999, Berry, Cross et al. 2009, Guo, Shi et al. 2010, Fansuri, Prasetyoko et al. 2012). In addition, the use of class F fly ash has also more recently been used in the manufacture of geopolymers, thus diverting it from the waste stream into a useful material for the replacement of Portland cement (Meyer 2009, Shayan, Xu et al. 2013).

Fly ash as an industrial by-product contains silicate materials which have been used as an alternative binder material to ordinary Portland cement. The fly ash produced can be categorized as either class F or class C (ASTM 2012). Class F fly ash is produced from burning anthracite and bituminous coals, while class C fly ash is produced from sub-bituminous and lignite. In Australia only, lignite is referred to as brown coal, whereas in Europe both sub-bituminous coal and lignite are called brown coal (Geoscience Australia and ABARE 2010). Australian brown coal fly ash is categorized as neither class F nor class C based on chemical composition according to ASTM C618-12 (ASTM 2012) due to the high Sulphur content.

Annual production of brown coal worldwide in 2008 was estimated to be 938 million tonnes compared to 5,762 million tonnes of black coal. The largest producers of brown coal are Germany, Russia and the USA, with Australia the 4th largest producer of brown coal worldwide, being responsible for 7% of the total production and has 25% of the world's brown coal total reserve (Geoscience Australia and ABARE 2010).

A study of carbon dioxide equivalent (CO_2-e) emission comparing geopolymer with ordinary Portland cement concrete (Turner and Collins 2013) showed that the CO_2-e of geopolymer concrete was approximately 9% less than that of concrete with 100% ordinary Portland cement binder. This contrasted with an earlier study where the CO_2-e of geopolymer concrete ranged from 26-80% less than that of ordinary Portland cement concrete (Davidovits 1994b, Duxson, Provis et al. 2007, Stengel, Reger et al. 2009). Despite only a 9% CO_2-e reduction attributable to the use of geopolymer concrete, fly ash has an important advantage as it is a by-product which would be a waste product to be disposed of with associated costs (Meyer 2009). Existing stockpiles of fly ash and bottom ash will be enough to produce alkali-activated fly ash geopolymer concrete for centuries to come.

At present class F fly ash is the most commonly used binder material in the synthesis of alkali-activated binder (Guo, Shi et al. 2010). Activation of fly ash involves using a highly alkaline solution which will then form an inorganic binder through a polymerization process e.g. dissolution, speciation equilibrium, gelation, reorganization, polymerization and hardening (Duxson, Provis et al. 2007). This material is known as geopolymer concrete, with several commercial products recently coming on to the market (Davidovits 2011). This geopolymer concrete gives similar strength to both ordinary Portland cement and blended cements.

The formation of $[M_z(AlO_2)_x(SiO_2)_y \cdot nMOH \cdot mH_2O]$ gel has been identified as a dominant step in the formation of an amorphous structure of geopolymer with the OH^- ion acting as a reaction catalyst during the activation process (Xu and

Van Deventer 2000, Fernández-Jiménez and Palomo 2005). Davidovits (2005) has categorized the geopolymer structure as being based on the ratio of Si/Al (Davidovits 2005). The initial development of fly ash geopolymer was undertaken using class F fly ash, as a higher proportion of silica (SiO_2) and/or the sum of SiO_2 and alumina (Al_2O_3) is needed to ensure that sufficient potential reactive constituent is present in the fly ash. The activation process for geopolymer concretes is attributable to the activation of the aluminosilicate by high concentration alkali rather than the activation of the fly ash by the calcium hydroxide ($Ca(OH)_2$) produced by the hydration of the ordinary Portland cement. Therefore if the proportion of aluminosilicate in brown coal fly ash is sufficient it may be feasible to produce brown coal fly ash geopolymer concrete.

Some previous research has been undertaken using class C fly ash (also referred to as high calcium fly ash) to explore the feasibility of using it as a binder in geopolymer concrete (Guo, Shi et al. 2009, Chindaprasirt, Chareerat et al. 2011). However, little research has been undertaken to date on the feasibility of using brown coal fly ash (Bankowski, Zou et al. 2004, Škvára, Kopecký et al. 2009) and there is no commercial use of the material in the construction industry with the majority of the material being sent to landfill at present.

1.2. Research significance

Presently brown coal fly ash is not used as a binder in concrete (Macphee, Black et al. 1993, CIA 2011), with the majority of the brown coal fly ash produced stored in ponds or sent to landfill. Preliminary research on geopolymer mortar using a high aluminosilicate brown coal fly ash as 100% replacement of ordinary Portland cement demonstrated compressive strength comparable to those obtained from ordinary Portland cement mortar (Law, Molyneaux et al. 2013). This demonstrated the potential to produce geopolymer concrete using Australia-Victoria brown coal fly ash, and more generally all brown coal fly ash worldwide. This potential use of brown coal fly ash could result in utilization of

an industrial by-product produced from coal burning power stations presently disposed of directly into the environment.

1.3. Aim, objective and scope

The aim of the research is to investigate the possibility of using brown coal fly ash as a binder to produce geopolymer concrete, specifically Australia-Victoria brown coal fly ash. In addition to the development of brown coal fly ash geopolymer concrete, the properties of the brown coal fly ash geopolymer mortar and concrete will be assessed. The specific objectives will include:

a) Review of brown coal fly ash, class C fly ash and class F fly ash and their geopolymerization mechanisms.
b) Production of brown coal fly ash geopolymer mortar, and development of an optimum mix design to produce brown coal fly ash geopolymer concrete.
c) Evaluation of the reaction kinetics and microstructural development of brown coal fly ash geopolymeric formulations.

The research contributes to the development of environmentally friendly binders for geopolymer concrete using waste by-product material. While the use of fly ash as both a replacement material for cement and to produce geopolymer concrete has become established practice, most of the fly ash used at present is class F and class C. Little research has been undertaken on the feasibility of using brown coal fly ash as waste product. As such, this study undertakes novel research on the potential use of brown coal fly ash as a binder in manufacture of geopolymer concrete. The research may provide the opportunity for potentially diverting a waste stream into a useful material.

1.4. Structure of the thesis

The thesis will be structured into seven chapters, as describes below:

Chapter one is the introduction, this chapter describes the development of brown coal fly ash geopolymer concrete as an alternative binder for concrete. The research significance is also described in this chapter along with the aim, objectives and the scope of study.

Chapter two is a literature review, this chapter reviews the literature on the environmental impacts of the production of ordinary Portland cement, the use of coal as primary energy source, the production and utilisation of fly ash as a by-product, the history of alkali activation of cementitious materials, the reaction mechanism and properties of fly ash geopolymer concrete. The properties and characteristics of the different classes of fly ash are also explained. The key factors in development of brown coal fly ash geopolymer concrete will be also discussed.

Chapter three is the methodology, this chapter presents the experimental methods employed in the development of alkali activated brown coal fly ash geopolymer mortar and concrete. This chapter also describes the materials used to produce the brown coal fly ash geopolymer mortar and concrete and the experimental methods used in the testing of the geopolymer mortar and concrete.

Chapter four discusses the geopolymer mortar, this chapter reports the experimental studies on the development of alkali activated brown coal fly ash geopolymer mortar. The experimental investigation included optimising the mix design, curing regimes, mechanical properties and microstructure analysis.

Chapter five covers geopolymer concrete, this chapter reports the experimental studies on the development of alkali activated brown coal fly ash geopolymer concrete. It covers the experimental and testing applied to brown coal fly ash geopolymer concrete. The experimental investigation and testing varied from mechanical properties, curing regimes, NDT and durability to microstructure analysis.

Chapter six is a general discussion, this chapter discusses the development of brown coal fly ash geopolymer concrete, the background, development of an optimum mix design to produce brown coal fly ash geopolymer concrete and the analysis and implications of the experimental program. The analysis is based on the testing applied to brown coal fly ash geopolymer mortar and concrete.

Chapter seven is the conclusion, this chapter reports the main findings and conclusions of the research. This chapter also includes future prospects and recommendations for further research.

References

ADAA (2007). Coal Combustion Products Handbook, Ash Development Association of Australia, Cooperative Research Centre for Coal in Sustainable Development.

ASTM (2012). ASTM C618-12. Standard Specification for Coal Fly Ash and Raw or Calcined Natural Pozzolan for Use in Concrete. West Conshohocken, US., ASTM International.

Bankowski, P., L. Zou and R. Hodges (2004). "Reduction of metal leaching in brown coal fly ash using geopolymers." Journal of Hazardous Materials 114(1–3): 59-67.

Berry, M., D. Cross and J. Stephens (2009). Changing the Environment: An Alternative "Green" Concrete Produced without Portland Cement. 2009 World of Coal Ash (WOCA) Conference. Lexington, KY, USA.

Chindaprasirt, P., T. Chareerat, S. Hatanaka and T. Cao (2011). "High-Strength Geopolymer Using Fine High-Calcium Fly Ash." Journal of Materials in Civil Engineering 23(3): 264-270.

CIA (2011). Recommended Practice Geopolymer Concrete. Sydney, Concrete Institute of Australia.

Davidovits, J. (1994a). "Geopolymers: Man-Made Rock Geosynthesis and the Resulting Development of Very Early High Strength Cement." Journal of Materials Education 16(2/3): 48.

Davidovits, J. (1994b). "Global Warming Impact on the Cement and Aggregates Industries." World Resource Review 6(2): 263-278.

Davidovits, J. (2005). Geopolymer chemistry and sustainable Development. The Poly(sialate) terminology: a very useful and simple model for the promotion and understanding of green-chemistry. Geopolymers, Green Chemistry and

Sustainable Development Solutions. J. Davidovits. Saint-Quentin, France, Institut Géopolymère: 9-15.

Davidovits, J. (2011). Geopolymer Chemistry and Applications 3rd edition, Institut Géopolymère.

Duxson, P., A. Provis, J. L. Lukey, G. C. Van Deventer, A. Fernández-Jiménez and J. S. J. Palomo (2007). "Geopolymer technology: The current state of the art." Journal of Materials Science 42(9): 16.

Duxson, P., J. L. Provis, G. C. Lukey and J. S. J. van Deventer (2007). "The role of inorganic polymer technology in the development of 'green concrete'." Cement and Concrete Research 37(12): 1590-1597.

Fansuri, H., D. Prasetyoko, Z. Zhang and D. Zhang (2012). "The effect of sodium silicate and sodium hydroxide on the strength of aggregates made from coal fly ash using the geopolymerisation method." Asia-Pacific Journal of Chemical Engineering 7(1): 73-79.

Fernández-Jiménez, A. and A. Palomo (2005). "Composition and microstructure of alkali activated fly ash binder: Effect of the activator." Cement and Concrete Research 35(10): 1984-1992.

Geoscience Australia and ABARE (2010). Australian Energy Resource Assessment. Canberra, Commonwealth of Australia (Geoscience Australia).

Guo, X., H. Shi, L. Chen and W. A. Dick (2009). Performance and Mechanism of Alkali-Activated Complex Binders of High-Ca Fly Ash and other Ca-Bearing Materials. 2009 World Of Coal Ash (WOCA) Conference. Lexington, KY, USA.

Guo, X., H. Shi, L. Chen and W. A. Dick (2010). "Alkali-activated complex binders from class C fly ash and Ca-containing admixtures." Journal of Hazardous Materials 173(1–3): 480-486.

Keyte, L. M. (2009). 2. Fly Ash Glass Chemistry and Inorganic Polymer Cements. Geopolymers - Structure, Processing, Properties and Industrial Applications. J. L. Provis and J. S. J. van Deventer, Woodhead Publishing.

Law, D. W., T. K. Molyneaux, A. Wardhono, R. Dirgantara and D. Kong (2013). The Use Brown Coal Fly Ash To Make Geopolymer Concrete. ACCTA 2013, Johannesburg.

Macphee, D. E., C. J. Black and A. H. Taylor (1993). "Cements Incorporating Brown Coal Fly Ash from The Latrobe Valley Region of Victoria, Australia." Cement and Concrete Research 23(3): 507-517.

Malhotra, V. (2008). "Role of fly ash in reducing greenhouse gas emissions during the manufacturing of portland cement clinker." Advances in Concrete Technologies in the Middle East: 19-20.

Manz, O. E. (1997). "Worldwide production of coal ash and utilization in concrete and other products." Fuel 76(8): 6.

Meyer, C. (2009). "The greening of the concrete industry." Cement and Concrete Composites 31(8): 601-605.

Naik, T. R. (2008). "Sustainability of concrete construction." Practice Periodical on Structural Design and Construction 13(2): 98-103.

Naik, T. R. and S. S. Singh (1993). Fly Ash Generation and Utilization - An Overview. Recent Trend in Fly Ash Utilization.

Oscar, E. (1999). "Coal Fly Ash: a retrospective and future look." Fuel 78(2): 133-136.

Shayan, A., A. Xu and F. Adndrew-Phaedonos (2013). Field Performance of Geopolymer Concrete, Used as a Measure Towards Reducing Carbon Dioxide Emission. Concrete in Australia. North Sydney, Engineers Media. 39: 10.

Škvára, F., L. Kopecký, V. Šmilauer and Z. Bittnar (2009). "Material and structural characterization of alkali activated low-calcium brown coal fly ash." Journal of Hazardous Materials 168(2–3): 711-720.

Stengel, T., J. Reger and D. Heinz (2009). "LCA of geopolymer concrete–what is the environmental benefit." Proceedings Concrete 9.

Turner, L. K. and F. G. Collins (2013). "Carbon dioxide equivalent (CO2-e) emissions: A comparison between geopolymer and OPC cement concrete." Construction and Building Materials 43(0): 125-130.

Xu, H. and J. S. J. Van Deventer (2000). "The geopolymerisation of alumino-silicate minerals." International Journal of Mineral Processing 59(3): 247-266.

CHAPTER 2

LITERATURE REVIEW

2.1. Overview

This chapter reviews the literature on the environmental impact of the use of coal as a primary energy sources and the production of ordinary Portland cement. The history of alkali activation of cementitious material and the reaction mechanism are also described. The various classes of fly ash, in particular the Australia brown coal fly ash used in this project and its characteristic are also explained.

2.2. Environmental Issues

2.2.1 Ordinary Portland cement production

Concrete is the world's most consumed man-made material, with Portland cement being most common binding material for concrete products. Portland cement has been employed for centuries due to its durability, dependability and low embodied energy (Naik 2008).

The production of Portland cement as the main binder material in concrete does however raise a number of environmental concerns regarding the energy consumption and the emission of CO_2 (Davidovits 1994b, Malhotra 2005, Berry, Cross et al. 2009, Aïtcin and Mindess 2011). The production of the Portland cement requires a large amount of energy and at the same time produces a large quantity of CO_2 as result of the calcination process during the manufacturing. Malhotra (2004) breaks down the sources of greenhouse gas CO_2 emissions in the manufacturing of Portland cement as shown in Table 2.1 (Malhotra 2004), while Davidovits (2005), Table 2.2 compared the energy needs along with the greenhouse gas CO_2 emissions between ordinary Portland cement and geopolymeric cement (Davidovits 2005).

Table 2.1 Source of greenhouse gas CO_2 emissions in the production of Portland cement (Malhotra 2004)

Source of CO_2 emissions	**Percentage**
Calcination process	50 – 55
Fuel combustion	40 – 50
Use of electric power	0 – 10

Table 2.2 Energy needs and greenhouse CO_2 emissions, ordinary Portland cement vs geopolymeric cement (Davidovits 2005)

Cement type	**Energy needs MJ/tonne**			**CO_2 emissions tonne/tonne**
	Calcination	**Crushing**	**Total**	
Portland	3200	430	3420	1.00
Geopolymeric	600	390	990	0.15 – 0.20

According to Naik (2008), the manufacture of Portland cement worldwide in 2004 contributed about 2 billion tonnes of greenhouse gas CO_2 emission, corresponding to about 7% of total worldwide greenhouse gas. Moreover, the cement production is predicted to double from about 2.5 billion tonnes in 2006 to about 5 million tonnes by 2020. Accordingly the greenhouse gas CO_2 emission of cement production will increase similarly by 2020 (Naik 2008).

Concrete is by far the most widely used material around the world (Aïtcin and Mindess 2011), next to water, with around 10 billion tonnes produced each year (Meyer 2009). Table 2.3 shows the annual world material production in 2007. This level of production comes with considerable effects on the environment: the use of vast amounts of raw materials, a large energy consumption and a large volume of CO_2 emitted during the manufacture of cement; plus the large volume of water required during the production of concrete.

Table 2.3 Annual world production of material in 2007 (Aïtcin and Mindess 2011)

Material	**Production in tonnes**
Concrete	~ 13 billion
Coal	6.5 billion
Crude oil	~ 3.8 billion
Portland cement	2.36 billion
Steel	1.34 billion
Wheat	606.4 million
Salt	200 million
Sugar	162 million

Aïtcin and Mindess (2011) consider the need to reduce the environmental impact of cement and concrete production in the light of sustainable development concepts, and consider approaches to making concrete more sustainable. These include:

- the use of higher strength concretes
- making concrete more durable
- replacing up to half of the Portland cement with supplementary cementing materials (SCMs)
- using fillers
- manufacturing Portland cement more efficiently
- using waste materials as fuels
- using recycled concrete, and other industrial wastes, as aggregate sources
- finding ways to capture and store or sequester CO_2 emissions
- using cement kiln dust in some applications
- using less water
- improving structural design and building codes.

Some approaches would be expected to be more effective than others and some are less likely to be employed in developing countries due to the associated cost and lack of the technology.

Substituting the major part of Portland cement by pozzolanic material or supplementary cementitious materials is potentially the most effective way of decreasing both energy consumption and the production of greenhouse gases. Each kilogram of substitution reduces by about 1 kg the emission of CO_2, and saves the energy required to produce 1 kg of cement.

Presently there are numerous supplementary cementing materials (SCM) or pozzolanic material (PM) available, primarily by-products or wastes of other industrial processes, several of which are already used. These are interground or blended with the cement at the cement plant, or substituted for cement at the batch plant. The levels of substitution can be 50-70% of the Portland cement. These supplementary cementing materials include: fly ash, ground granulated blast furnace slag, silica fume, metakaolin and calcined clay, natural pozzolans, and rice husk ash (Papadakis and Tsimas 2002, Malhotra 2005, Naik 2008, Aïtcin and Mindess 2011, Thomas 2013).

Therefore the use of supplementary materials for blended cement or even a 100% replacement of ordinary Portland cement would have a significant impact on the environment.

2.2.2 Coal production

Coal currently supplies around 30% of primary energy and plays a vital role in electricity generation worldwide with 41% of global electricity provide by coal (WCA 2015). In Australia coal fuelled 72% of Australian electrical power generation in 2012-2013 (French and Smitham 2007, ESAA 2015). Thus while electricity provided by renewable energy sources is increasing, at present it only satisfies a small proportion of the global demand for power generation. As such, coal use will continue for many years in the future, given the huge reserves of coal available worldwide. Indeed a study has identified that coal burning power

stations produce low cost power, and has a high 'energy returned' to 'energy invested' ratio, which is second only to hydro-power generation plants (Table 2.4)(Rangan 2010).

Table 2.4 Energy returned to energy invested ratio of power generation plants (Rangan 2010)

Power generation plant	**Energy returned to Energy invested Ratio**
Hydro	100
Coal	80
Oil	35
Wind	18
Solar	6 – 20
Nuclear	15
Biofuels	3

It is estimated that there are over 860 Giga tonnes of proven coal reserves worldwide, which is enough to last over 118 years at current rates of production. Coal reserves are available in almost every country worldwide, with recoverable reserves in over 70 countries. More than 80% of global reserves are found in five countries, which the largest reserves in North America, Russia, China, India and Australia respectively (Barnes 2010, WCA 2015). Figure 2.1 shows coal reserves by country for the top 9 countries or regions (Barnes 2010, Heidrich, Feuerborn et al. 2013).

According to the International Energy Agency, over 6745 million tonnes of hard/black coal and 1040 million tonnes of brown coal/lignite are currently produced annually worldwide (IEA 2012).

Coal is generally differentiated into black and brown coal. Black coal produces more thermal energy than brown coal. In Australia, anthracite, bituminous and sub-bituminous coals are called black coal and lignite as brown coal, whereas in

Europe, both sub-bituminous coal and lignite are referred to as brown coal (Table 2.5). Australia brown coal is currently considered to be unsuitable for export and is used exclusively to generate electricity in domestic power stations (Geoscience Australia and ABARE 2014).

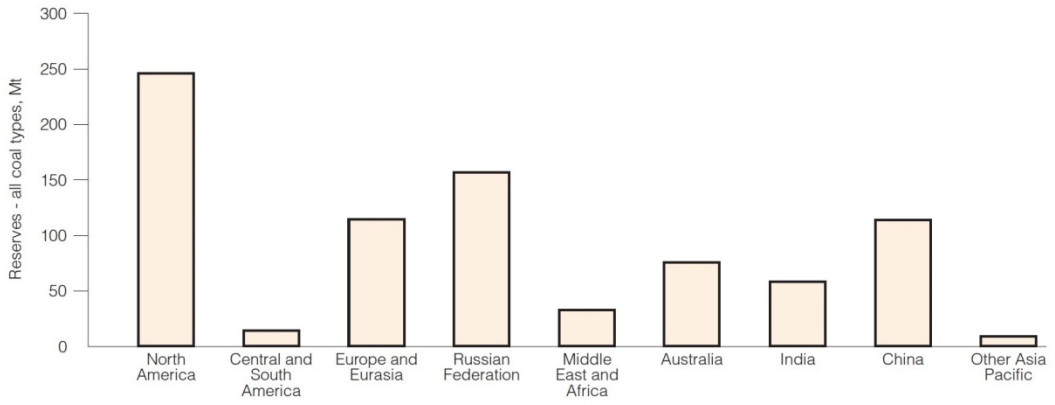

Figure 2.1 Proven coal reserves worldwide (Heidrich, Feuerborn et al. 2013)

Table 2.5 Coal classification terminology (Geoscience Australia and ABARE 2014)

Coal rank	**Australian terminology**	**European terminology**
Anthracite	Black coal	Black coal
Bituminous coal	Black coal	Black coal
Sub-bituminous coal	Black coal	Brown coal
Lignite	Brown coal	Brown coal

Estimated in 2014, Australia's recoverable Economic Demonstrated Resource (EDR) of black coal was at 62.6 Giga tonnes comprising 9% of the world's recoverable resources, with most of it located in Queensland (60%) and New South Wales (37%). Australia's recoverable EDR brown coal of 44.2 Giga tonnes was approximately 19% of the world's recoverable resources, nearly all located in Victoria with 93% deposited in the Latrobe Valley (Britt, Summerfield et al.

2015). The Latrobe Valley field is one of the largest single brown coal fields in the world.

The ash produced during pulverised coal combustion which is transported by the combustion gases and then captured, usually in an electrostatic precipitator, is known conventionally as fly ash and sometimes referred to as Pulverised Fuel Ash (PFA) (Barnes 2010). The most common applications for fly ash are as blended cement and cement raw material (Barnes 2010). Cement manufacturers have increasingly used fly ash both as a source of silica, and as a blend material, enabling them to produce more environmentally friendly, cost effective cements, while reducing overall CO_2 emissions, energy and use of natural aggregates.

2.2.3 Coal combustion products

The coal powered power stations around the world produce huge quantities of Coal Combustion Products (CCPs) every year. The coal combustions products are the by-products generated from coal-fired power plants. These by-products include (WCA 2015):

- fly ash
- bottom ash
- boiler slag
- flue gas desulphurisation gypsum
- others types of material such as fluidised bed combustion ash, cenospheres, and scrubber residues.

Fly ash and bottom ash are the major coal combustion products from pulverised firing. About 80-90% of the ash residue from power stations is recovered as fly ash while the remaining 10-20% is bottom ash. Boiler slag and flue gas deposits accounting for little of the overall residue.

Worldwide, fly ash production was 900 million tonnes per year in 2005 and it is anticipated to increase up to about 2000 million tonnes in 2020 (Malhotra 2008).

In 2005 Australia produced around 13 million tonnes of CCPs or ash with only 33% or around 4 million tonnes being “effectively utilised” (defined as sold or used in a beneficial manner), the remainder is deposited into ponds or landfill mixed with bottom ash (ADAA 2007, Keyte 2009). The Ash Development Association of Australia data on ash production and use in Australia from 1992 to 2005 is shown in Figure 2.2 (ADAA 2007).

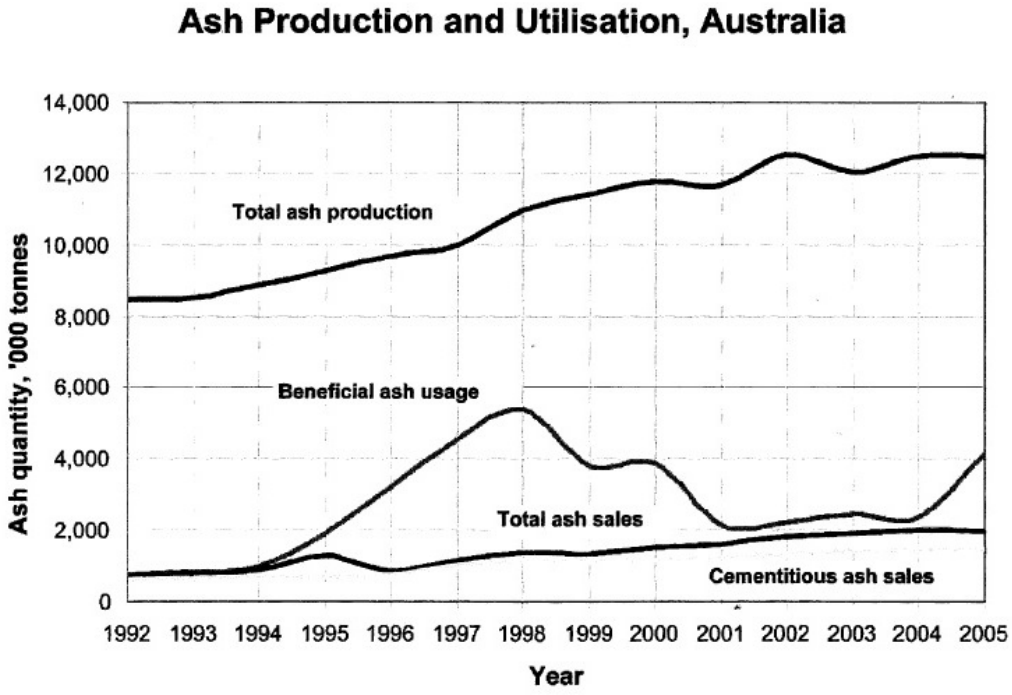

Figure 2.2 Ash production and utilization in Australia 1992 to 2005 (ADAA 2007)

Figure 2.2 presents a 14 year picture of fly ash and bottom ash production and utilisation. In 2005, 15.8% or 1.397 million tonnes were sold primarily for cementitious application. The main contributors to total ash sales were cementitious and non-cementitious applications:

- Pre-mixed concrete
- Road stabilisation
- Blended cement products
- Controlled low strength fills

- Asphaltic fillers
- Underground mining applications
- Agricultural uses

The utilization of the ash is categorised as (Heidrich 2003):

a) Category 1 – Ash materials sold for the use in cement production, blended cement manufacture, binder supplement.
b) Category 2 – All uses not included in Category 1 or 3. This includes ash sold for use in road stabilisation, asphaltic fillers, controlled low strength material and bulk fill, where a small amount of cement is added as a stabiliser.
c) Category 3 – All uses of ash where no other binders are added to the ash, e.g. Bulk fill, road bases non-stabilised, agricultural applications.
d) Beneficial use – Use of ash in projects where benefits could have resulted in reduced direct handling costs, used in an in-kind nature to the benefit of external or internal groups, e.g. Mine site remediation, void backfilling, site haul roads. Placement in ash pond is not considered a beneficial use.

However, approximately half of the "beneficial use" for cementitious applications comes from black coal fly ash, with most of the lignite brown coal fly ash dumped into ponds. More than a million tonnes of brown coal fly ash is captured by electrostatic precipitators in the State of Victoria annually, in 2005 1.3 million tonnes were produced, most of which went to land-fill (ADAA 2007). The fly ash, bottom ash and clinker is mixed with water to form slurry and conveyed to a settling pond, then stored as stockpile ash.

2.3. Fly Ash

Fly ash is a very fine ash removed by the dust collection systems from the exhaust gases of power plants and is predominantly spherical glassy particles together with some crystalline matter and unburnt carbon from the combustion gases. ASTM C618-12 defines fly ash as "the finely divided residue that results

from the combustion of ground or powdered coal and that is transported by flue gasses" (ASTM 2012). The Australian Standard AS 3582.1 defines fly ash as "solid material extracted from the flue gases of a boiler fired with pulverised coal" (AS-3582.1 1998). ASTM C618 is the standard specification for coal fly ash and raw or calcined natural pozzolan for use in concrete and AS 3582.1 is the Australian Standard for supplementary cementitious materials for use with Portland and blended cement.

2.3.1 Classification of fly ash

Fly ash is generally pozzolanic and rarely cementitious depending on its mineralogical composition, fine particle size and amorphous character. ASTM C 618 (1993) defines pozzolans as "silicious and aluminous materials which in themselves possess little or no cementitious value but will, in finely divided form and in the presence of moisture, chemically react with $Ca(OH)_2$ at normal temperatures to form compounds possessing cementitious properties."

The fly ashes produced by different power stations are not equally pozzolanic, moreover a significant variation in the chemical composition is observed despite the same source and type of burning coal, so not all fly ashes are suitable for use as a binder in concrete (French and Smitham 2007, Siddique 2008). Several factors that could cause coal burning power stations to produce fly ash that is an inherently variable material according to Siddique (2008) are:

- the type and mineralogical composition of the coal,
- degree of coal pulverization,
- type of furnace and oxidation conditions including air-to-fuel ratio, and
- the manner in which fly ash is collected, handled and stored before use.

In addition, the fly ash properties may also vary within the same plant with the same source of coal because of load conditions over a twenty four hour period (Siddique 2008). This unpredictability variation of chemical composition is a serious disadvantage and one of the main challenges of utilizing fly ash.

ASTM C618-12 specifies the chemical and physical requirements of fly ash and natural pozzolans for use in concrete (Table 2.6).

Table 2.6 Requirements for fly ash and natural pozzolans for use in concrete (ASTM 2012)

Requirements		**Fly ash classification**		
		N	**F**	**C**
Chemical requirements				
$SiO_2 + Al_2O_3 + Fe_2O_3$	min %	70.0	70.0	50.0
SiO_2	max %	4.0	5.0	5.0
Moisture content	max %	3.0	3.0	3.0
Loss on ignition	max %	10.0	6.0	6.0
Physical requirements				
Fineness:				
Amount retained on 45µm sieve	max %	34	34	34
Strength activity index				
With Portland cement, at 7 days	min %	75	75	75
With Portland cement, at 28 days	min %	75	75	75
Water requirement	max %	115	105	105
Soundness				
Autoclave expansion or contraction	max %	0.8	0.8	0.8
Uniformity requirements				
Density, variation	max %	5	5	5
Percent retained on 45µm, variation	max %	5	5	5

The individual fly ash classes are defined as:

Class N: Raw or calcined natural pozzolans, such as some diatomaceous earths; opaline cherts and shales; tuffs and volcanic ashes or pumicites, calcined or uncalcined; and various materials requiring calcination to induce satisfactory properties, such as some clays and shales.

Class F: Fly ash normally produced from burning anthracite or bituminous coal (but may also be produced from subbituminous coal and from lignite) falls in this category. This class of fly ash exhibits pozzolanic.

Class C: Fly ash normally produced from lignite or sub-bituminous coal is the only material included in this category. This class of fly ash, in addition to having pozzolanic properties, also has some cementitious properties.

According to French and Smitham (2007) the ASTM C 618 (2012) classification may not be directly applicable to or adequately reflect the variability found in Australian fly ash both with respect to chemistry and mineralogy (French and Smitham 2007). Classification of the three grades Australian fly ash, according to Australian Standard AS 3582.1, are shown in Table 2.7.

Table 2.7 Classification of fly ash according to Australian standard AS 3582.1

Grade	**Fineness, by mass passing 45µm sieve % minimum**	**Loss on ignition, % maximum**	**Moisture content % maximum**	**SO_3 content % maximum**
Fine	75	4.0	1.0	3.0
Medium	65	5.0	1.0	3.0
Coarse	55	6.0	1.0	3.0

Both the ASTM C 618 and Australian Standard AS 3582.1 classification may be overly simplistic and fail take into account other important characteristic such as mineralogy so as an overall rating system of classification and characteristic would be useful for all end-users of fly ash (French and Smitham 2007).

The chemical composition of coal fly ash in Australia varies significantly, with most of the commercially available source having low calcium content that can be used in Portland cement concrete (Keyte 2009). This fly ash with a relatively low concentration of calcium typically referred to as class F fly ash, is normally produced from burning black coal (anthracite or bituminous coal). The high

content of calcium in the fly ash could interfere the polymerization process and change the microstructure (Rangan 2010). Victoria brown coal fly ash although produced from brown coal (lignite) may well only exhibit a low concentration of calcium. Development of geopolymer concrete that can utilise large amounts of brown coal fly ash is of particular interest.

2.3.2 Fly ash utilisation

The major chemical constituents of the ash are silica, alumina and oxides of calcium and iron. Due to the fineness, pozzolanic and sometimes self-cementitious nature, fly ash has been widely used as a replacement material in cement and concrete in the construction industry (Siddique 2008, Blissett and Rowson 2012). The use of fly ash, an industrial by-product from coal burning power stations, as a replacement material for Portland cement is well established. Figure 2.3 shows breakdown of the uses of fly ash in Europe, with the major use is either as a raw material or as an additive (Blissett and Rowson 2012).

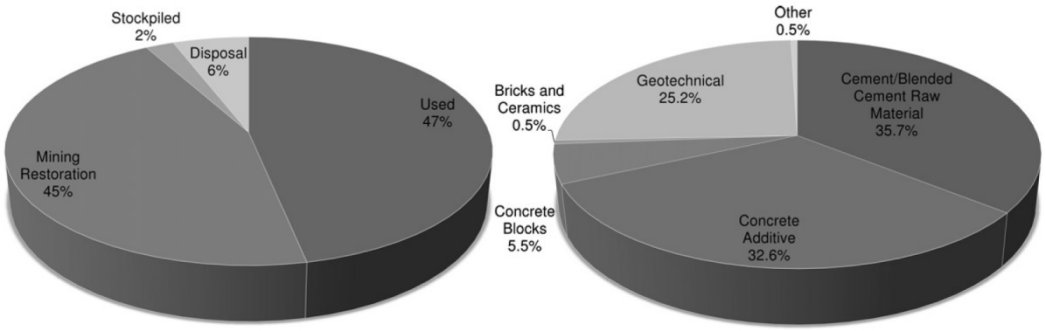

Figure 2.3 Fly ash utilisation trends 2008 in Europe and a breakdown of the used component of the trends (Blissett and Rowson 2012)

The fly ash produced can be categorised as either, class F or class C fly ash. Class F fly ash is produced from burning anthracite and bituminous coals, while class C fly ash is produced from sub-bituminous coals and lignite. In Australia, lignite is

also known as brown coal, accordingly class F and C fly ash are from black coal and brown coal fly ash is from brown coal.

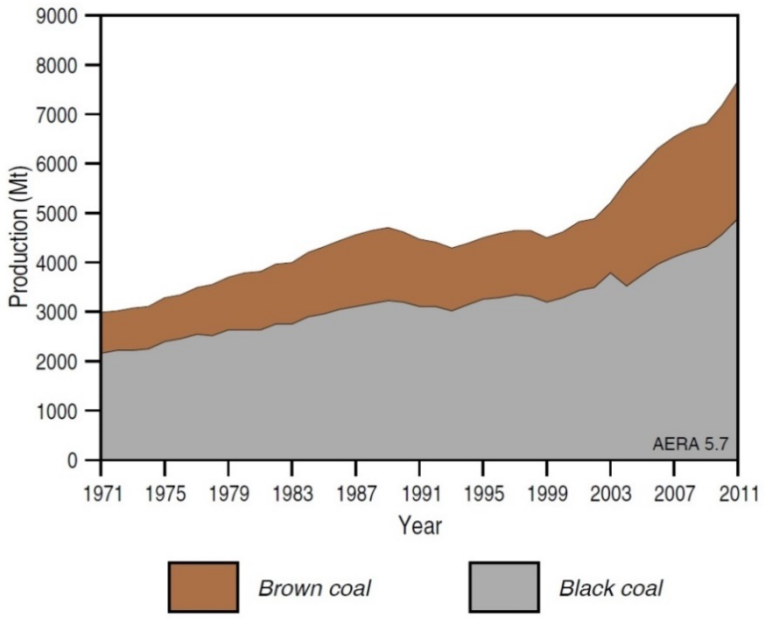

Figure 2.4 World production by coal type (Geoscience Australia and ABARE 2014)

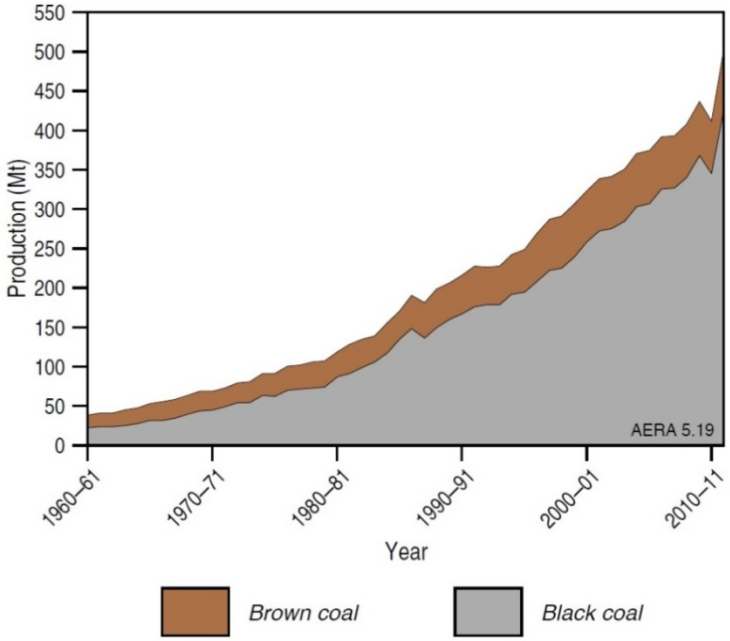

Figure 2.5 Australian production by coal type (Geoscience Australia and ABARE 2014)

World coal production in 2011 totalled 7.6 billion tonnes. Of the total coal production, black coal accounted for 64%, while brown coal accounted for the remaining 36%. Australian coal production in 2011-2012 was estimated to be around 504 million tonnes, black coal accounted for 85% and brown coal 15% (Geoscience Australia and ABARE 2014). Figure 2.4 shows the world production of coal by type, and Figure 2.5 shows the Australian production of coal by type.

The majority of fly ashes used in concrete are low-calcium fly ash (ASTM C 618, class F) which exhibit pozzolanic action. These pozzolanic materials require $Ca(OH)_2$ in order to form effective products, thus have predominantly been used in blended cement as a partial replacement of Portland cement or either as a raw material or as an additive (Papadakis and Tsimas 2002, Ahmaruzzaman 2010, Blissett and Rowson 2012). Whereas, high-calcium fly ash (ASTM C 618, class C) apart from being pozzolanic and containing significant quantities of CaO, can exhibit a self-cementitious (hydraulic) activity. This can also be used in combination with Portland cement to gather the essential $Ca(OH)_2$ activation from its hydration (Papadakis and Tsimas 2002, Malhotra 2005).

2.3.3 Geopolymer concrete

The term ”geopolymer” was first applied by Davidovits in 1979, it refers to alkali-activated aluminosilicate binders formed by alkali silicate activation of aluminosilicate materials. These binders are formed by the reaction of an alkali, generally in liquid form, with the silicon (Si) and the aluminium (Al) from a source material of geological origin or in by-product materials such as fly ash and rice husk ash. As the chemical reaction that takes place is a polymerization process the term geopolymer was then used to represent those binders (Davidovits 1993, Rangan 2010). Later on the name geopolymer came to be widely accepted for materials based on fly ash and other aluminosilicate sources (Duxson, Lukey et al. 2007). Geopolymers are often coupled with alkali-activated cements, which

were originally developed by Glukhovsky in the 1950s. Glukhovsky published the term “soil cements” for the binders and “soil silicate“ for the concrete.

Geopolymers are member of the family of inorganic polymers. The geopolymer structure is an alkali aluminosilicate gel with a framework similar to the microstructure of a zeolite, except lacking long-range order (crystallinity) (Hardjito and Rangan 2005, CIA 2011).

The silicate and aluminate content within fly ash are the main contributors to the geopolymer reaction, while a high content CaO could affected the rate of reaction and cause rapid setting and altered workability (Diaz, Allouche et al. 2010). Due to the variation in the fly ash chemical composition, class F fly ash so far is the most commonly used in the synthesis of this alkali-activated binder. The high content of amorphous alumina-silicate phases and greater workability have made class F is preferred material in geopolymer and cement application (Sindhunata 2006).

2.3.4 Reaction mechanism

Davidovits (2005) categorised the geopolymer structure based on the ratio of Si/Al and proposed poly(sialate) as the molecular structure of geopolymers based on silico-aluminates, Figure 2.6 (Davidovits 2005). The tetrahedral structures, i.e SiO_4 and AlO_4, are linked in an alternating pattern sharing oxygen atoms to compose the sialate network. Sialate is an acronym for silicon-oxo-aluminate the base unit which condense together to form larger polymeric structures called poly(sialates). Polysialates are chain and ring polymers with Si^{4+} and Al^{3+} in IV-fold coordination with oxygen (Davidovits 2005, Radford, Grabher et al. 2009).

The polymerization process involves a rapid chemical reaction under alkaline conditions with the aluminosilicates present in the fly ash. The geopolymer produced is a member of the family of inorganic polymers with a chemical composition similar to natural zeolitic materials, except the microstructure is amorphous (Davidovits 1994d, Hardjito and Rangan 2005, Rangan 2010). The alkali silicates or hydroxides used as the activating agents achieve this

requirement by providing either potassium (K^+) or sodium (Na^+) ions into the matrix. The aluminosilicate have been grouped in three families depending on the atomic ratio of Si/Al that may be 1, 2, or 3 (Davidovits 1994c).

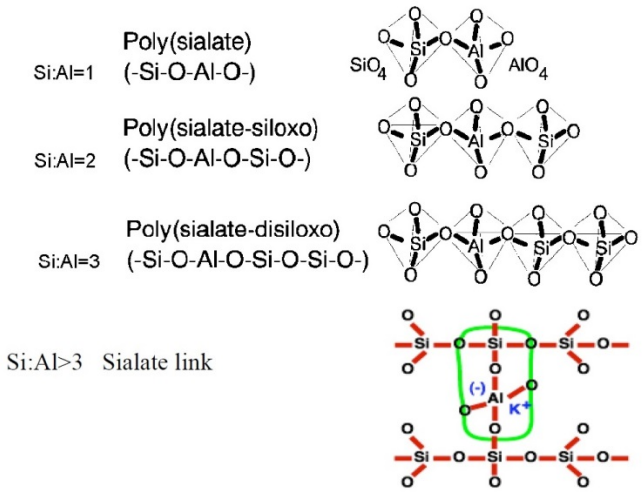

Figure 2.6 The chemical structures of polysialate (Davidovits 2005)

A schematic representation of the geopolymerization process (which is exothermic) according to Davidovits (1994) shown on Figure 2.7:

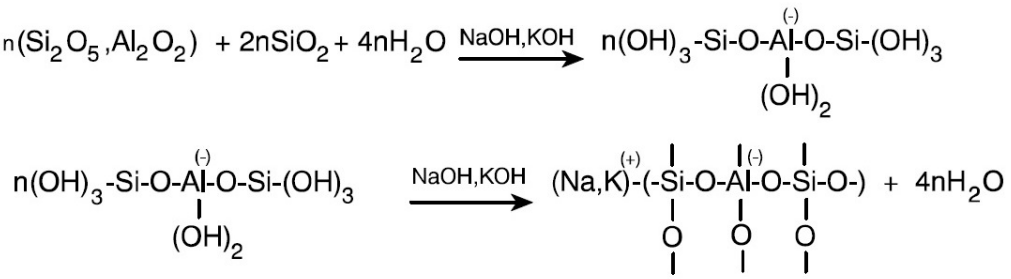

Figure 2.7 Schematic of geopolymerization (Davidovits 1994d)

It has been assumed that the syntheses are carried out through oligomers consisting of two or three monomers which provide the actual unit structures of the three dimensional macromolecular structure (Davidovits 1994d). Van Jaarsveld (1997) considered that the description is an oversimplification. Under

reaction conditions where temperature cannot be exactly controlled, a wide range of related materials could be expected to form (Van Jaarsveld, Van Deventer et al. 1997). Rangan (2010) refined the reaction mechanism, identifying the first step, orthosialate, as a "geopolymer precursor" and the second step as the formation of the "geopolymer backbone", Figure 2.8.

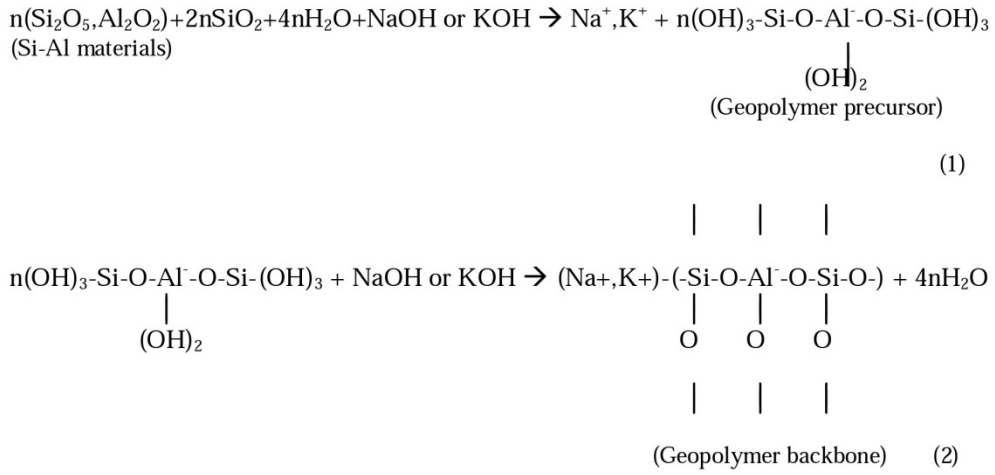

Figure 2.8 Refined schematic equation (Rangan 2010)

Furthermore, Rangan (2010) showed that water in a geopolymer reaction provides workability and plays no role in the chemical reaction. This is in contrast to the chemical reaction with Portland cement where water is consumed in the hydration process. In geopolymerization water is expelled during the curing and drying stages, creating nano-pores in the matrix which play a key role in the mechanical and durability performance of the geopolymer (Rangan 2010).

Fernández-Jiménez et al. (2004) proposed a model for the reaction mechanism of the fly ash particles themselves, Figure 2.9 (Fernández-Jiménez, Palomo et al. 2004). The model shows that the reaction product is generated both inside and outside the shell of the sphere. The chemical attack starts on the surface of a particle, leading to the formation of the reaction product around the surface of the fly ash particle. However, the reaction on the surface also results in the

formation of a hole in the surface of the particle exposing the inner core leading to geopolymerization within the core of the fly ash particle. This bi-directional process will continue until the ash particle is completely or almost completely consumed (Figure 2.9.a-b).

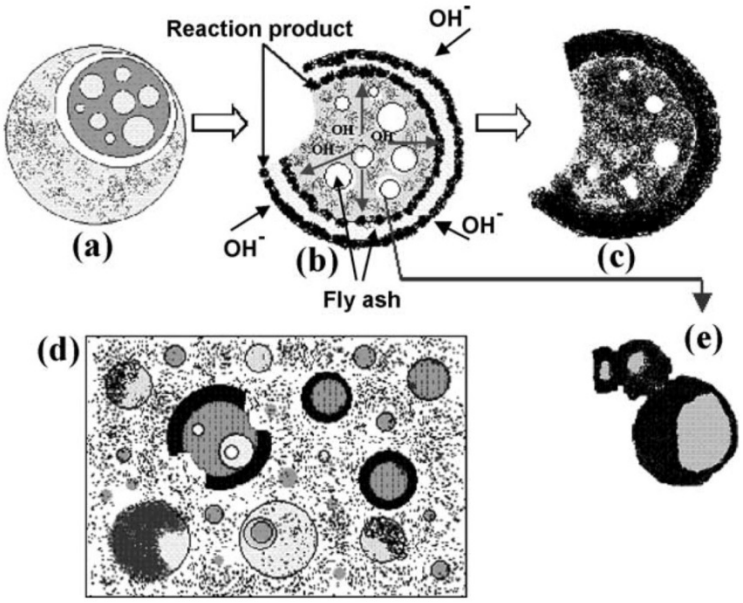

Figure 2.9 Descriptive model of the alkali activation (Fernández-Jiménez, Palomo et al. 2004)

This initial chemical reaction when the fly ash particles react with the alkaline solution is termed the dissolution process. The dissolution process involves extensive precipitation of reaction products on the surface layer of the fly ash particles, as a consequence this layer might cover some of the smaller spheres and prevent contact with the alkaline medium (Figure 2.9.e), resulting in some unreacted fly ash particles in the geopolymer matrix formed (Figure 2.9.d). Overall the formation of the surface layer coupled with the internal reaction filling the space within the fly ash particles results in the forming of a dense matrix.

The process described can vary locally from one point in the matrix and is not necessarily uniform throughout the gel, depending on the distribution of particle

size and the local chemistry such as pH. As a result, several morphologies may occur in a single paste such as: unreacted particles, partially dissolved particles and fully reacted particles, Figure 2.9.d.

A general mechanism for the alkali activation of materials primarily comprising silica and alumina proposed by Glukhovsky in 1950s divided the process into three phases: (a) destruction-coagulation, (b) coagulation-condensation, and (c) condensation-crystallization. A number of authors have elaborated on and extended the Glukhovsky theory in order to explain the entire geopolymerization process (Duxson, Provis et al. 2007).

Duxson et al. (2007) proposed a much simplified conceptual model for the reaction mechanism for geopolymerization (Figure 2.10). The model identifies the principal processes as the activation of solid alumina-silicate into an inorganic alkali aluminasilicate binder through a polymerization process, which consists of a number of steps:

- dissolution,
- speciation equilibrium,
- gelation,
- reorganization,
- polymerization and hardening.

Although the conceptual model is presented as a stepwise process the individual steps actually occur concurrently.

During geopolymerization, the dissolution of the solid particles at the surface which releases aluminate and silicate has been identified as the rate determining step in the formation of the geopolymeric gel matrix, Figure 2.10 (Dissolution), although the actual process of particle-to-gel conversion has not been definitively confirmed.

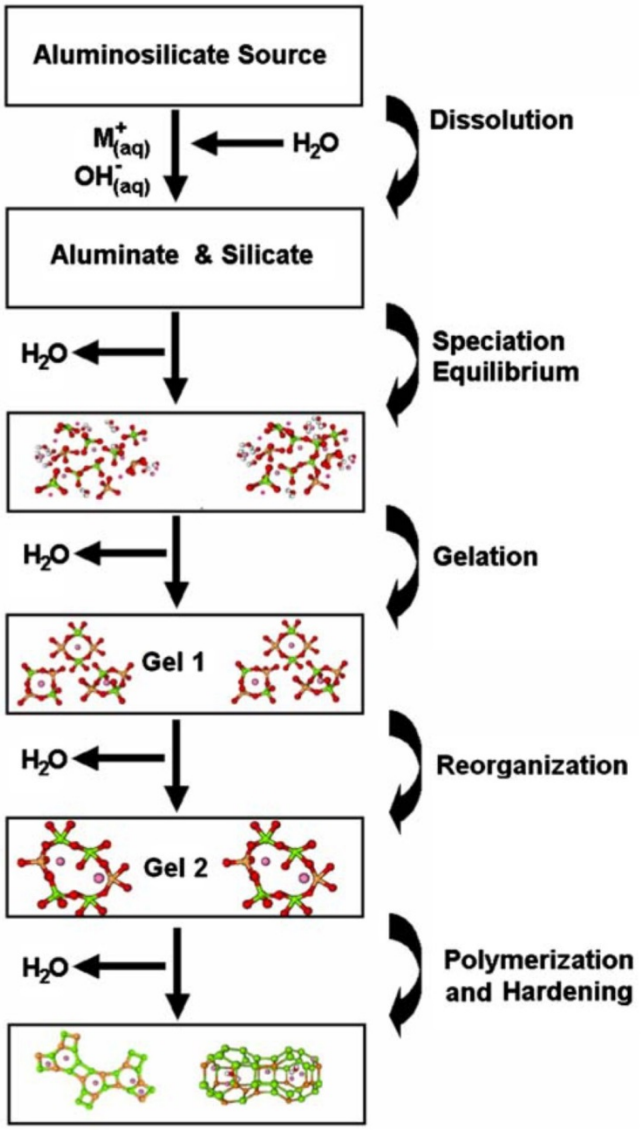

Figure 2.10 Conceptual model for geopolymerization (Duxson, Provis et al. 2007)

Once the species have been released by dissolution into the aqueous phase, a complex mixture of silicate, aluminate and aluminosilicate species is formed. When a sufficient concentration of reactants is achieved this then results in the formation of the gel. This process releases the water that was nominally consumed during dissolution. As such, water plays the role of a reaction medium, but resides within pores in the gel. This type of gel structure is commonly referred to as bi-phasic, with the aluminosilicate binder and water forming the two phases. The time for the supersaturated aluminosilicate solution to form a

continuous gel varies considerably with raw material, processing conditions and solution composition and synthesis conditions, such that some systems never gel. The three-dimensional aluminosilicate structure attributed to geopolymers is created after gelation as the system continues to rearrange and reorganize to produce the gel networks and pore connectivity (growth) Figure 2.10.

Furthermore, Duxson et al. (2007) identified two successive and controlling stages which are nucleation and growth. Nucleation is the dissolution of the aluminosilicate material and formation of polymeric species, known as destruction-coagulation and coagulation-condensation phases in Glukhovsky's proposed mechanism. These are highly dependent on thermodynamic and kinetic parameters. Growth is the condensation-crystallization phase, the third step on the Glukhovsky mechanism, when the nuclei reach a critical size and crystal begin to develop. This process is a structural reorganization which forms the microstructure of the material and the nano-pore distribution which is critical in determining the physical and durability properties of the geopolymer (Duxson, Provis et al. 2007, Rangan 2010).

Provis (2006) proposed an extended model Figure 2.12, outlining the reaction kinetic model for geopolymerization based on the Faimon model Figure 2.11 (Faimon 1996). The aluminosilicate weathering model of Faimon only allows for dissolution of a primary mineral into aluminate and silicate monomers. The aluminate and silicate monomers are then linked via both addition and autocatalytic polymerization routes, with the creation of an unclear 'secondary mineral' phase. The extended kinetic reaction model of Provis suggested a chemical reaction sequence for responsible for geopolymers formation. The reaction sequence is a result of the pH of the geopolymer reaction slurry being higher than Faimon's mineral weathering model. The higher pH will initiate the geopolymerization reaction which will be completed in a much shorter time frame. The products of the reaction will then consist of both a gel and a zeolitic phase, with the gel to zeolite conversion happening over an extended curing period, shown as grey arrow in Figure 2.12 (Provis 2006).

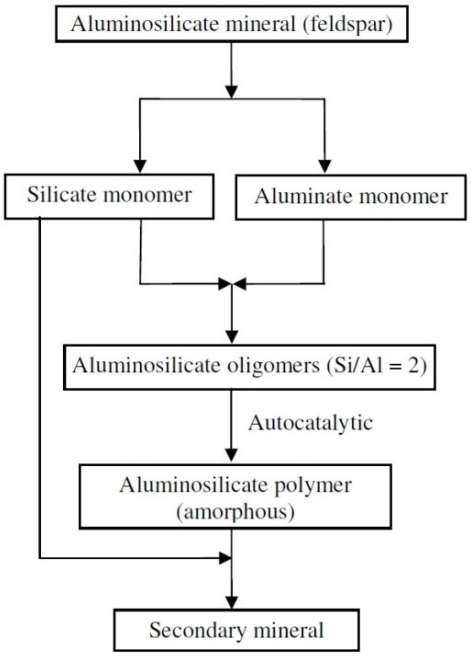

Figure 2.11 Faimon (1996) aluminosilicate weathering model (Provis 2006)

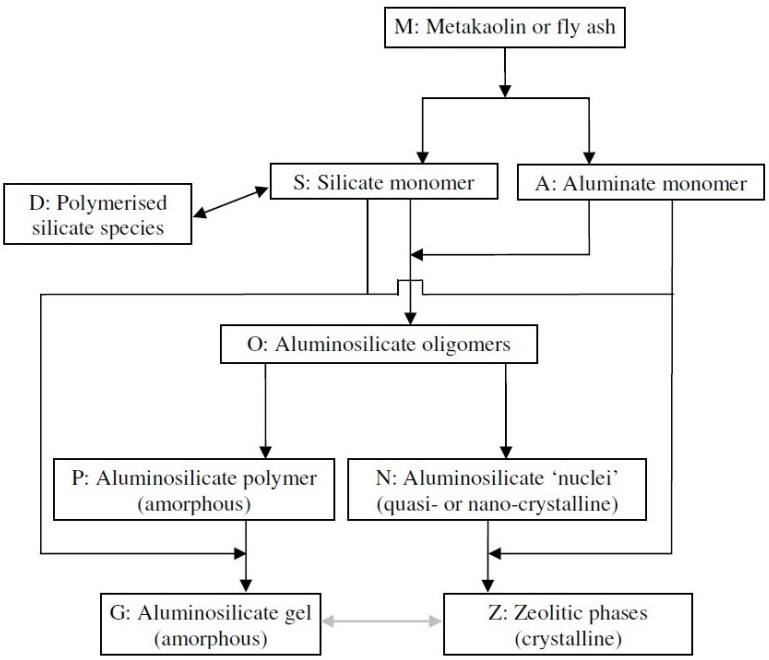

Figure 2.12 Reaction sequence of geopolymerization extended model (Provis 2006)

Based on the extended model of the geopolymerization reaction sequence proposed by Provis, Pacheco-Torgal (2008) further modified the model, identifying the gel/zeolite interconversion as a one way process called transformation, Figure 2.13 (Pacheco-Torgal, Castro-Gomes et al. 2008). Provis subsequently presented a simplified schematic of the chemical reaction steps during geopolymerization, separate from physical processes, such as sorption of particles surface and gel drying which happen simultaneously Figure 2.14 (Provis and Rees 2009).

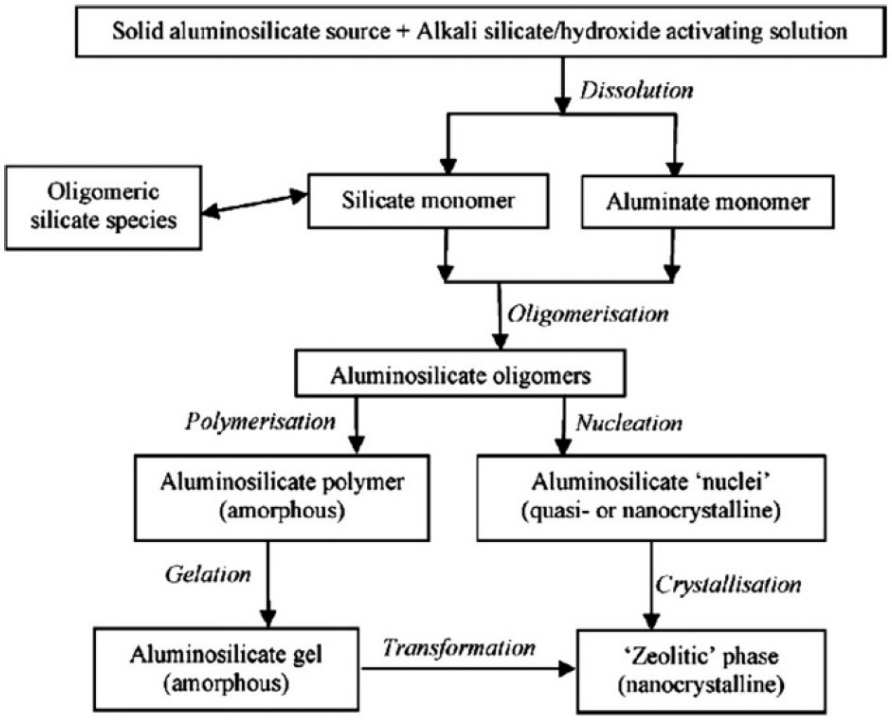

Figure 2.13 Schematic outline of the reaction process in geopolymerization (Pacheco-Torgal, Castro-Gomes et al. 2008)

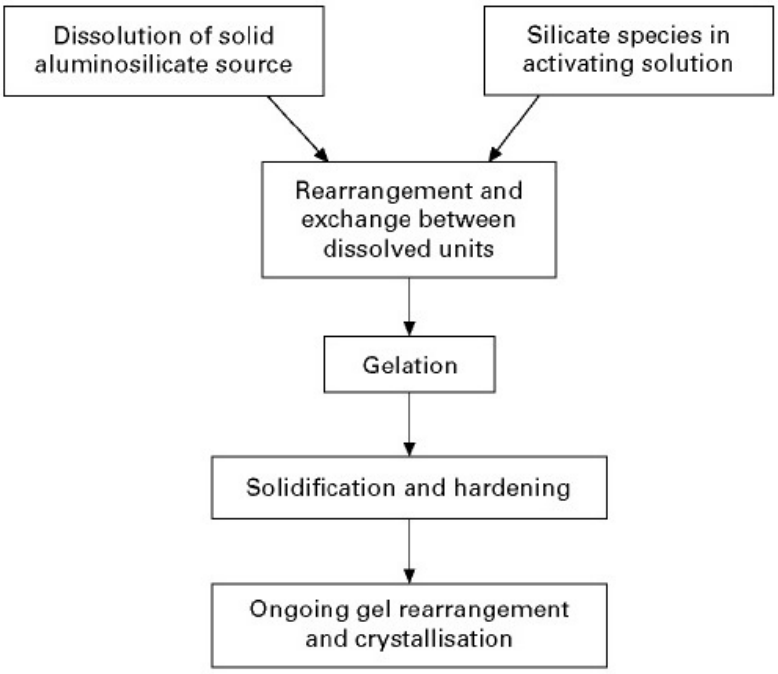

Figure 2.14 Simplified chemical reaction during geopolymerization (Provis and Rees 2009)

As stated the extent of dissolution of alumino-silicate materials has been identified as a dominant step in formation of an amorphous structure of geopolymer, with the OH^- ion acting as a reaction catalyst during the activation process (Xu and Van Deventer 2000, Fernández-Jiménez, Palomo et al. 2004). Xu et al. (2000) proposed a reaction scheme for the polycondensation process of geopolymerization from aluminosilicate materials by taking in to account the differences between zeolite and geopolymers (Figure 2.15). The geopolymers, with the shorter setting and hardening times, will form a firmly packed polycrystalline structure which give better mechanical properties than zeolite with lower density and cage-like crystalline structure (Xu and Van Deventer 2000). Depending on the composition of the fly ash and activator the gel formed can be represented as $[M_z(AlO_2)_x(SiO_2)_y \cdot nMOH \cdot mH_2O]$. The proposed reaction scheme being:

$$Al\text{–}Si\ material(s) + MOH(aq) + Na_2SiO_3(s\ or\ aq) \quad (2.1)$$

$$\text{Al–Si material(s)} + [\text{M}_z(\text{AlO}_2)_x(\text{SiO}_2)\cdot n\text{MOH}\cdot m\text{H}_2\text{O}]\cdot\text{gel} \quad (2.2)$$

$$\text{Al–Si material(s)} + [\text{M}_a(\text{AlO}_2)_a(\text{SiO}_2)_b\cdot n\text{MOH}\cdot m\text{H}_2\text{O}]\cdot\text{gel} \quad (2.3)$$

Figure 2.15 Geopolymers schematic with amorphous structure

The particle size, the extent of dissolution of alumina-silicate and the concentration of the alkaline solution will affected the amount of alumina-silicate material needed for schematic 2.1 and 2.2. A finer particle size will give a higher extent of dissolution resulting in a relatively lower concentration of alkali required to dissolve alumina-silicate particles to produce a gel. However, it should be noted that seldom is the solid phase of alumina-silicate particles totally converted to the gel phase. According to Palomo et al. (1992), the undissolved alumina-silicate contained in geopolymer can behave as reinforcement of the matrix (Xu and Van Deventer 2000).

2.3.5 Brown coal fly ash geopolymer concrete

At present brown coal fly ash is not used as a binder in concrete as it tends to show little geopolymer reaction and is more likely to be classified a non- reactive filler (Macphee, Black et al. 1993, CIA 2011). To date little research has been undertaken on the feasibility of using brown coal fly ash as a waste product (Bankowski, Zou et al. 2004, Škvára, Kopecký et al. 2009). Tennakon et al. (2014) studied using unblended 100% brown coal fly ash and blended brown coal fly ash with class F and slag, while Law et al. (2013) studied using 100% of brown coal fly ash (Law, Molyneaux et al. 2013, Tennakoon, Sagoe-Crentsil et al. 2014).

The suitability of brown coal fly ash as a binder will depend on its inherent physical and chemical properties. Research undertaken on class F fly ash suggested the main characteristics of a fly ash to produce optimal binding

properties were: a percentage of unburned material lower than 5%, Fe_2O_3 content not higher than 10%, a low content of CaO, content of reactive silica between 40–50%, percentage of particles with size lower than 45 µm between 80 and 90%, and also high content of vitreous phase (Fernández-Jiménez and Palomo 2003). In contrast, according to van Jaarsveld et al. (2002) and the Concrete Institute of Australia (2011), a high level of calcium within the fly ash could lead to improved compressive strength of geopolymer concrete (van Jaarsveld, van Deventer et al. 2002, CIA 2011). The particle size, amorphous content, morphology and the origin of fly ash are other factors that have been identified as potentially influencing the suitability of fly ash as a binder (Hardjito and Rangan 2005).

2.4. Alkaline activator, modulus and dosage

2.4.1 Type of alkaline activator

The main difference between geopolymer concrete and Portland cement concrete is the binder. The silicon and aluminium oxides in the fly ash react with alkaline liquid (alkaline activator) become soluble reactants to form geopolymer paste that binds the loose aggregates and other unreacted materials. The compressive strength and the workability of geopolymer concrete are influenced by the proportions and properties of the constituent materials that make the geopolymer paste (Rangan 2010).

One factor that influences geopolymerization is related to the metal oxide ratios of the soluble reactants such SiO_2/M_2O, SiO_2/Al_2O_3, M_2O/H_2O and M_2O/Al_2O_3, where M is either sodium or potassium.

Several types of solutions with different chemical and physical properties have been used as activators in geopolymeric synthesis. The chemical and physical properties of each solutions play a role in determining the properties and value of synthesized geopolymer produced (Provis 2009). The most alkaline solution usually used in geopolymerization is a combination of sodium hydroxide (NaOH)

or potassium hydroxide (KOH) and sodium silicate or potassium silicate (Provis 2009, Rangan 2010). Some other activating solutions are carbonates, aluminates and even water, but currently none of these have seen commonly use in the synthesis of aluminosilicate geopolymers (Provis 2009).

Previous geopolymer paste and mortar research using class F fly ash as a binder discovered that activation with sodium hydroxide, sodium silicate, or blended sodium hydroxide and sodium silicate has given good strength more than 40 MPa (Bakharev 2005, Fernández-Jiménez and Palomo 2005, Adam 2009, Wardhono 2015). The combination of sodium hydroxide and sodium silicate was chosen as the alkaline activator for this study.

2.4.2 Activator modulus, dosage of activator and water content

The interaction of several parameters on the compressive strength of fly ash geopolymer concrete is complex. An experimental study on the development and properties of low-calcium fly ash-based geopolymer concrete by Hardjito and Rangan (2005) has shown the following:

- Higher concentration (in terms of molarity) of sodium hydroxide solution results in higher compressive strength of fly ash-based geopolymer concrete.
- Higher the ratio of sodium silicate-to-sodium hydroxide ratio by mass, higher is the compressive strength of fly ash-based geopolymer concrete.
- As the ratio of water-to-geopolymer solids by mass increases, the compressive strength of fly ash-based geopolymer concrete decreases.

The polymerization process requires highly alkaline solution as it involves a substantially fast chemical reaction under alkaline conditions on Si-Al minerals. The geopolymer structures are based on the ratio of Si/Al, consequently the extent of dissolution of Si and the Si to Al ratio are significant factors in geopolymerization. Changing the Al/Si ratio could produce geopolymers with a range of physical and mechanical properties (Barbosa, MacKenzie et al. 2000). Previous research has considered the effect of the ratio of alkaline solutions such

as SiO_2/Na_2O on the polymerization process (Barbosa, MacKenzie et al. 2000, Chindaprasirt, Chareerat et al. 2007, Guo, Shi et al. 2010, Chindaprasirt, Chareerat et al. 2011, Li, Ma et al. 2013).

Duxson et al. (2007) pointed out the importance of the ratio SiO_2/Na_2O as it significantly modifies the degree of polymerization of the dissolved species in an alkali silicate solution, and will influent the structure and properties geopolymer gel synthesized (Duxson, Provis et al. 2007). The concentration will be contingent on the water content which is also very important in the dissolution process of the solid aluminosilicate.

The geopolymerization reaction depends on the chemical properties of the fly ash, the availability of soluble silicates and aluminates, and the concentration of added NaOH (Fansuri, Prasetyoko et al. 2012). Several factors need to be considered to assess the viability of producing geopolymer mortar and concrete from brown coal fly ash: the chemical composition of brown coal fly ash (French and Smitham 2007), the liquid to solid ratio of the mixture (Lloyd and Rangan 2010, Fansuri, Prasetyoko et al. 2012) and the Alkali Modulus of the activator (Li, Ma et al. 2013).

Alkali modulus of the activator or Activator Modulus (AM) and dosage of activator are important parameters in geopolymer mix design. The AM is defined as the mass ratio of SiO_2/Na_2O in alkaline activator while the dosage of activator is the ratio of Na_2O/fly ash.

$$\mathrm{AM} = \frac{\mathrm{SiO_2\ in\ alkaline\ activator\ solution}}{\mathrm{Na_2O\ in\ alkaline\ activator\ solution}} \qquad \text{(Equation 2.1)}$$

$$\mathrm{Dosage\ of\ activator} = \frac{\mathrm{Na_2O\ in\ alkaline\ activator\ solution}}{\mathrm{fly\ ash}} \qquad \text{(Equation 2.2)}$$

The activator modulus AM and dosage activator applied by several researchers of geopolymer mortar and concrete are presented in Table 2.8.

Table 2.8 Activator Modulus and dosage of activator of geopolymer

Research authors	**Activator**	
	Modulus	**Dosage** (%)
Fernández-Jiménez and Palomo (2005)	0.037 – 1.23	5.55 – 14.9
Hardjito and Rangan (2005)	1.31 – 1.36	5.3 – 5.7
Wallah and Rangan (2006)	1.31	5.7
Sumajouw and Rangan (2006)	1.09	6.8
Skavara, Kopecky et al. (2006)	1 – 1.6	6 – 10
Adam (2009)	0.75 – 1.50	7.5 – 15.0

Fansuri et al. (2012) discussed the variation of the water content as the Liquid to Solid ratio (L/S) of the mixture. Water content will provided a medium for the soluble silicates and aluminates to polymerise (Fansuri, Prasetyoko et al. 2012). Water content or the total mass of water is the sum of the mass of water contained in the sodium silicate solution and the sodium hydroxide solution plus the mass of extra water (if present) in the mixture. Despite water playing no role in the chemical reaction, the nano-pores resulting from the water being expelled during the curing and further drying stages will affected the performance of the geopolymer (Rangan 2010).

Water provides a medium for the soluble silicates and aluminates to polymerise during the condensation reaction, which also produces water molecules. However, excessive water will reduce the condensation rate and could also causes segregation in the geopolymer mixture. Rangan (2010) proposed using a water to geopolymer solids (liquid to solid ratio, L/S) to account for the water in the mixture. The liquid is the total mass of water, which is the sum of the mass of water contained in the sodium silicate solution, the mass of water used in the making of the sodium hydroxide solution and the mass of added water if present in the mixture (Rangan 2010). In addition coarse and fine aggregates used for geopolymer mortar and concrete should be in a saturated surface-dry (SSD) condition. This is to ensure the aggregates are neither to be dry to absorb water

from the mixture nor be too wet to add water to the mixture (Lloyd and Rangan 2010).

2.5. Other factors affecting geopolymer concrete performance

The polymerization process in the geopolymer binder/gel has been identified as being due to a number of factors, the alkali modulus of the activator and silicate and alumina ratio, the particle size distribution and surface area, the amorphous content and zeta potential (Hardjito, Wallah et al. 2004, Duxson, Provis et al. 2005, Duxson, Lukey et al. 2006, Fernandez-Jimenez, Palomo et al. 2006, Duxson, Mallicoat et al. 2007, Gunasekara, Law et al. 2015).

The performance of geopolymer concrete in term of compressive strength depends on the polymerization process. The polymerization is influenced by chemical composition and physical properties of the fly ash. Considerable research has been published on the effects of chemical composition and physical properties on compressive strength (Álvarez-Ayuso, Querol et al. 2008, Rickard, Temuujin et al. 2012, Tennakoon, Nazari et al. 2014).

Particle size distribution of the fly ash has also been identified as affecting the reactivity (Fernández-Jiménez and Palomo 2003) but is not considered the main parameter in determining compressive strength (Tennakoon, Nazari et al. 2014). Tennakoon et al. (2014) pointed to characteristic parameters that could effects the evolution of compressive strength of geopolymer pastes i.e SiO_2/Al_2O_3 and Al_2O_3/Na_2O. They revealed that strength evolution mainly depends on the distribution of SiO_2 and Al_2O_3 in the starter fly ash rather than their ratios (Tennakoon, Nazari et al. 2014).

Duxson, et al. (2005) found that the Si/Al ratio affects the microstructure and pore volume distribution of sodium activated geopolymers. The increase of the Si/Al ratio appears to produce an homogeneous product with smaller dispersed pores (Duxson, Provis et al. 2005).

The dissolution process of geopolymerization starts on the surface of a fly ash particle, when its reacts with the alkaline solution (Fernández-Jiménez, Palomo et al. 2004). While the core of a fly ash particle as it is not directly exposed, will depend on dissolution rates of the surface layers (Kukier, Ishak et al. 2003). The elements on the surface are susceptible to leaching in an aqueous environment. The surface layer of fly ash particles contains significant readily leachable elements with the most common anionic groups being silicate ($–O–SiO_2^-$) and aluminate ($–O–AlO^-$) (Iyer 2002, Gunasekara, Law et al. 2015). Gunasekara et. al (2015) reported Ca is the principal element leached from fly ash, and the Ca^{2+} influences the pH of the fly ash-water system influencing the zeta potential of the raw fly ash (Gunasekara, Law et al. 2015). Therefore it can be concluded that the process is not necessary uniform throughout and the gel and can vary locally depending on the distribution of particle size, chemical composition, elemental distribution and pH. Several morphologies may occur in the matrix such as unreacted particles, partially dissolved and fully reacted particles (Fernández-Jiménez, Palomo et al. 2004).

The amorphous content of fly ash has also been identified as critical for the first step of the geopolymerization process as it is easier to dissolve with the major reaction product developed in the alkali activation of fly ash being an amorphous aluminosilicate gel (Fernández-Jimenez, de la Torre et al. 2006).

2.6. Temperature and curing

Previous research reported that elevated temperature or heat curing is an important factor for the activation of fly ash, as its assists the chemical reaction that occurs in the geopolymer paste. Temperature significantly affects the structural transition from the amorphous to the crystalline, while the curing condition will affected the micro and nano structure of geopolymers. Curing temperature, curing time and condition influences the compressive strength of geopolymer concrete (Bakharev 2005, Sindhunata 2006, Chindaprasirt, Chareerat et al. 2007, Criado, Fernández-Jiménez et al. 2010, Lloyd and Rangan 2010).

Temperature and time of elevated curing applied in previous research are presented in Table 2.9 (Swanepoel and Strydom 2002, van Jaarsveld, van Deventer et al. 2002, Bakharev 2005, Chindaprasirt, Chareerat et al. 2007, Kong, Sanjayan et al. 2007, Law, Molyneaux et al. 2013).

Table 2.9 Elevated temperature curing of geopolymer

Research authors	**Elevated curing**	
	Temp. (°C)	**Time** (h)
Swanepoel and Strydom (2002)	40 – 70	6 – 72
van Jaarsveld, van Deventer et al. (2002)	30 – 70	6 – 48
Bakharev (2005)	75 – 90	6 – 24
Chindaprasirt, Chareerat et al. (2007)	30 – 90	24
Kong, Sanjayan et al. (2007)	80	24
Law, Molyneaux et al. (2013)	80 – 120	24

Bakharev (2005) reported that a 24 hours curing at room temperature was beneficial for strength development contrary to Chindaprasirt et al. (2002) who reported that a delay in the time before the sample was placed in the oven had no effect on the strength (Bakharev 2005, Chindaprasirt, Chareerat et al. 2007).

Van Jaarsveld et al. (2002) reported that prolonged curing at elevated temperature will not increase the compressive strength. A longer curing time will produce dehydration and excessive shrinkage as the gel contracts without transforming to a more semi-crystalline form. This structural transition was also observed by other researchers (van Jaarsveld, van Deventer et al. 2002).

Criado al. (2010) concluded that the curing condition plays a key role in the micro and nano structural development of the reaction product. Curing at relative humidity of over 90%, in which the pastes are kept in air-tight containers resulted in dense and compact materials. In contrast, curing at relative humidity

of 40-50% with the paste in direct contact with the atmosphere produces a granular, porous material (Criado, Fernández-Jiménez et al. 2010).

Previous research on brown coal fly ash has identified that curing at elevated temperature of 120 ^{o}C for 24 hours gave the optimum compressive strength (Law, Molyneaux et al. 2013).

2.7. Durability of geopolymer concrete

Good durability is a major factor for success of concrete as a construction material and ensuring the design and service life of a structure is achieved (Papadakis, Vayenas et al. 1991). Durability of concrete is the ability to resist weathering action, chemical attack, abrasion, or any process of deterioration as a result of a variety of physical and chemical processes (ACI.201.2R-08 2008).

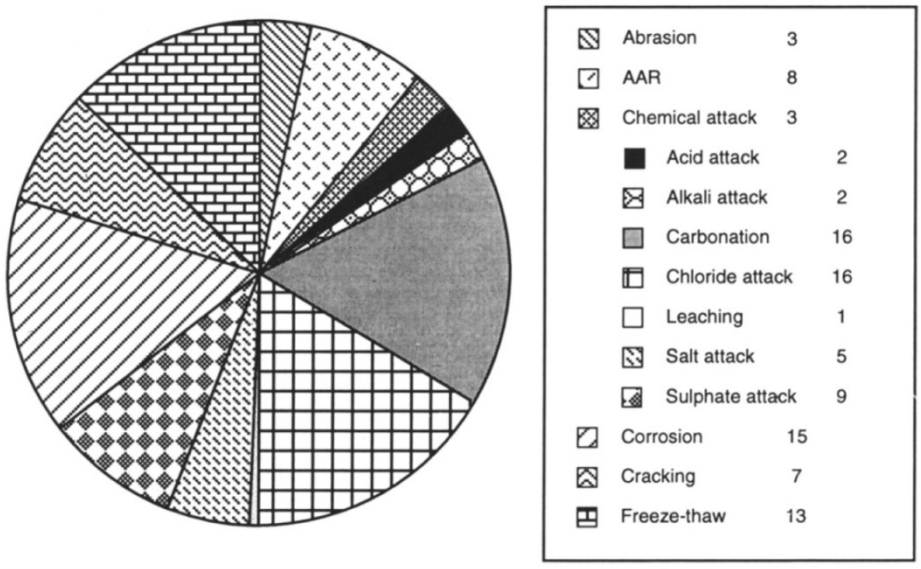

Figure 2.16 Reference to percentages assigned to the contribution of various mechanisms affecting durability (Basheer, Chidiact et al. 1996)

Basheer et al. (1996) reviewed more than 400 published papers, and reported the deterioration mechanisms most studied (Figure 2.16). The review indicates the physical and chemical mechanisms of deterioration for reinforced concrete

finding that carbonation, chloride attack and corrosion were the most common cause of concrete deterioration (Basheer, Chidiact et al. 1996).

Isgor (2001) defines durability of concrete as the resistance of concrete to physical and chemical attack either from external (interaction with the environment) and/or internal agents (interaction among its constituents), and divided the deterioration of reinforced concrete structures into three main types shown on Figure 2.17 (Isgor 2001):

1. Physical deterioration, due to cracking, abrasion, fire and frost.
2. Chemical deterioration, due alkali aggregate reaction, leaching and sulphate and acid attack.
3. Reinforcement corrosion, due chloride attack and carbonation.

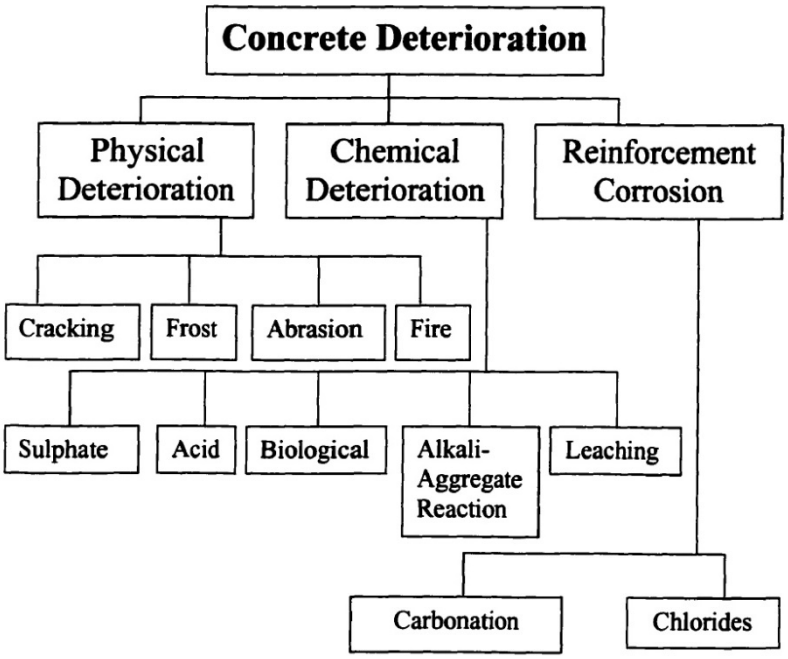

Figure 2.17 Deterioration of reinforced concrete structures (Isgor 2001)

Carbonation and chloride attack are two most processes responsible for the common damage problems related to reinforced concrete structures. Diffusion

of CO_2 from the environment together with chloride ingress mechanism plays an important role in deterioration of concrete.

Durability properties of concrete are influenced and controlled by the number, type, size and distribution of pores present in the paste and the aggregate constituents and the bond between them, permeability is influenced by the pore size distribution and continuity (Basheer, Kropp et al. 2001). Microstructure is of particular importance for durability as a matter it defines all aspects of durability. The distribution of pore sizes control mass transfer which is central to almost all aspects of durability (Lloyd, Provis et al. 2009, Bernal, Bílek et al. 2014).

Despite the underlying mechanisms of degradation of alkali activated binders are not always same as OPC based binders, and cannot always be tested in precisely the same ways (Provis 2013), the series of concrete durability investigation still apply to the geopolymer concrete, as further investigation is required to determine the mechanical properties and durability characteristic of the geopolymer concrete for use in the construction industry.

2.8. Summary of chapter 2

Chapter 2 on literature review could be summarised as follows:

1) The intrinsic chemical composition of brown coal fly ash is the significant factor in order to be able to produce geopolymer concrete.
2) Ratio and modulus of alkali activators, water content and curing are some of most important factors in designing and producing geopolymer concrete mixtures.
3) The silicate and alumina ratio, the particle size distribution and surface area, the amorphous content and zeta potential are some other factors identify influences the polymerization process within the geopolymer binder/gel.
4) Curing temperature, curing time and condition influence the compressive strength of geopolymer concrete.

5) Geopolymer concrete, like all concretes, must meet the mechanical strength and workability requirements of civil construction, and be durable over extended service life.
6) Based on the chemical composition of Victoria brown coal fly ash, it may be possible to make geopolymer concrete from Victoria brown coal fly ash.

References

ACI.201.2R-08 (2008). Guided to Durable Concret : Reported by ACI Commitee 201. Michigan, USA, American Concrete Institute.

ADAA (2007). Coal Combustion Products Handbook, Ash Development Association of Australia, Cooperative Research Centre for Coal in Sustainable Development.

Adam, A. (2009). Strength and durability properties of alkali activated slag and fly ash-based geopolymer concrete. PhD, RMIT University.

Ahmaruzzaman, M. (2010). "A review on the utilization of fly ash." Progress in Energy and Combustion Science 36(3): 327-363.

Aïtcin, P.-C. and S. Mindess (2011). Sustainability of Concrete. Abingdon, Oxon, CRC Press.

Álvarez-Ayuso, E., X. Querol, F. Plana, A. Alastuey, N. Moreno, M. Izquierdo, O. Font, T. Moreno, S. Diez and E. Vázquez (2008). "Environmental, physical and structural characterisation of geopolymer matrixes synthesised from coal (co-) combustion fly ashes." Journal of Hazardous Materials 154(1): 175-183.

AS-3582.1 (1998). Australian Standard 3582.1. Supplementary Cementitious Materials for Use with Portland and Blended Cement. Part 1: Fly ash. Australia, Standards Australia.

ASTM (2012). ASTM C618-12. Standard Specification for Coal Fly Ash and Raw or Calcined Natural Pozzolan for Use in Concrete. West Conshohocken, US., ASTM International.

Bakharev, T. (2005). "Geopolymeric materials prepared using Class F fly ash and elevated temperature curing." Cement and Concrete Research 35(6): 1224-1232.

Bankowski, P., L. Zou and R. Hodges (2004). "Reduction of metal leaching in brown coal fly ash using geopolymers." Journal of Hazardous Materials 114(1–3): 59-67.

Barbosa, V. F. F., K. J. D. MacKenzie and C. Thaumaturgo (2000). "Synthesis and characterisation of materials based on inorganic polymers of alumina and silica:

sodium polysialate polymers." International Journal of Inorganic Materials 2(4): 309-317.

Barnes, I. (2010). "Ash utilisation–impact of recent changes in power generation practices." IEACC Centre (Ed.) 1.

Basheer, L., J. Kropp and D. J. Cleland (2001). "Assessment of the durability of concrete from its permeation properties: a review." Construction and building materials 15(2): 93-103.

Basheer, P., S. Chidiact and A. Long (1996). "Predictive models for deterioration of concrete structures." Construction and Building Materials 10(1): 27-37.

Bernal, S. A., V. Bílek, M. Criado, A. Fernández-Jiménez, E. Kavalerova, P. V. Krivenko, M. Palacios, A. Palomo, J. L. Provis and F. Puertas (2014). Durability and testing–degradation via mass transport. Alkali Activated Materials, Springer: 223-276.

Berry, M., D. Cross and J. Stephens (2009). Changing the environment: an alternative “Green” concrete produced without Portland cement. Proc., World of Coal Ash Conf., Lexington, KY, USA.

Blissett, R. and N. Rowson (2012). "A review of the multi-component utilisation of coal fly ash." Fuel 97: 1-23.

Britt, A. F., D. Summerfield, A. Whitaker, P. Kay, D. C. Champion, D. Huston, A. B. Senior, M. Sexton, D. Roberts, S. J. Wright and A. Schofield (2015). Australia's Identified Mineral Resources 2015, Geoscience Australia, Canberra.

Chindaprasirt, P., T. Chareerat, S. Hatanaka and T. Cao (2011). "High-Strength Geopolymer Using Fine High-Calcium Fly Ash." Journal of Materials in Civil Engineering 23(3): 264-270.

Chindaprasirt, P., T. Chareerat and V. Sirivivatnanon (2007). "Workability and Strength of coarse high calcium fly ash geopolymer." Cement and Concrete Composites 29(3): 224-229.

CIA (2011). Recommended Practice Geopolymer Concrete. Sydney, Concrete Institute of Australia.

Criado, M., A. Fernández-Jiménez and A. Palomo (2010). "Alkali activation of fly ash. Part III: Effect of curing conditions on reaction and its graphical description." Fuel 89(11): 3185-3192.

Davidovits, J. (1993). From Ancient, CONCRETE TO GEOPOLYMERS. Arts et Metiers Mag. France, Geopolymer Institute. 180: 8.

Davidovits, J. (1994b). "Global Warming Impact on the Cement and Aggregates Industries." World Resource Review 6(2): 263-278.

Davidovits, J. (1994c). "High-alkali cements for 21st century concretes." Special Publication 144: 383-398.

Davidovits, J. (1994d). Properties of geopolymer cements. First international conference on alkaline cements and concretes.

Davidovits, J. (2005). Geopolymer chemistry and sustainable Development. The Poly(sialate) terminology: a very useful and simple model for the promotion and understanding of green-chemistry. Geopolymers, Green Chemistry and Sustainable Development Solutions. J. Davidovits. Saint-Quentin, France, Institut Géopolymère: 9-15.

Diaz, E., E. Allouche and S. Eklund (2010). "Factors affecting the suitability of fly ash as source material for geopolymers." Fuel 89(5): 992-996.

Duxson, P., G. C. Lukey and J. S. van Deventer (2006). "Evolution of gel structure during thermal processing of Na-geopolymer gels." Langmuir 22(21): 8750-8757.

Duxson, P., G. C. Lukey and J. S. J. van Deventer (2007). "The thermal evolution of metakaolin geopolymers: Part 2 – Phase stability and structural development." Journal of Non-Crystalline Solids 353(22–23): 2186-2200.

Duxson, P., S. Mallicoat, G. Lukey, W. Kriven and J. Van Deventer (2007). "The effect of alkali and Si/Al ratio on the development of mechanical properties of metakaolin-based geopolymers." Colloids and Surfaces A: Physicochemical and Engineering Aspects 292(1): 8-20.

Duxson, P., A. Provis, J. L. Lukey, G. C. Van Deventer, A. Fernández-Jiménez and J. S. J. Palomo (2007). "Geopolymer technology: The current state of the art." Journal of Materials Science 42(9): 16.

Duxson, P., J. L. Provis, G. C. Lukey, S. W. Mallicoat, W. M. Kriven and J. S. Van Deventer (2005). "Understanding the relationship between geopolymer composition, microstructure and mechanical properties." Colloids and Surfaces A: Physicochemical and Engineering Aspects 269(1): 47-58.

ESAA. (2015). "Energy Supply Association of Australia." Retrieved April, 2015, from https://esaa.com.au/policy/data_and_statistics-_energy_in_australia.

Faimon, J. (1996). "Oscillatory silicon and aluminum aqueous concentrations during experimental aluminosilicate weathering." Geochimica et cosmochimica acta 60(15): 2901-2907.

Fansuri, H., D. Prasetyoko, Z. Zhang and D. Zhang (2012). "The effect of sodium silicate and sodium hydroxide on the strength of aggregates made from coal fly ash using the geopolymerisation method." Asia-Pacific Journal of Chemical Engineering 7(1): 73-79.

Fernández-Jimenez, A., A. G. de la Torre, A. Palomo, G. López-Olmo, M. M. Alonso and M. A. G. Aranda (2006). "Quantitative determination of phases in the alkali activation of fly ash. Part I. Potential ash reactivity." Fuel 85(5–6): 625-634.

Fernández-Jiménez, A. and A. Palomo (2003). "Characterisation of fly ashes. Potential reactivity as alkaline cements." Fuel 82(18): 2259-2265.

Fernández-Jiménez, A. and A. Palomo (2005). "Composition and microstructure of alkali activated fly ash binder: Effect of the activator." Cement and Concrete Research 35(10): 1984-1992.

Fernández-Jiménez, A., A. Palomo and M. Criado (2004). "Microstructure development of alkali-activated fly ash cement: a descriptive model." Cement and Concrete Research 35(6): 1204-1209.

Fernandez-Jimenez, A. M., A. Palomo and C. Lopez-Hombrados (2006). "Engineering properties of alkali-activated fly ash concrete." ACI Materials Journal 103(2): 106-112.

French, D. and J. Smitham (2007). Fly Ash Characteristics and Feed Coal Properties. Pullenvale, Qld 4069, Australia, Cooperative Research Centre for Coal in Sustainable Development.

Geoscience Australia and ABARE (2014). Australian Energy Resource Assessment. Canberra, Commonwealth of Australia (Geoscience Australia).

Gunasekara, C., D. W. Law, S. Setunge and J. G. Sanjayan (2015). "Zeta potential, gel formation and compressive strength of low calcium fly ash geopolymers." Construction and Building Materials 95: 592-599.

Guo, X., H. Shi and W. A. Dick (2010). "Compressive strength and microstructural characteristics of class C fly ash geopolymer." Cement and Concrete Composites 32(2): 142-147.

Hardjito, D. and B. V. Rangan (2005). Development and Properties of Low-Calcium Fly Ash-Based Geopolymer Concrete, Research Report GC 1. Perth, Australia, Curtin University of Technology.

Hardjito, D., S. E. Wallah, D. M. Sumajouw and B. V. Rangan (2004). "On the development of fly ash-based geopolymer concrete." ACI Materials Journal-American Concrete Institute 101(6): 467-472.

Heidrich, C. (2003). Ash Utilisation-an Australian Persepctive. 2003 International Ash Utilization Symposium. University of Kentucky, Center for Applied Energy Research

Heidrich, C., H.-J. Feuerborn and A. Weir (2013). Coal combustion products: a global perspective. World coal ash WOCA conference, Lexington, KY.

IEA (2012). Coal Information 2012 with 2011 data, International Energy Agency.

Isgor, B. O. (2001). Durability model for chloride and carbonation induced steel corrosion in reinforced concrete members. PhD, Carleton University.

Iyer, R. (2002). "The surface chemistry of leaching coal fly ash." Journal of Hazardous Materials 93(3): 321-329.

Keyte, L. M. (2009). 2. Fly Ash Glass Chemistry and Inorganic Polymer Cements. Geopolymers-Structure, Processing, Properties and Industrial Applications. J. L. Provis and J. S. J. van Deventer, Woodhead Publishing.

Kong, D. L., J. G. Sanjayan and K. Sagoe-Crentsil (2007). "Comparative performance of geopolymers made with metakaolin and fly ash after exposure to elevated temperatures." Cement and Concrete Research 37(12): 1583-1589.

Kukier, U., C. F. Ishak, M. E. Sumner and W. P. Miller (2003). "Composition and element solubility of magnetic and non-magnetic fly ash fractions." Environmental Pollution 123(2): 255-266.

Law, D. W., T. K. Molyneaux, A. Wardhono, R. Dirgantara and D. Kong (2013). The Use Brown Coal Fly Ash To Make Geopolymer Concrete. ACCTA 2013, Johannesburg.

Li, X., X. Ma, S. Zhang and E. Zheng (2013). "Mechanical Properties and Microstructure of Class C Fly Ash-Based Geopolymer Paste and Mortar." Materials 6(4): 1485-1495.

Lloyd, N. A. and B. V. Rangan (2010). Geopolymer Concrete with Fly Ash. Second International Conference on Sustainable Construction Materials and Technologies. Universita Politecnica delle Marche, Ancona, Italy.

Lloyd, R. R., J. L. Provis and J. S. van Deventer (2009). "Microscopy and microanalysis of inorganic polymer cements. 1: remnant fly ash particles." Journal of materials science 44(2): 608-619.

Macphee, D. E., C. J. Black and A. H. Taylor (1993). "Cements Incorporating Brown Coal Fly Ash from The Latrobe Valley Region of Victoria, Australia." Cement and Concrete Research 23(3): 507-517.

Malhotra, V. (2004). Role of supplementary cementing materials and superplasticizers in reducing greenhouse gas emissions. Proceedings of ICFRC International Conference on Fiber Composites, High-Performance Concrete, and Smart Materials, Chennai, India.

Malhotra, V. (2005). Global warming, and role of supplementary cementing materials and superplasticisers in reducing greenhouse gas emissions from the manufacturing of portland cement. The 1st Panhellenic Conference on the Utilization of industrial by-products in Construction, Thessaloniki, Greece, EVIPAR.

Malhotra, V. (2008). "Role of fly ash in reducing greenhouse gas emissions during the manufacturing of portland cement clinker." Advances in Concrete Technologies in the Middle East: 19-20.

Meyer, C. (2009). "The greening of the concrete industry." Cement and Concrete Composites 31(8): 601-605.

Naik, T. R. (2008). "Sustainability of concrete construction." Practice Periodical on Structural Design and Construction 13(2): 98-103.

Pacheco-Torgal, F., J. Castro-Gomes and S. Jalali (2008). "Alkali-activated binders: A review: Part 1. Historical background, terminology, reaction mechanisms and hydration products." Construction and Building Materials 22(7): 1305-1314.

Papadakis, V. and S. Tsimas (2002). "Supplementary cementing materials in concrete: Part I: efficiency and design." Cement and Concrete Research 32(10): 1525-1532.

Papadakis, V. G., C. G. Vayenas and M. N. Fardis (1991). "Physical and Chemical Characteristics Affecting the Durability of Concrete." ACI Materials Journal 8(2): 11.

Provis, J. L. (2006). Modelling the formation of geopolymers. PhD, University of Melbourne.

Provis, J. L. (2009). 4. Activating Solution Chemistry for Geopolymers. Geopolymers-Structure, Processing, Properties and Industrial Applications. J. L. Provis and J. S. J. van Deventer, Woodhead Publishing.

Provis, J. L. (2013). "Geopolymers and other alkali activated materials: why, how, and what?" Materials and Structures 47(1-2): 15.

Provis, J. L. and C. A. Rees (2009). 7. Geopolymer Synthesis Kinetics. Geopolymers-Structure, Processing, Properties and Industrial Applications. J. L. Provis and J. S. J. van Deventer, Woodhead Publishing.

Radford, D., A. Grabher and J. Bridge (2009). "Inorganic Polymer Matrix Composite Strength Related to Interface Condition." Materials 2(4): 2216-2227.

Rangan, B. V. (2010). Fly Ash-Based Geopolymer Concrete. The International Workshop on Geopolymer Cement and Concrete, Mumbai, India.

Rickard, W. D., J. Temuujin and A. van Riessen (2012). "Thermal analysis of geopolymer pastes synthesised from five fly ashes of variable composition." Journal of non-crystalline solids 358(15): 1830-1839.

Siddique, R. (2008). Coal Fly Ash. Waste Materials and By-Products in Concrete, Springer Berlin Heidelberg: 177-234.

Sindhunata (2006). A Conceptual Model of Geopolymerisation. PhD, The University of Melbourne.

Skavara, F., L. Kopecky, J. Nemecek and Z. Bittnar (2006). "Microstructure of Geopolymer Materials Based on Fly Ash." Ceramics − Silikáty 50(4): 7.

Škvára, F., L. Kopecký, V. Šmilauer and Z. Bittnar (2009). "Material and structural characterization of alkali activated low-calcium brown coal fly ash." Journal of Hazardous Materials 168(2–3): 711-720.

Sumajouw, M. D. J. and B. V. Rangan (2006). Low-Calcium fly ash-based geopolymer concrete: Reinforced beams and columns, Research Report GC 3. Perth, Australia, Curtin University of Technology.

Swanepoel, J. C. and C. A. Strydom (2002). "Utilisation of fly ash in a geopolymeric material." Applied Geochemistry 17(8): 1143-1148.

Tennakoon, C., A. Nazari, J. G. Sanjayan and K. Sagoe-Crentsil (2014). "Distribution of oxides in fly ash controls strength evolution of geopolymers." Construction and Building Materials 71(0): 72-82.

Tennakoon, C., K. Sagoe-Crentsil, J. G. Sanjayan and A. Shayan (2014). Early Age Properties of Alkali Activated Brown Coal Fly Ash Binders. Advanced Materials Research, Trans Tech Publ.

Thomas, M. (2013). Supplementary cementing materials in concrete, CRC Press.

Van Jaarsveld, J. G. S., J. S. J. Van Deventer and L. Lorenzen (1997). "The potential use of geopolymeric materials to immobilise toxic metals: Part I. Theory and applications." Minerals Engineering 10(7): 659-669.

van Jaarsveld, J. G. S., J. S. J. van Deventer and G. C. Lukey (2002). "The effect of composition and temperature on the properties of fly ash- and kaolinite-based geopolymers." Chemical Engineering Journal 89(1–3): 63-73.

Wallah, S. E. and B. V. Rangan (2006). Low-Calcium fly ash-based geopolymer concrete: Long-term properties, Research Report GC 2. Perth, Curtin University of Technology.

Wardhono, A. (2015). The Durability of Fly Ash Geopolymer and Alkali-Activated Slag Concretes. PhD, RMIT University.

WCA. (2015). "World Coal Asscociation." Coal Matters Retrieved April, 2015, from http://www.worldcoal.org/.

Xu, H. and J. S. J. Van Deventer (2000). "The geopolymerisation of alumino-silicate minerals." International Journal of Mineral Processing 59(3): 247-266.

CHAPTER 3

METHODOLOGY

3.1. Overview

This chapter presents details of the experimental methods employed in the development and testing of alkali activated brown coal fly ash geopolymer mortar and concrete. The properties and specification of the materials used to produce the brown coal fly ash geopolymer mortar and concrete are described. The geopolymer mortar and concrete test program and parameters are also explained.

3.2. Materials

3.2.1 Brown Coal Fly Ash, La Trobe Valley-Victoria

The fly ash used in this study came from La Trobe Valley, Victoria, Australia. The La Trobe Valley contains large deposits of low-rank Lignite coal also known as Brown Coal. The brown coal fly ash was supplied from 3 major Power Stations in Victoria: Loy Yang (AGL), Yallourn (Energy Australia) and Hazelwood (GDF-SUEZ Australian Energy).

ASTM (ASTM 2012) defines fly ash into 2 classes, class F and class C. Class F is produced from burning anthracite and bituminous coals, while class C is produced from lignite and sub-bituminous coals (Figure 3.1). Both have pozzolanic properties, and in addition to this, class C also has some cementitious properties and the total calcium (CaO) content is typically higher than class F. ASTM C618-12 also differentiates the fly ash based on the minimum percentage of silicon dioxide (SiO_2), aluminium oxide (Al_2O_3) and iron oxide (Fe_2O_3), and the maximum sulphur trioxide (SO_3) content. The minimum combined content of silicon dioxide, aluminium oxide and iron oxide is 70% and 50% for class F and

class C respectively. The maximum sulphur trioxide (SO_3) content is 5.0% for both classes of fly ash.

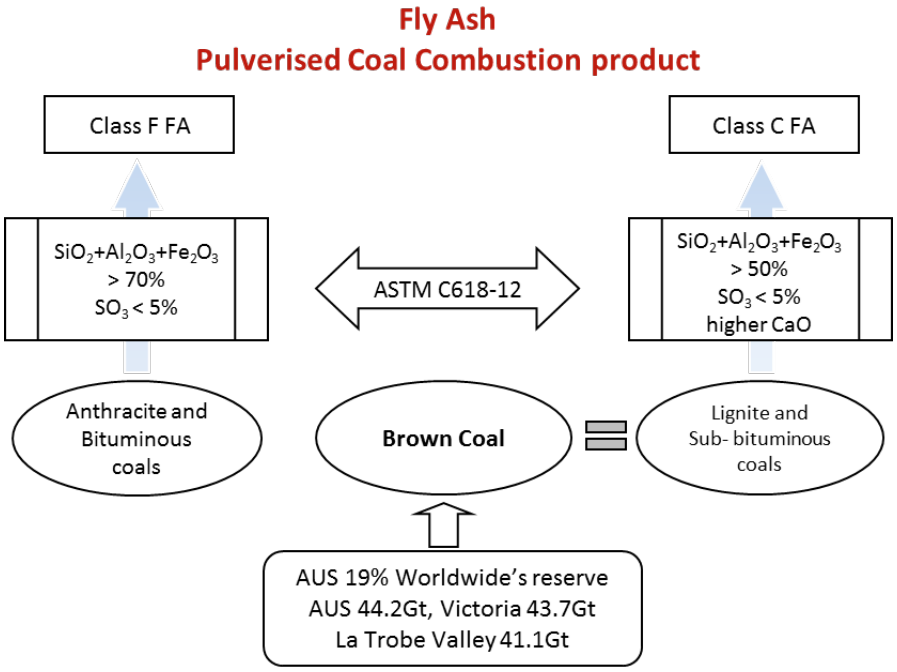

Figure 3.1 Classification of fly ash (ASTM 2012)

The brown coal fly ash supplied was obtained directly from the precipitator with no pre-treatment prior to casting. Considerable variation in colour and texture were noted from current La Trobe Valley brown coal fly ash materials supplied (Figure 3.2).

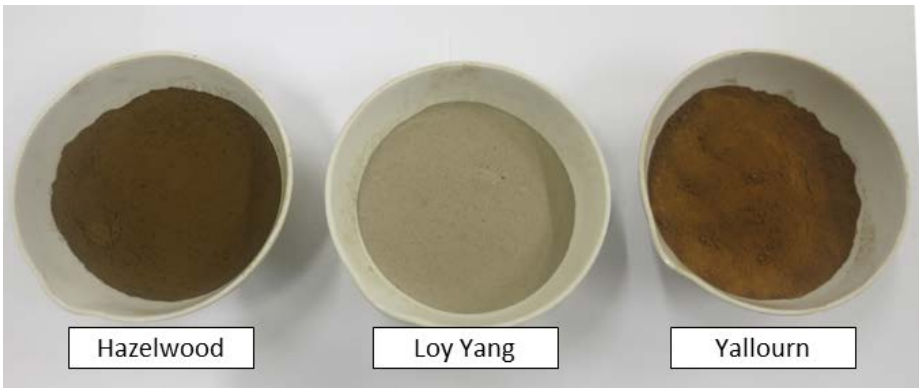

Figure 3.2 La Trobe Valley brown coal fly ash: Hazelwood, Loy Yang and Yallourn

Table 3.1 shows chemical composition of La Trobe Valley brown coal fly ash previously reported and the current materials supplied. The SiO_2, Al_2O_3 and Fe_2O_3 contents varied significantly between Yallourn, Hazelwood, and Loy Yang. The CaO content of Yallourn and Hazelwood brown coal fly ash (as usually found with class C fly ash) are significantly higher than Loy Yang brown coal fly ash, while the SiO_2, Al_2O_3 and Fe_2O_3 are significantly lower than Loy Yang.

Table 3.1 Chemical composition of brown coal fly ash materials

Oxide %	**Brown Coal Fly Ash**			**La Trobe Valley Class C Fly Ash[1]**		
	Loy Yang	**Yallourn**	**Hazelwood**	**Loy Yang**	**Yallourn**	**Hazelwood**
SiO_2	47.52	6.48	2.94	60.4	1.4	6.6
Al_2O_3	17.29	2.24	2.20	13.3	2.1	1.8
Fe_2O_3	5.98	16.74	18.20	8.5	24.5	8.7
CaO	2.25	29.91	31.40	1.0	12.3	28.4
MgO	4.63	15.58	15.85	2.2	18.0	18.8
K_2O	0.50	0.48	0.36	1.2	0.4	0.4
Na_2O	6.26	4.27	3.88	2.1	11.0	4.5
TiO_2	1.26	0.33	0.22	1.7	0.1	0.2
P_2O_5	0.74	1.47	1.16			
SO_3	13.03	19.57	20.59	3.4	21.7	15.6
Cl				<0.1	<0.1	3.4
Cl_2O	0.44	2.37	2.63			
Mn_2O	0.10	0.55	0.57			
LOI				7.6	8.2	11.7

[1]Macphee, Black et al. (1993)

A significant variation in the chemical composition was also observed from previously reported data despite the same source and type of burning coal (French and Smitham 2007). Based on the type of coal used and previously

published data the La Trobe Valley fly ash was classified as class C fly ash (Macphee, Black et al. 1993). However analysis of the chemical composition of the material supplied for this study could not be categorized into either of those two classes of ASTM C618-12. This is due to the high SO_3 content in all samples and the percentage of SiO_2, Al_2O_3 and Fe_2O_3 in the Yallourn and Hazelwood samples (Table 3.2). As such, the term Brown Coal Fly Ash is used instead of class C fly ash for all materials.

Table 3.2 La Trobe Valley brown coal fly ash as per ASTM C618-12

Fly Ash Component	**$SiO_2 + Al_2O_3 + Fe_2O_3$ (%)**	**SO_3 (%)**	**CaO (%)**
ASTM C618-12 Class F	≥ 70	≤ 5	-
ASTM C618-12 Class C	≥ 50	≤ 5	-
Loy Yang	70.79	13.03	2.25
Yallourn	25.46	19.57	29.91
Hazelwood	23.34	20.59	31.40

Figure 3.3 shows the element mapping image of La Trobe Valley brown coal fly ash taken using Scanning Electron Microscopy (SEM). The mapping image simply displays the six oxidation elements of raw brown coal fly ash i.e SiO_2, Al_2O, Fe_2O_3, Na_2O, CaO and SO_3. The Loy Yang brown coal fly ash is dominated by SiO_2 and Al_2O, while Hazelwood and Yallourn are dominated by CaO, SO_3 and Fe_2O_3.

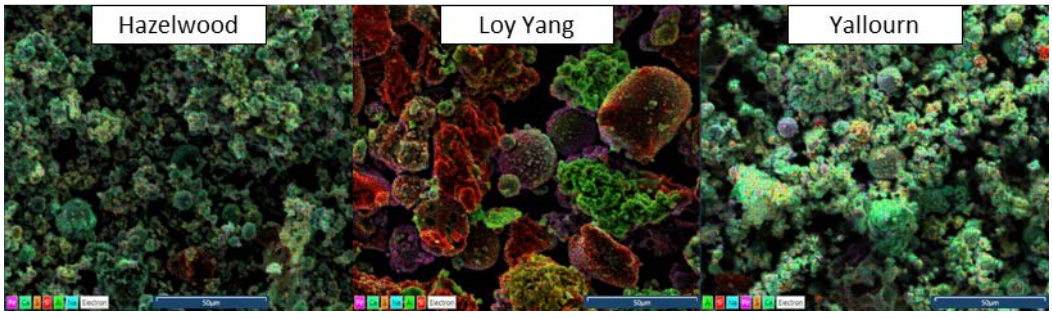

Figure 3.3 Element mapping image of La Trobe Valley brown coal fly ash: Hazelwood, Loy Yang, and Yallourn

3.2.2 Alkaline activators

The alkaline activator used in this study was a combination of sodium silicate (Na_2SiO_3) and sodium hydroxide (NaOH) solution. A grade D sodium silicate (Na_2SiO_3) combined with a high alkaline solution of 15 M sodium hydroxide (NaOH) solution were used as the alkali activator. The properties of a grade D sodium silicate (Na_2SiO_3) solution used, a 2.00 ratio of 1.52 g/cc density with composition of 14.7% Na_2O, 29.4% SiO_2 and 55.90% water are shown in Table 3.3.

Table 3.3 Chemical and physical properties of liquid sodium silicate (Na2SiO3)

Product Name	**Grade D, PQ Australia Pty. Ltd.**
Na_2O%.wt	14.5 – 14.9
SiO_2%.wt	29.1 – 29.7
Solids%.wt	43.6 – 44.6
Ratio (SiO_2 % / Na_2O %)	1.95 – 2.05
Density, g/cc @ 20°C	1.50 – 1.53
Viscosity, cps @ 20°C	250 – 450

3.2.3 Fine aggregate

The fine aggregate (sand) used for the development of brown coal fly ash geopolymer mortar and concrete was obtained from Langwarin source, Victoria, Australia, with a fineness modulus of 2.03 conforming to the Australian Standard AS 1141.5, 2000. Typical grading of the fine aggregate is shown in Table 3.4 (Wardhono 2015).

Table 3.4 Typical grading of the fine aggregate (sand)

Test sieve size	Retained (%)	Cumulative passing (%)	Specification passing (%)
4.75 mm	0.4	99.6	90 – 100
2.36 mm	4.6	95.0	85 – 97
1.18 mm	7.9	87.1	70 – 95
600 µm	13.2	74.0	45 – 80
300 µm	36.4	37.6	25 – 47
150 µm	34.4	3.2	0 – 15
75 µm	2.9	0.3	0 – 5
PAN	0.3	0.0	0

3.2.4 Combined aggregates

According to previous research, coarse and fine aggregates used by the concrete industry are suitable to use for geopolymer concrete and mortar. Thus, aggregate grading curves currently used in concrete practice are applicable in the case of geopolymer concrete (Hardjito and Rangan 2005, Sumajouw and Rangan 2006, Wallah and Rangan 2006, Siddique 2008).

The combined aggregates used for the development of brown coal fly ash geopolymer concrete were a combination of fine aggregate, 7 mm and 10 mm coarse aggregates. The fine aggregate was from Langwarin source, the coarse aggregates were from the Mawson Lake Cooper quarry, Victoria, Australia. The moisture condition of the fine and coarse aggregates were oven dried condition (at 105°C for 24hours). Typical grading of the aggregate and combination of aggregates are shown in Table 3.5. The combined aggregate is combination of 43% of sand (fine aggregate), 38% of 10 mm and 19% of 7 mm coarse aggregates. Those percentages of combined aggregates were adopted from previous research at RMIT University with the same source of the aggregates (Adam

2009). The fine aggregate was uncrushed sand and the coarse aggregates were crushed basalt aggregate.

Table 3.5 Grading of aggregate and the combined aggregate

Test sieve size	Aggregate			Combination
	Fine	7 mm	10 mm	
19.00 mm	100.0	100.0	100.0	100.0
9.50 mm	100.0	100.0	100.0	100.0
6.70 mm	100.0	96.0	100.0	99.24
4.75 mm	99.6	36.0	21.0	57.65
2.36 mm	95.0	3.0	2.0	42.18
1.18 mm	87.1	0.0	1.0	37.83
600 µm	74.0	1.0	0.0	32.01
300 µm	37.6	0.0	0.0	16.17
150 µm	3.2	0.0	0.0	1.38
75 µm	0.3	0.0	0.0	0.13
PAN	0.0	0.0	0.0	0.00

3.3. Mix design

The key mix design parameters as in Recommended Practice Geopolymer Concrete published by Concrete Institute of Australia (2011) to optimize the paste and aggregate skeleton are:

a) Fluids to Binder ratio by mass. ("Fluids" = total water + sodium/potasium silicate + sodium/potassium hydroxide). Increasing this parameter increases workability (and material costs). As such it should be set as low as possible whilst still achieving the required paste rheology (and concrete workability). To produce very high strength concretes, very low water contents (highly concentrated alkaline solutions) must be used.

b) Si:Al ratio. The ratio of silicon to aluminium ions in the hardened matrix (i.e in the solution after dissolution has occurred) controls the physical properties of the geopolymer network. For low calcium systems the preferred ratio is about 2:1.

c) SiO_2:Na_2O ratio. The concentration of required Si ions in the activator varies with the reactivity of the binder feedstock but typically a SiO_2: Na_2O ratio in the range 0.5 to 1.5 will contain the optimum, based on trial concrete strength testing.

d) H_2O:Na_2O ratio by mass. The alkali concentration determines the rate and degree of dissolution. Very high concentrations (low H_2O:Na_2O) produce stronger geopolymer matrices and very low concentrations produce zeolites instead of geopolymers.

3.4. Mix design proportions

The proportion of mixtures was calculated using the absolute volume method (Neville 2011) based on previous research (Adam 2009), which assumed that the volume of compacted mortar is equal to the sum of the absolute volumes of all ingredients. The initial mix design of brown coal fly ash geopolymer mortar was replicated from previous research at RMIT University, Melbourne, Australia using the same source of Loy Yang brown coal fly ash (Law, Molyneaux et al. 2013). The composition of the initial mix design in proportion to 1 kg unit of brown coal fly ash binder is given in Table 3.6. The content of the brown coal fly ash in the mixture was also evaluated as the mass ratio of the fly ash to the total weight of the mix (wt% FA).

Table 3.6 Composition of initial replicated mix design (kg)

Mixture	Fly Ash	Sand	Na_2SiO_3	NaOH	Fly Ash content (%wt)
Loy Yang 1	1	2.782	0.571	0.170	22.11

The liquid mass (water content) was determined taking into account all of the water in the mixed alkali activators (including water quantity of Na_2SiO_3 and NaOH solutions). The solid mass was determined by accounting for all solid materials of the binder and aggregate including the solid content of the Na_2SiO_3 and NaOH solutions (Lloyd and Rangan 2010). Hence, the solid is the sum of the fly ash, the mass of sodium hydroxide solids used to make the sodium hydroxide solution, and the mass of solids in the sodium silicate solution (i.e the mass of Na_2O and SiO_2).

The NaOH used is a ready-made 15 M NaOH solution. However, the exact mass of NaOH solids in a solution was not provided. Therefore the mass of NaOH solids was obtained from interpolation of measured mass of NaOH solids adopted by Hardjito (2005). Consequently the mass of NaOH solids of the 15 M NaOH solution is 424.41 grams per kg of 15 M NaOH solution. This will contribute 42.44% NaOH to the mass of solid in the mixture, subsequently a 15 M NaOH solution will contribute 57.56% H_2O (water) to the mass of liquid (Hardjito and Rangan 2005).

The activator modulus and dosage of activator of the initial mix design are given in Table 3.7 (see Equation 2.1 and 2.2 in Chapter 2 Section 2.4.2).

Table 3.7 Initial mix design activator modulus and dosage of activator

Mixture	**Activator**	
	Modulus (AM)	**Dosage** (%)
Loy Yang 1	1.202	14

The activator modulus influences the polymerization process by having a significant influence on the dissolution process of the solid aluminosilicate. The alkaline solution of the mixture will change due to the dissolution of the precursor FA (i.e the dissolution of the solid aluminosilicate will contribute to the Alkali Modulus).

To account for the impact of the composition of the FA a modified activator modulus (AM_m), is calculated to include the silicon dioxide and sodium oxide content from the fly ash.

$$\mathrm{AM_m} = \frac{\mathrm{SiO_2}}{\mathrm{Na_2O}} \qquad \text{(Equation 3.1)}$$

The modified activator modulus and dosage, calculated to include the content from the fly ash based on the initial mix design (Table 3.6) is shown in Table 3.8.

Table 3.8 Initial mix design activator modulus and dosage of activator take into account the Loy Yang brown coal fly ash content

Mixture	**Activator**	
	Modulus (AM_m)	**Dosage (%)**
Loy Yang 1	3.178	21.6

The impact of the chemical composition of the FA on the silicate to aluminate (SiO_2/Al_2O_3), aluminosilicate to sodium ($SiO_2+Al_2O_3/Na_2O$), sodium to silicate (Na_2O/SiO_2), dosage of activator (Na_2O/fly ash binder) and the liquid to solid ratio (L/S) of the binder paste are shown in Table 3.9.

Table 3.9 Ratio and modulus of the initial mix design Loy Yang brown coal fly ash geopolymer mortar

Ratio and Modulus	**Loy Yang 1**
Silicate to aluminate (SiO_2/Al_2O_3)	3.720
Aluminosilicate to sodium ($SiO_2+Al_2O_3/Na_2O$)	4.033
Sodium to silicate (Na_2O/SiO_2) or ($1/AM_m$)	0.315
Dosage of activator (Na_2O/fly ash binder)	0.216
Liquid to Solid ratio (L/S) of the binder paste	0.315

Trial mixing was carried out based on previous work using the same source of Loy Yang brown coal fly ash (Law, Molyneaux et al. 2013). Based on the previous work, mix variations were designed to consider the chemical composition of Loy Yang brown coal fly ash, the liquid to solid ratio of the mixture, the alkali modulus of the activator (SiO_2/Na_2O), and the weight percentage of brown coal fly ash (Fly Ash wt%).

Mixes designs for Yallourn and Hazelwood brown coal fly ash were subsequently based on optimum mix design determined for the Loy Yang brown coal fly ash, taking into consideration the specific chemical composition of these materials. The mix proportions for Yallourn and Hazelwood brown coal fly ash considered the SiO_2 content, which was significantly lower than the Loy Yang brown coal fly ash and instead of using the ratio of SiO_2/Na_2O, these mixes were designed using the ratio of the sum of silica (SiO_2) and alumina (Al_2O_3) to Na_2O.

Loy Yang brown coal fly ash geopolymer concrete mix design was derived from the optimum mix design of Loy Yang brown coal fly ash geopolymer mortar. The fine aggregate (sand) proportion of the optimum mortar mix was substituted by a combination of aggregates: 43% of fine aggregate, 38% of 10 mm and 19% of 7 mm coarse aggregates. The percentages of the combined aggregates were adopted from previous research at RMIT University (Adam 2009). The fine aggregate was uncrushed sand and the coarse aggregates were crushed basalt aggregate, the aggregates were in oven dried condition.

The mix design of OPC concrete as a control was adopted from previous research at RMIT University with the same source of aggregate and combination (Adam 2009). The mix design composition of OPC concrete as control is given in Table 3.10. The fine aggregate was uncrushed sand and the coarse aggregates were crushed basalt aggregate, the aggregates were in saturated surface condition.

Table 3.10 Mix design composition of OPC concrete as control (kg/m^3)

Mixture	OPC	Aggregates			Water
		Sand	7 mm	10 mm	
OPC Control	427.8	783.7	346.3	692.5	222.5

3.5. Mixing, curing and testing

3.5.1 Mixing of geopolymer mortar

The mixing for all brown coal fly ash geopolymer mortar specimens was undertaken using a 5-litre Hobart mixer (Figure 3.4).

The mixing procedure for the brown coal fly ash geopolymer mortar was:

1. The binder (brown coal fly ash) and fine aggregate were mix for 1-2 minute by hand, until a uniform mix was obtained.
2. The alkaline activator (sodium silicate and sodium hydroxide), about a quarter of the volume, was added to the mixture.
3. The mixer was run at slow speed (140±5 r/m) for 2 minutes, then the remaining of the alkali activator was added to the mixture and the mixer was run for a further 2 minutes.
4. The mixer speed was then increased to medium (285±10 r/m) for 2 minutes, then run at slow speed for another 4 minutes.
5. The mix was then poured into 50 mm cube moulds, compacted with two-layer placing and tamping, and vibrated for 1 minute on a vibrating table.

Brown coal fly ash geopolymer mortar specimens were produced for compressive strength test and microstructural analysis.

Figure 3.4 Brown coal fly ash geopolymer mortar: fly ash, sodium hydroxide and sodium silicate; mixing; and moulding.

3.5.2 Mixing of geopolymer concrete

The mixing for Loy Yang brown coal fly ash geopolymer concrete specimens was undertaken using a 60 litre mixer (Figure 3.5).

The mixing procedure for the brown coal fly ash geopolymer concrete was:

1. The binder (brown coal fly ash), fine aggregate and coarse aggregate were mix for 2 minute by mixer.
2. The alkaline activator (sodium silicate and sodium hydroxide), about a quarter of the volume, was added to the mixture.
3. The mixer was run for 2 minutes, then the remaining of the alkali activator was added to the mixture and the mixer was run for 4 minutes.
4. The mix was then poured into moulds as presented in Table 3.11 and vibrated for 1 minute on vibrating table.

Table 3.11 Type of moulds for testing specimen of Loy Yang brown coal fly ash geopolymer concrete.

No	Moulds	Size	Test
1	Cube	100 mm x 100 mm x 100 mm	Compressive strength, Carbonation, Chloride diffusion, Monitoring of elevated temperature curing.
2	Block	300 mm x 300 mm x 100 mm	Water permeability, NDT
3	Cube	200 mm x 200 mm x 200 mm	Monitoring of elevated temperature curing
4	Cube	300 mm x 300 mm x 300 mm	Monitoring of elevated temperature curing
5	Cube	50 mm x 50 mm x 50 mm	Microstructure analysis, Monitoring of elevated temperature curing

Figure 3.5 Loy Yang brown coal fly ash geopolymer concrete: mixing; moulding; and elevated temperature curing.

3.5.3 Elevated temperature curing

Heat curing or elevated temperature curing is a very important factor during geopolymerization processes as its assists the chemical reaction that occurs in the geopolymer paste. Temperature, time and condition of curing influence the compressive strength of geopolymer concrete as well as affected the micro and nano structure of geopolymer. The curing conditions were based on previous research which had identified that 120 ^{o}C gave the optimum compressive strength, demonstrating significant improvement in strength compared to curing at lower temperatures, 80 – 100 ^{o}C (Law, Molyneaux et al. 2013),

A preliminary trial was performed using different periods of curing time of 8, 10, 12 and 14 hours. The preliminary investigation found 12 hours of curing period gave the best compressive strength for the initial Loy Yang brown coal fly ash geopolymer mortar mixture (Table 3.12 and Figure 3.6).

As such a curing temperature duration of 12 hours was chosen for this study both for geopolymer mortar and concrete. Under standard curing conditions applied the specimens were left at room temperature for 24 hours before put in the oven for elevated temperature curing of 120 ^{o}C for 12 hours. The specimens were wrapped with heat resistant cling film to reduced evaporation. The specimens were demoulded and left at the room temperature before testing.

Table 3.12 Compressive strength of Loy Yang brown coal fly ash geopolymer mortar vs elevated temperature curing time

Curing time (hours)	**Compressive strength (MPa)**	
	Mean	SD
8	8.97	1.15
10	19.16	1.08
12	26.38	1.95
14	24.98	2.84

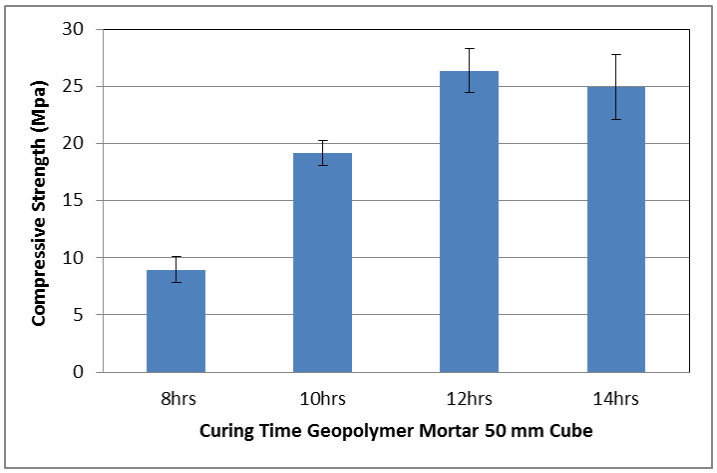

Figure 3.6 The compressive strength of Loy Yang brown coal fly ash geopolymer mortar vs elevated temperature curing time

3.5.4 Elevated temperature curing monitoring

A further investigation was undertaken in order to provide an understanding of how the temperature profile was distributed inside the specimen. The optimum Loy Yang brown coal fly ash geopolymer specimens were selected for this trial. The samples were 50 mm cube geopolymer mortar, and 50, 100, 200 and 300 mm cubes concrete specimens. A thermocouple was installed at various locations within the samples, Figure 3.7. The temperature changes were monitored during the elevated temperature curing.

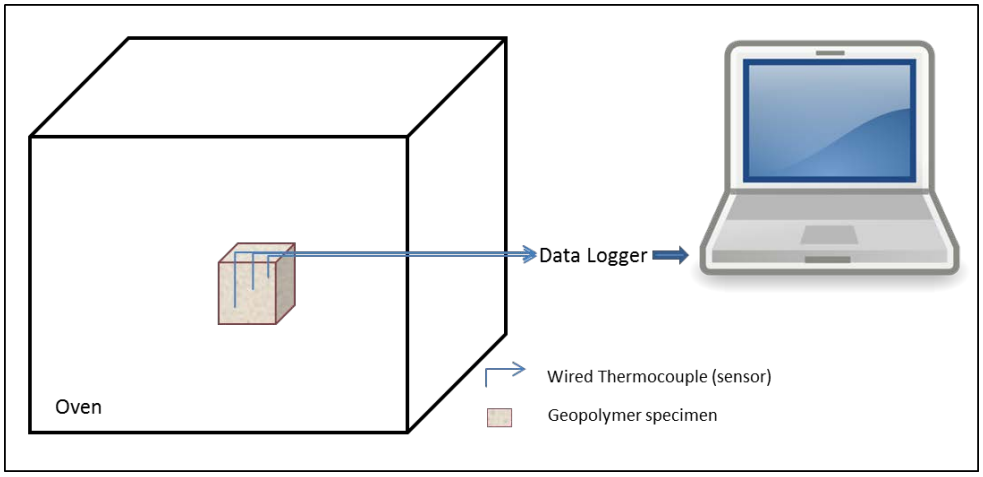

Figure 3.7 Schematic of geopolymer specimen elevated temperature monitoring

In the 50 mm cube geopolymer mortar and concrete specimens the thermocouple was positioned in the center of the sample, which was 25 mm from each surface (Figure 3.8). In the 100 mm cube geopolymer concrete the probes were position along centerline at the 25, 50, and 75 mm distance from the side and from the top surface (Figure 3.9). In the 200 and 300 mm cubes the probes were positioned at 25 mm interval from the side along the centerline with the depth increased by 25 mm from the top surface respectively.

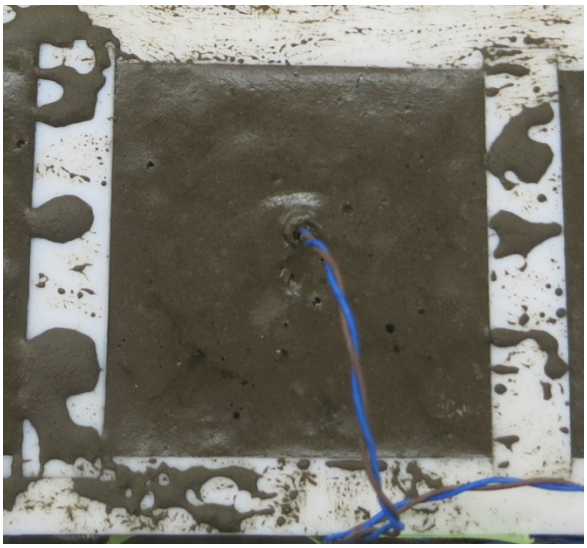

Figure 3.8 Mortar sample for elevated temperature monitoring with thermocouple installed

Additional samples were prepared for microstructural analysis. The samples cured at 120°C with different time periods i.e for 4, 6, 8, 10, 12 and 14 hours.

The activation of fly ash by alkali activator of geopolymer following elevated temperature curing was observed using several techniques. Fourier Transform Infrared Spectroscopy (FTIR), X-Ray Diffraction (XRD), and Scanning Electron Microscope (SEM) with Energy Dispersive X-Ray spectroscopy (EDX) (Swanepoel and Strydom 2002, van Jaarsveld, van Deventer et al. 2002, Bakharev 2005, Criado, Fernández-Jiménez et al. 2010).

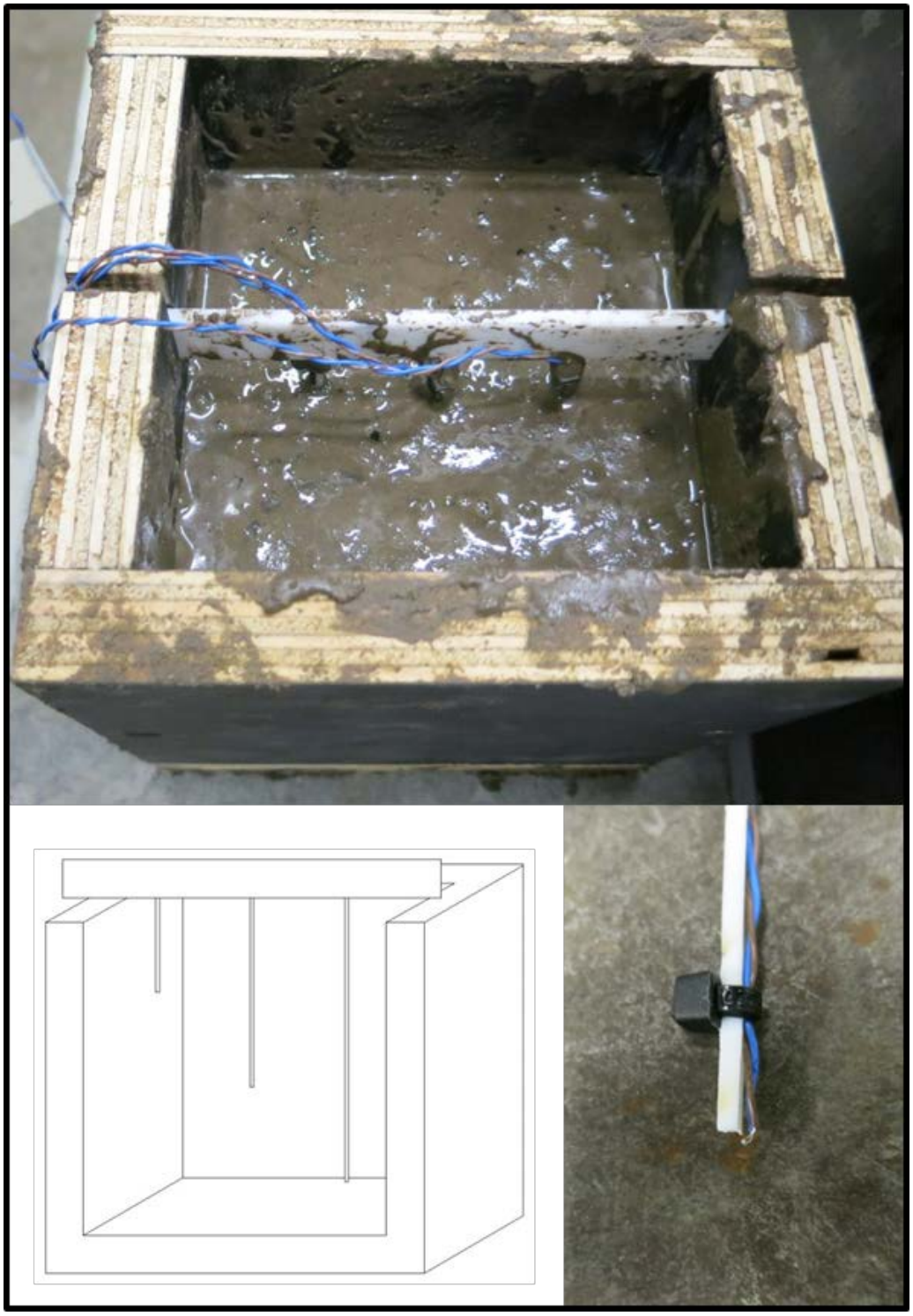

Figure 3.9 Brown coal fly ash geopolymer concrete with thermocouples installed, sketch of mould and thermocouple sensor frame, and the thermocouple tip.

3.5.5 Compressive strength testing

Compressive strength assessment of mortar and concrete were performed on a Universal Testing Machine, Tecnotest, and MTS machines in accordance with BS EN 12390-3. All compression tests were performed with a loading rate of 1 MPa/minute and the load recorded at the point of cube failure. Three cubes were tested for each sample of geopolymer mortar and concrete. The sizes of the specimen were 50 mm cubes for brown coal fly ash geopolymer mortar and 100 mm cubes for brown coal fly ash geopolymer concrete. Figure 3.10 and Figure 3.11 shows the brown coal fly ash geopolymer mortar, geopolymer concrete and OPC concrete specimens for the compression strength testing.

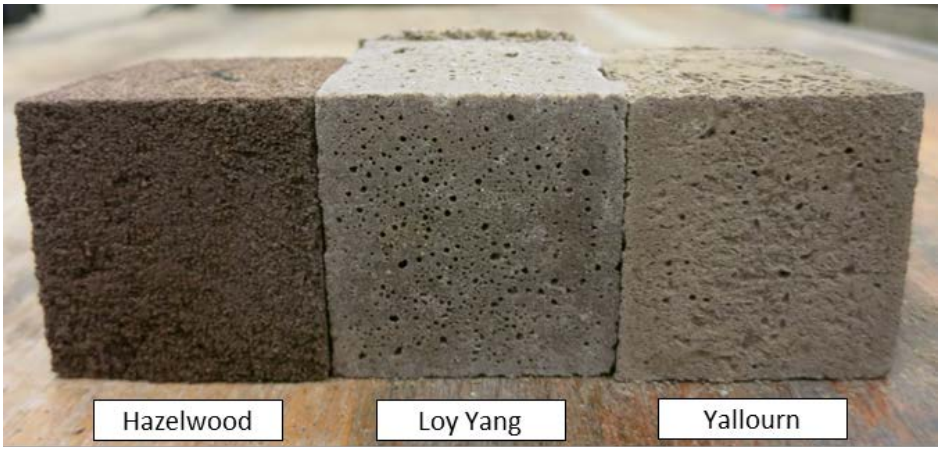

Figure 3.10 La Trobe Valley brown coal fly ash geopolymer mortar: Yallourn, Loy Yang and Hazelwood

The compressive strength was calculated from the applied load at the point of cube failure. The average of three tests are reported. The compressive strength of the specimen was calculated using the formula as follows:

$$\sigma = \frac{\mathrm{F}}{\mathrm{A}} \qquad \text{(Equation 3.2)}$$

Where: σ = the compressive strength (MPa)

F = the force applied (N)

A = the cross-sectional area (mm^2)

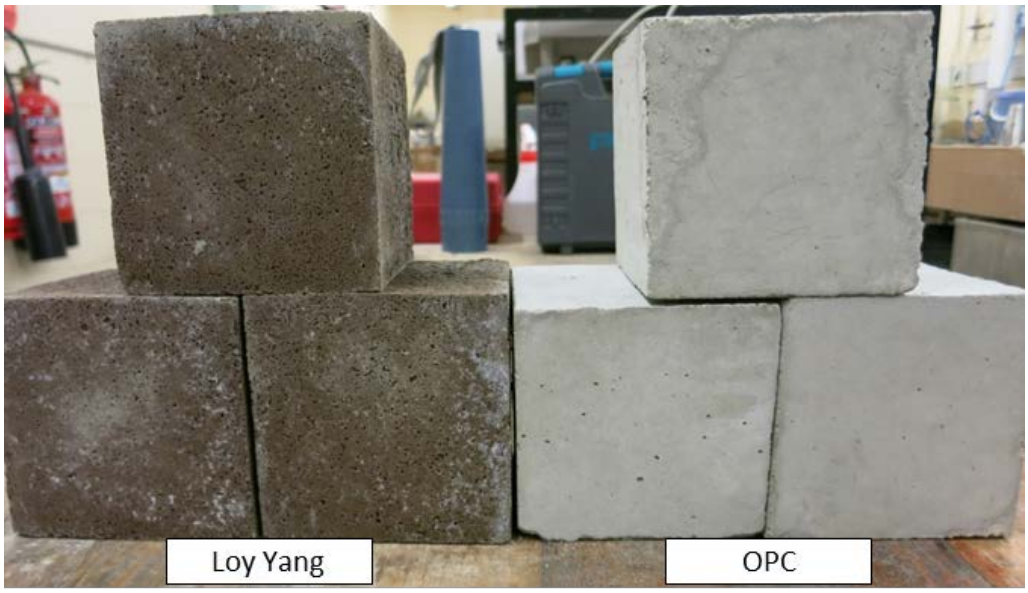

Figure 3.11 Loy Yang brown coal fly ash geopolymer concrete and OPC concrete

3.6. Microstructural analysis

Microstructural studies are essential in order to understand the mechanism of geopolymerization, the physical properties and characteristics of the brown coal fly ash material and the geopolymer mortar/concrete produced. Particle size analyser, Scanning Electron Microscopy (SEM) with Energy Dispersive X-Ray Spectroscopy (EDX), X-Ray Diffraction (XRD), Fourier Transform Infrared Spectroscopy (FTIR), Mercury intrusion porosimetry (MIP), and Zeta Potential are the methods used to investigate the microstructure properties of brown coal fly ash geopolymer.

Microscopy analysis using SEM was undertaken to identify microstructural features of brown coal fly ash and geopolymer produced e.g. to acquire surface

images and to record micrographs. SEM in combination with EDX was utilised to determine the chemical composition, elemental distribution, and an additional tool for semi-quantitative analysis of the specimens. The microscopy analysis was undertaken using a FEI Quanta 200 ESEM with Oxford X-MaxN 20 EDXS Detector in high vacuum mode with a Secondary Electron (SE) detector as well as a Backscattered Electron (BSE) detector. The microscope was coupled with an Oxford Aztec EDS Detector for elemental analysis. The image, chemical composition and analysis were gathered under high vacuum and a high voltage of 15–30keV, with the spot size varying from 5–10. The SEM samples were carbon coated and were prepared unpolished and polished from fractured and sawn surfaces. The samples were cut to a size of 3–7 mm in height and approximately 10 mm in diameter.

The mineralogical characteristic to identify the crystalline phase of the content was undertaken using a Bruker XRD instrument. The particle distribution of brown coal fly ash and the surface area were determined using a Malvern Particle size analyser (Mastersizer). A Malvern Zetasizer (nano series) was used to measure the zeta potential of the brown coal fly ash and geopolymer particles. Pore distribution analysis was conducted using a Micrometrics mercury AutoPore IV 9500 VI.09 intrusion porosimeter.

A Perkin-Elmer-Spectrum 100 FTIR spectrometer was used to acquire specimen FTIR absorption spectrum. The equipment was equipped with the universal attenuated total reflectance (ATR) top plate and a diamond crystal. Spectra were recorded at a scan speed of 0.2cm/s and a spectral resolution of $4cm^{-1}$, and with data normalised using the Spectrum software (Perkin-Elmer). The powder for testing was manually ground and filtered using a 75 micron sieve as required.

3.7. Durability properties

A range of non-destructive tests (NDT) and durability tests were performed to determine the durability properties and characteristic of the Loy Yang brown coal

fly ash geopolymer concrete. The NDT durability investigation of the Loy Yang brown coal fly ash geopolymer concrete was carried out adopting the OP cement concrete as a control.

3.7.1 Non Destructive Testing (NDT)

The range of non-destructive test methods that were implemented on Loy Yang brown coal fly ash geopolymer concrete and the OP cement concrete control samples were:

Schmidt Rebound Hammer

The Schmidt Rebound Hammer measures the rebound of a spring-loaded mass impacting against the surface of the sample. The hammer impacts the concrete at a defined energy with its rebound dependent on the hardness of the concrete, this hardness is measured by the test equipment. The test was conducted using a Schmidt Type N hammer (Figure 3.12) in according to ASTM standard (ASTM-C805-02 2003). Striking points were uniformly distributed to reduce the influence of coarse aggregates distribution and averages of the rebound value calculated. Two cuboid Loy Yang brown coal fly ash geopolymer concrete specimens of 300 mm width x 300 mm length x 100 mm height were tested at 28 and 90 days after casting and average values for each data point was considered.

Figure 3.12 Schmidt Rebound Hammer equipment

Electrical resistivity

The corrosion risk of concrete can be assessed by measuring the electrical resistivity of the concrete specimen. The electrical resistivity of concrete is an important parameter in determining the potential intensity of the initiated corrosion process. In concrete with low resistivity the corrosion rate may be high compared to high resistivity concrete (Song and Saraswathy 2007).

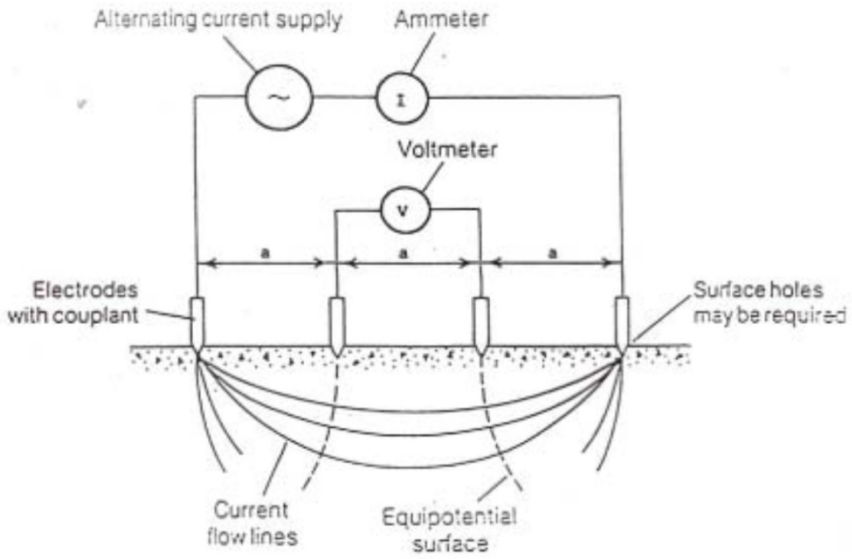

Figure 3.13 Schematic of Wenner 4 probes resistivity meter (IAEA 2002)

The Wenner four probes method was adopted for *in situ* electrical resistivity measurements. The equipment consists of four electrodes (2x inner and 2x outer) which are placed in a straight line on the concrete surface at equal spacing (Figure 3.13). The surface electrical resistivity is measured using a fully integrated four point 50 mm spacing Wenner RESIPOD resistivity probe, sourced from Proceq (Figure 3.14). The resistivity reading was reported in the range of 0 – 100 kΩcm. Duplicate Loy Yang brown coal fly ash geopolymer concrete specimens, 300 mm width x 300 mm length x 100 mm height, were tested at 28 and 90 days after casting.

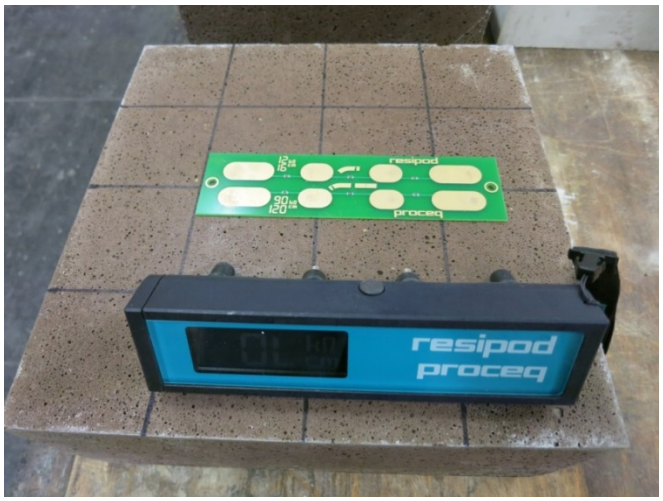

Figure 3.14 Electrical resistivity test equipment

The testing procedure for the resistivity tests was as follows:

- Calibrate the instrument using the calibration instrument.
- Place and hold the probe firmly on the surface of specimens.
- Record the resistivity (kΩcm) and the current (%) readings.
- Take a minimum of 10 readings per specimen.

The relationship between the risk of corrosion and the resistivity measurements can be predicted on the basis of resistivity measurement as shown on Table 3.13 (IAEA 2002).

Table 3.13 Guide for interpretation of corrosion risk from resistivity measurement (IAEA 2002).

Resistivity (Ωcm)	**Corrosion risk**
Less than 5,000	Very high
5,000 – 10,000	High
10,000 – 20,000	Low / Moderate
Greater than 20,000	Negligible

Ultrasonic pulse velocity

The Ultrasonic Pulse Velocity (UPV) was measured in accordance with ASTM standard (ASTM-C957-09 2009). The UPV is used to determine the density and quality of a material based on the speed of a stress wave passing through the medium which is related to the elasticity-density. The UPV testing apparatus according to the ASTM (ASTM-C957-09 2009) consists of a pulse generator, a pair of transducers, a time measuring circuit, a time display unit and connecting cables. The UPV was measured with a pulse of longitudinal vibration produced by an electro-acoustical transducer and received by another transducer after travelling a known path.

The testing procedure of UPV test was as follows:

- Setup the instrument by connecting the transducers to the UPV equipment.
- Calibrate the instrument using the calibration cylinder.
- A conductive coupling gel was applied to the transducers to ensure good contact with the concrete surface
- Put and hold transducers firmly against each end of specimens.
- Record the transit time (μs) and the pulse velocity (m/s) reading.
- Take a minimum of 10 readings per specimen.

The pulse velocity was calculated using ASTM C597-02 as follows:

$$V = \frac{\mathrm{L}}{\mathrm{T}} \qquad \text{(Equation 3.3)}$$

Where: V = the pulse velocity (m/s)

L = the distance between centers of transducers faces (m)

T = the transit time (s)

The transit time is measured using the TICO Ultrasonic Pulse Velocity instrument from Proceq (Figure 3.15). Duplicate Loy Yang brown coal fly ash geopolymer

concrete specimens, 300 mm x 300 mm x 100 mm, were tested at 28 and 90 days after casting. The transit time (T) and the pulse velocity (V) were determined. The quality of the concrete is predicted on the basis of the pulse velocity as shown on Table 3.14 (IAEA 2002).

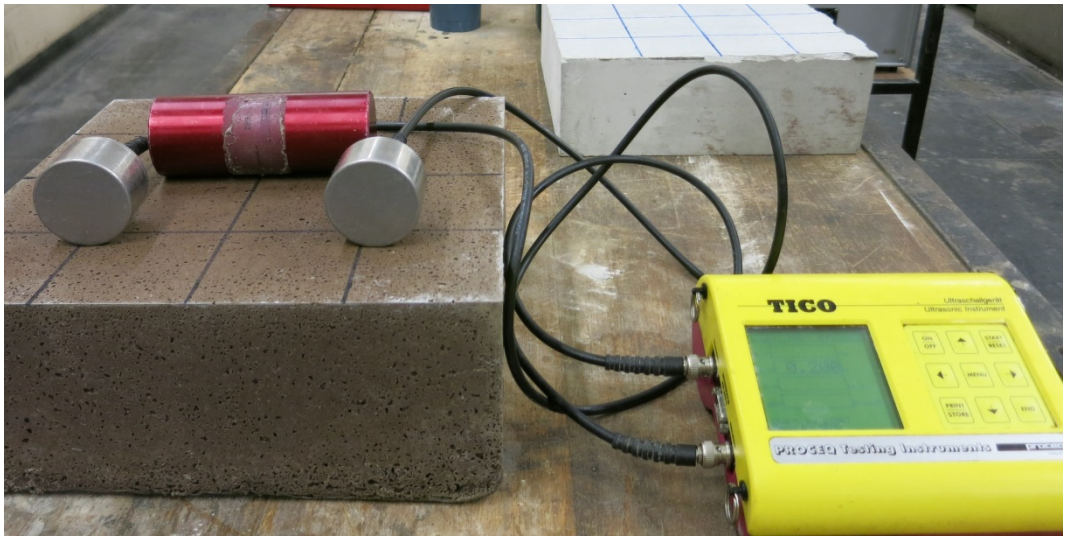

Figure 3.15 Ultrasonic Pulse Velocity instrument

Table 3.14 Clasification of the quality of concrete on the basis of pulse velocity (IAEA 2002).

Longitudinal pulse velocity (km/s.10^3)	**Quality of concrete**
> 4.5	Excellent
3.5 – 4.5	Good
3.0 – 3.5	Doubtful
2.0 – 3.0	Poor
< 2.0	Very poor

Air permeability and water absorption (sorptivity)

The permeability of concrete at the surface is a major factor in determining the durability (Montgomery, Basheer et al. 1993, Claisse, Ganjian et al. 2003, Torrent and Luco 2007). The air permeability and water absorption (sorptivity) tests were performed using the Autoclam Permeability System (Figure 3.16). This permeability test allows for a rapid analysis of the air and water absorption (sorptivity) of the concrete face by a non-destructive method.

Duplicate Loy Yang brown coal fly ash geopolymer concrete specimens 300 mm x 300 mm x 100 mm were tested at 28 and 90 days after casting. The test was carried out at one location on each of specimen with the air permeability test being carried out prior to the water absorption (sorptivity) test.

The air permeability test involves a pressure of 500 mBar applied to the specimen test surface using Autoclam, and its decay is monitored over a period of 15 minutes (Amphora-NDT 2014). The resulting test data from the 5^{th} minutes to 15^{th} minutes when plotted as the natural logarithm of pressure against the time, Ln(pressure)/min is reported as the Air Permeability Index (API). If the pressure reaches zero before finalising the test duration of 15 minutes, the data from the beginning to end of the test can be used to determine the slope, a coefficient of intrinsic permeability (in m^2) (Torrent and Luco 2007). The protective quality of the concrete can be predicted on the basis of Autoclam Air Permeability Index as shown on Table 3.15 (Amphora-NDT 2014).

The water absorption (sorptivity) test is undertaken following the air permeability test at the same test location (Basheer, Montgomery et al. 1991). This test involves the measurement of water penetrating into the concrete at a constant pressure of 20 mBar for test duration of 15 minutes. The autoclam equipment monitors the volume of water that penetrates the concrete specimen at a constant pressure for 15 minutes duration. The resulting test data from the 5^{th} minutes when plotted as the volume of water absorbed against the square root of time $m^3/\sqrt{min}$ is reported as the Autoclam Sorptivity Index (Amphora-

NDT 2014). The protective quality of the concrete can be predicted on the basis of Autoclam Sorptivity Index as shown on Table 3.16 (Amphora-NDT 2014).

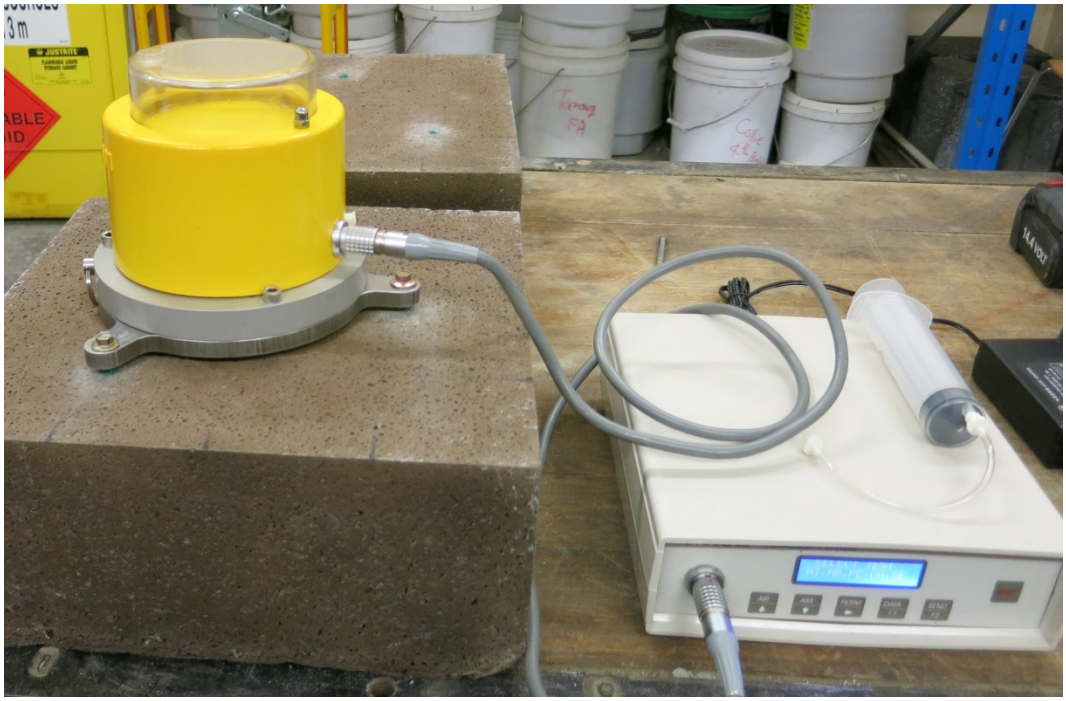

Figure 3.16 Autoclam equipment for air permeability and water absorption (sorptivity) experiments.

Table 3.15 Protective quality based on Autoclam Air Permeability Index (Amphora-NDT 2014).

Autoclam Air Permeability Index **Ln (Pressure)/min**	**Protective quality**
≤ 0.10	Very good
> 0.10 ≤ 0.50	Good
> 0.50 ≤ 0.90	Poor
> 0.90	Very poor

Table 3.16 Protective quality based on Autoclam Sorptivity Index (Amphora-NDT 2014).

Autoclam Sorptivity Index $m^3 \times 10^{-7}/\sqrt{min}$	**Protective quality**
≤ 1.30	Very good
> 1.30 ≤ 2.60	Good
> 2.60 ≤ 3.40	Poor
> 3.40	Very poor

3.7.2 Chloride diffusion

The salt ponding test to evaluate the chloride resistance of Loy Yang brown coal fly ash geopolymer concrete was performed in this study. The chloride ponding test was done in accordance with AASHTO (AASHTO-T-259 1997) and ASTM (ASTM-C1543-02 2003) standards. The test determined chloride diffusion coefficient (D_a) and the surface concentration (C_s).

The specimens were 100 mm concrete cubes. All sides, other than the cast face, are painted with an epoxy to ensure unidirectional chloride ingress. The test was carried out for a duration of 90 days after casting. The chloride solution used was a 3% NaCl solution in accordance with ASTM (ASTM-C1543-02 2003). The specimens were submerged into the solution and the solution was renewed every 14 days (Figure 3.17). The container was closed to prevent the evaporation. The specimens were removed from the chloride solution at 90 days and slice at three different thicknesses corresponded to depth increment of 0-20 mm, 20-40 mm and 40-100 mm. Each slice was ground and pulverized using a ring mill machine to 150µm. The powder from each slice was sent to an accredited laboratory to determine the chloride content according to AASHTO standard (AASHTO-T-259 1997). The chloride diffusion coefficient (Da) and the

surface concentration (Cs) were calculated by plotting the chloride profiles and determining the best fit curve using Fick's 2nd Law (Crank 1979).

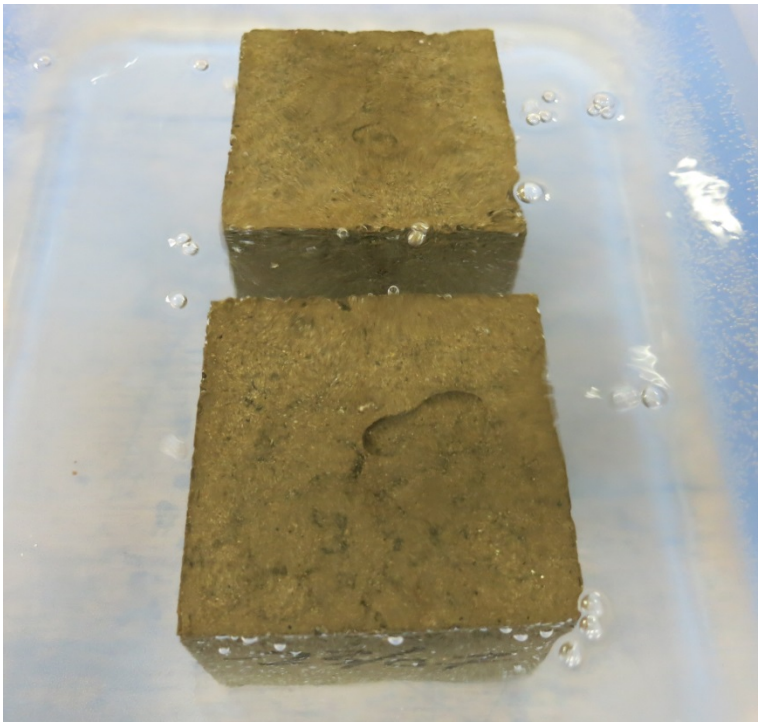

Figure 3.17 Loy Yang brown coal fly ash geopolymer concrete in the salt ponding test container

3.7.3 Carbonation

The carbonation test was performed to assess the carbonation depth ingression in Loy Yang brown coal fly ash geopolymer concrete. The actual process of carbonation in the real world is a long term reaction. The carbonation experiment was performed using an accelerated carbonation chamber. The Loy Yang brown coal fly ash geopolymer concrete was exposed to CO_2 in an environment where three variables: the temperature, the relative humidity and the CO_2 concentration could be controlled. The carbonation chamber used for the accelerated carbonation tests was a Climatron Growth Cabinet sourced from Thermoline Scientific. The environment of accelerated carbonation chamber is

set to the concentration of CO_2 of 2% ± 1%, the temperature of 20°C ± 1°C and the relative humidity of 70% ± 1%.

The specimens were 100 mm concrete cubes. All sides, other than the cast face, are painted with an epoxy to ensure unidirectional ingress. The test was performed at 7 and 28 days. At the intervals the specimens were taken out of the chamber and the depth of carbonation were measured. The depth of carbonation of Loy Yang brown coal fly ash geopolymer concrete specimens was measured by treating the surface of freshly sliced specimen with a pH indicator which was prepared by mixing a 1% solution of phenolphthalein with water in accordance with the RILEM standard (RILEM 1994). The depth of carbonation was measured based on the change of colour on the surface of the specimen. In the non-carbonated part of the specimen where the concrete was still highly alkaline, purple-red coloration was seen. While in the carbonated part of the specimen, where (due to the carbonation) the alkalinity was reduced, no coloration occurred. An average carbonation depth was then taken from the cross-sectioned slices.

3.8. Summary of chapter 3

Chapter 3 on methodology could be summarised as follows:

1) The fly ash used is classified as neither class C or class F thus the term brown coal fly ash will be used for all fly ash materials used to prepare geopolymer mortar and concrete specimens.
2) The fly ash used for geopolymer mortar and concrete specimens came from 3 major Power Stations in La Trobe Valley, Victoria: AGL Loy Yang, Energy Australia Yallourn and GDF-SUEZ Australian Energy Hazelwood.
3) Mix variations of geopolymer mortar and concrete were considered the chemical composition of brown coal fly ash, the liquid to solid ratio of the mixture, the alkali modulus of the activator (SiO_2/Na_2O), and the weight percentage of brown coal fly ash (Fly Ash wt%).

4) Temperature inside the mortar and concrete specimens during elevated temperature curing were investigated to gather more understanding of how the temperature was distributed and affected the geopolymeric chemical reaction as well as the microstructure of the geopolymer.
5) The microstructural properties of brown coal fly ash geopolymer specimens were investigated using Particle size analyser, SEM-EDX, XRD, FTIR, Mercury intrusion porosimetry, and Zeta Potential.
6) The mechanical characteristic and durability properties of brown coal fly ash geopolymer concrete specimens were determined using the Schmidt Rebound Hammer test, the resistivity test, the ultrasonic pulse velocity test, the air permeability and sorptivity test, the chloride diffusion test, and the carbonation test.

References

AASHTO-T-259 (1997). AASHTO-T-259. Standard Method of Test for Resistance of Concrete to Chloride Ion Penetration. USA, AASHTO.

Adam, A. (2009). Strength and durability properties of alkali activated slag and fly ash-based geopolymer concrete. PhD, RMIT University.

Amphora-NDT (2014). Autoclam Permeability System, Operating Manual. Belfast, Northern Island, Amphora Technologies Ltd.

ASTM-C805-02 (2003). ASTM C805-02. Standard Test Method for Rebound Number of Hardened Concrete. USA, ASTM International.

ASTM-C957-09 (2009). ASTM C597-09. Standard test Method for Pulse Velocity through concrete. USA, ASTM International.

ASTM-C1543-02 (2003). ASTM C1543-02. Standard Test Method for Determining the Penetration of Chloride Ion into Concrete by Ponding. USA, ASTM International.

ASTM (2012). ASTM C618-12. Standard Specification for Coal Fly Ash and Raw or Calcined Natural Pozzolan for Use in Concrete. West Conshohocken, US., ASTM International.

Bakharev, T. (2005). "Geopolymeric materials prepared using Class F fly ash and elevated temperature curing." Cement and Concrete Research 35(6): 1224-1232.

Basheer, M., R. Montgomery and A. Long (1991). The'Autoclam'for Measuring the Surface Absorption and Permeability of Concrete on Site, Queen's University of Belfast, Department of Civil Engineering.

Claisse, P., E. Ganjian and T. Adham (2003). "In situ measurement of the intrinsic permeability of concrete." Magazine of concrete research 55(2): 125-132.

Crank, J. (1979). The mathematics of diffusion. England, Oxford university press.

Criado, M., A. Fernández-Jiménez and A. Palomo (2010). "Alkali activation of fly ash. Part III: Effect of curing conditions on reaction and its graphical description." Fuel 89(11): 3185-3192.

French, D. and J. Smitham (2007). Fly Ash Characteristics and Feed Coal Properties. Pullenvale, Qld 4069, Australia, Cooperative Research Centre for Coal in Sustainable Development.

Hardjito, D. and B. V. Rangan (2005). Development and Properties of Low-Calcium Fly Ash-Based Geopolymer Concrete, Research Report GC 1. Perth, Australia, Curtin University of Technology.

IAEA (2002). Guidebook on non-destructive testing of concrete structures. Vienna, Austria, International Atomic Energy Agency.

Law, D. W., T. K. Molyneaux, A. Wardhono, R. Dirgantara and D. Kong (2013). The Use Brown Coal Fly Ash To Make Geopolymer Concrete. ACCTA 2013, Johannesburg.

Lloyd, N. A. and B. V. Rangan (2010). Geopolymer Concrete with Fly Ash. Second International Conference on Sustainable Construction Materials and Technologies. Universita Politecnica delle Marche, Ancona, Italy.

Macphee, D. E., C. J. Black and A. H. Taylor (1993). "Cements Incorporating Brown Coal Fly Ash from The Latrobe Valley Region of Victoria, Australia." Cement and Concrete Research 23(3): 507-517.

Montgomery, F., P. Basheer and A. Long (1993). A comparison between the Autoclam permeability system and the Initial Surface Absorption Test. Proceeding of International Conference on Structural Faults and Repair.

Neville, A., M. (2011). Properties of Concrete. England, Pearson Education Limited.

RILEM (1994). RILEM Recommendations for the Testing and Use of Constructions Materials. CPC-18 Measurement of hardened concrete carbonation depth, RILEM.

Siddique, R. (2008). Coal Fly Ash. Waste Materials and By-Products in Concrete, Springer Berlin Heidelberg: 177-234.

Song, H.-W. and V. Saraswathy (2007). "Corrosion monitoring of reinforced concrete structures-a." Int. J. Electrochem. Sci 2: 1-28.

Sumajouw, M. D. J. and B. V. Rangan (2006). Low-Calcium fly ash-based geopolymer concrete: Reinforced beams and columns, Research Report GC 3. Perth, Australia, Curtin University of Technology.

Swanepoel, J. C. and C. A. Strydom (2002). "Utilisation of fly ash in a geopolymeric material." Applied Geochemistry 17(8): 1143-1148.

Torrent, R. and L. F. Luco (2007). Report 40: Non-Destructive Evaluation of the Penetrability and Thickness of the Concrete Cover-State-of-the-Art Report of RILEM Technical Committee 189-NEC, RILEM publications.

van Jaarsveld, J. G. S., J. S. J. van Deventer and G. C. Lukey (2002). "The effect of composition and temperature on the properties of fly ash- and kaolinite-based geopolymers." Chemical Engineering Journal 89(1–3): 63-73.

Wallah, S. E. and B. V. Rangan (2006). Low-Calcium fly ash-based geopolymer concrete: Long-term properties, Research Report GC 2. Perth, Curtin University of Technology.

Wardhono, A. (2015). The Durability of Fly Ash Geopolymer and Alkali-Activated Slag Concretes. PhD, RMIT University.

CHAPTER 4

BROWN COAL FLY ASH GEOPOLYMER MORTAR

4.1. Overview

This chapter presents research on brown coal fly ash geopolymer mortars. The research presented in this chapter includes brown coal fly ash from three power plants in Victoria, Australia: Loy Yang, Yallourn and Hazelwood. The chemical and physical characteristics of each material is analysed and a range of mix designs investigated to assess the feasibility of producing geopolymer mortars from brown coal fly ash, and the properties of the mortars produced.

4.2. Materials

4.2.1 La Trobe Valley-Victoria brown coal fly ash

A total of three brown coal fly ashes were investigated: Loy Yang, Hazelwood and Yallourn. The properties of these three La Trobe Valley brown coal fly ash are described in Chapter 3 Section 3.2.1.

4.2.2 Alkaline activators

The alkaline solution used as activator is a combination of sodium hydroxide (NaOH) and sodium silicate (Na_2SiO_3). The properties of sodium silicate and sodium hydroxide are presented in Chapter 3 Section 3.2.2.

4.2.3 Fine aggregate

The fine aggregate used had a fineness modulus of 2.03. As the water to geopolymer solid ratio is very critical the fine aggregate used were in an oven dried condition. The typical grading of fine aggregate is presented in Chapter 3 Section 3.2.3.

4.3. Mix design and proportions

4.3.1 Mix design

The initial trial mix designs for the brown coal fly ash geopolymer mortar were developed from previous research at RMIT University, Melbourne, Australia (Law, Molyneaux et al. 2013), Table 3.6 in Chapter 3 Section 3.4.

In order to optimize the mix design, the proportion of the materials were varied over a range of modified activator modulus (AM_m) and dosage of activator of the mortar mixtures.

A total of 6 mix compositions were investigated. The mix composition variations in proportion to 1 kg unit of Loy Yang brown coal fly ash are given in Table 4.1. For all mixes, the fly ash content was designed to have a minimum of 10% by weight of fly ash.

Table 4.1 Mix composition variation of Loy Yang brown coal fly ash geopolymer mortar mixtures (kg)

Mixture	Fly Ash	Sand	Na_2SiO_3	NaOH	Fly Ash content (%wt)
Loy Yang 1	1	2.782	0.571	0.170	22.11
Loy Yang 2	1	2.183	0.400	0.201	26.43
Loy Yang 3	1	6.011	1.301	0.075	11.92
Loy Yang 4	1	5.840	1.593	0.202	11.58
Loy Yang 5	1	5.550	1.387	0.188	12.31
Loy Yang 6	1	3.478	0.689	0.167	18.75
Loy Yang 7	1	6.152	1.389	0.089	11.59

The detailed AM, AM_m and dosage are summarized in Table 4.2 and the key composition ratios in Table 4.3. The AM and solution dosage of activator are based on the chemical composition of the solution only while AM_m and binder dosage of activator are calculated to include the content from the fly ash.

Table 4.2 Activator modulus, dosage of activator, and fly ash content of Loy Yang brown coal fly ash geopolymer mortar mixture

Mixture	Activator Modulus		Dosage of Activator (%)	
	AM	AM_m	Solution	Binder
Loy Yang 1	1.202	3.178	14.0	21.6
Loy Yang 2	0.942	3.164	12.5	20.0
Loy Yang 3	1.771	3.078	21.6	29.7
Loy Yang 4	1.559	2.599	30.0	38.7
Loy Yang 5	1.535	2.690	26.6	35.0
Loy Yang 6	1.296	3.097	15.6	23.3
Loy Yang 7	1.749	2.985	23.3	31.5

Table 4.3 Key composition ratios of Loy Yang brown coal fly ash geopolymer mortar mixture

Mixture	Modulus and ratio			
	SiO_2/Al_2O_3	Na_2O/Al_2O_3	$SiO_2+Al_2O_3/Na_2O$	Liquid to Solid
Loy Yang 1	3.720	1.170	4.033	0.315
Loy Yang 2	3.428	1.084	4.086	0.269
Loy Yang 3	4.961	1.611	3.699	0.480
Loy Yang 4	5.457	2.100	3.075	0.563
Loy Yang 5	5.106	1.898	3.216	0.522
Loy Yang 6	3.920	1.265	3.888	0.350
Loy Yang 7	5.110	1.712	3.569	0.501

The mix proportions of Loy Yang brown coal fly ash geopolymer mortars, Mass (kg) per m^3 of mix are given in Table 4.4.

Table 4.4 Mix design of Loy Yang brown coal fly ash geopolymer mortar, Mass (kg) per m^3 mix

Mixture	Fly Ash	Sand	Na_2SiO_3	NaOH
Loy Yang 1	513.1	1427.2	293.0	87.0
Loy Yang 2	612.9	1337.7	244.9	123.0
Loy Yang 3	279.0	1677.3	363.1	21.0
Loy Yang 4	263.0	1535.7	418.9	53.0
Loy Yang 5	282.0	1564.7	390.9	53.0
Loy Yang 6	437.1	1520.2	301.0	73.0
Loy Yang 7	269.9	1660.5	374.9	24.0

Hazelwood and Yallourn brown coal fly ash geopolymer mortars were designed based on the optimum mix design identified from the Loy Yang specimen mixes. In particular, the mix proportions for Hazelwood and Yallourn brown coal fly ash were calculated to consider the SiO_2 content which was significantly lower compared to the Loy Yang brown coal fly ash. As such, instead of using the SiO_2/Na_2O ratio, the mixes were designed using the ratio of the sum of SiO_2 and Al_2O_3 to Na_2O. The mix proportions of Hazelwood and Yallourn brown coal fly ash are given in Table 4.5. The AM_m and dosage of Hazelwood and Yallourn mixture 1–5 are summarized in Table 4.5 and key composition ratios Table 4.6.

Table 4.5 Mix design of Hazelwood and Yallourn brown coal fly ash geopolymer mortar, Mass (kg) per m^3 mix

Mixture	Fly Ash	Sand	Na_2SiO_3	NaOH	Water
Hazelwood 1	977.2	1005.2	164.0	10.0	114
Hazelwood 2	279.0	1677.3	363.1	21.0	0
Hazelwood 3	282.0	1564.7	390.9	53.0	0
Hazelwood 4	437.1	1520.2	301.0	73.0	0
Hazelwood 5	269.9	1660.5	374.9	24.0	0
Yallourn 1	263.0	1535.7	418.9	53.0	0
Yallourn 2	279.0	1677.3	363.1	21.0	0
Yallourn 3	282.0	1564.7	390.9	53.0	0
Yallourn 4	437.1	1520.2	301.0	73.0	0
Yallourn 5	269.9	1660.5	374.9	24.0	0

Table 4.6 Activator modulus and dosage of activator, and fly ash content of Hazelwood and Yallourn brown coal fly ash geopolymer mortar mixture

Mixture	Activator		Fly Ash content (%wt)
	Modulus (AM_m)	Dosage (%)	
Hazelwood 1	1.178	28.0	43.04
Hazelwood 2	1.617	21.6	11.92
Hazelwood 3	1.436	26.6	12.31
Hazelwood 4	1.189	15.6	18.75
Hazelwood 5	1.608	23.3	11.59
Yallourn 1	1.554	30.0	11.58
Yallourn 2	1.729	21.6	11.92
Yallourn 3	1.532	26.6	12.31
Yallourn 4	1.344	15.6	18.75
Yallourn 5	1.714	23.3	11.59

Table 4.7 Key composition ratios of Hazelwood and Yallourn brown coal fly ash geopolymer mortar mixture

Mixture	Modulus and ratio			
	SiO_2/Al_2O_3	Na_2O/Al_2O_3	$SiO_2+Al_2O_3/Na_2O$	Liquid to Solid
Hazelwood 1	3.580	3.038	1.507	0.201
Hazelwood 2	18.723	11.583	1.703	0.480
Hazelwood 3	19.865	13.838	1.508	0.522
Hazelwood 4	10.541	8.863	1.302	0.350
Hazelwood 5	19.897	12.373	1.689	0.501
Yallourn 1	23.847	15.350	1.619	0.563
Yallourn 2	20.007	11.572	1.815	0.480
Yallourn 3	21.131	13.791	1.605	0.522
Yallourn 4	11.956	8.897	1.456	0.350
Yallourn 5	21.162	12.350	1.794	0.501

4.4. Mixing, curing and testing

The mixing was as described in Chapter 3 Section 3.5.1. Elevated temperature curing was applied to the specimens as described in Chapter 3 Section 3.5.3. Compressive strength measurements of mortars were performed on a Universal Testing Machine with initial stroke of 1 mm/min. Three cubes were tested for each data point. The specimens were tested at 7 and 28 days after casting.

4.5. Experiments results

4.5.1 The compressive strength results – Loy Yang

The strength obtained ranged from 12.66 MPa, Mixture Loy Yang 4 at 28 days to 56.81 MPa, Mixture Loy Yang 3 at 7 days (Table 4.8 and Figure 4.1). The maximum strengths obtained are comparable to those obtained from previous research on class F and class C fly ash (Chindaprasirt, Chareerat et al. 2007, Ivan

Diaz-Loya, Allouche et al. 2011, Gunasekara, Law et al. 2015). The strengths are also consistent with those specified in AS 3600 for exposure category B1 and B2 which are indicative that brown coal fly ash geopolymer can produce compressive strengths acceptable for use in the construction industry (AS3600 2001).

Table 4.8 The compressive strength of Loy Yang brown coal fly ash geopolymer mortar

Mixture	**Compressive strength (MPa)**				
	7 days		**28 days**		**Average**
	Mean	SD	Mean	SD	
Loy Yang 1	21.49	3.84	22.65	3.43	22.07
Loy Yang 2	22.63	9.67	20.16	4.55	21.40
Loy Yang 3	56.81	13.22	43.16	6.36	49.99
Loy Yang 4	13.44	3.65	12.66	0.60	13.05
Loy Yang 5	20.68	4.90	25.27	3.44	22.98
Loy Yang 6	27.17	6.52	26.44	4.20	26.81
Loy Yang 7	32.72	11.8	28.77	4.13	30.75

The results show minimal variation between 7 and 28 days, which would be expected due to the elevated curing temperatures applied. Similar findings have been reported by other authors (Palomo, Grutzeck et al. 1999, Bakharev 2005, Sindhunata, Van Deventer et al. 2006). Heat curing is required to achieve activation of the binder. At ambient temperature the fly ash reaction is extremely slow so heat curing is required to accelerate the pozzolanic reaction (Hardjito, Wallah et al. 2004, Wang, Shah et al. 2004).

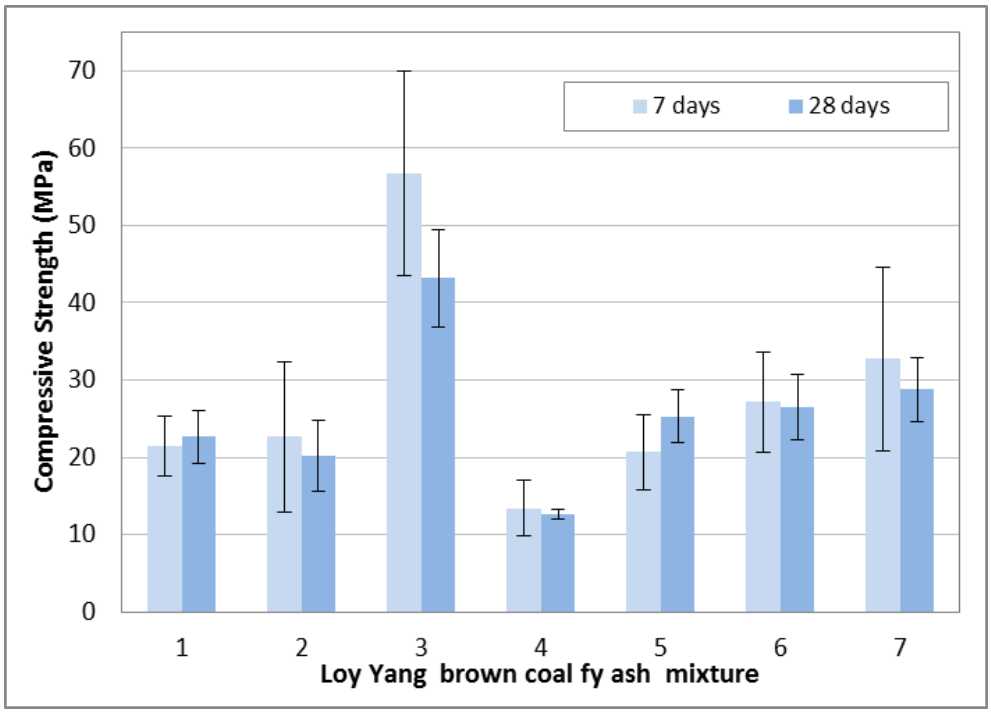

Figure 4.1 The compressive strength of Loy Yang brown coal fly ash geopolymer mortar

4.5.2 Modulus and dosage of activator, other activator ratio factors

Geopolymerization strongly depends on the chemical properties of the fly ash, the availability of soluble silicates and aluminates reactants, and the concentration of added NaOH. Geopolymerization has been identified as being influenced by the metal oxide ratios such as SiO_2/M_2O, SiO_2/Al_2O_3, M_2O/H_2O and M_2O/Al_2O_3 where M is either sodium or potassium (Davidovits 1994d). In this study the metal oxide ratios that would be anticipated to influence the geopolymerization would be the SiO_2/Na_2O, SiO_2/Al_2O_3, Na_2O/Al_2O_3 and the Na_2O/binder as the metal oxide used is sodium.

Figure 4.2 and Figure 4.3 show the effect on the compressive strength in relation to the AM_m, dosage of activator and key composition ratios.

The activator modulus and dosage of activator have been identified as playing an important role in determining compressive strength of geopolymer mortar strength (Fernández-Jiménez and Palomo 2005, Hardjito and Rangan 2005,

Skavara, Kopecky et al. 2006, Li, Ma et al. 2013). Figure 4.2 report an optimum range of activator modulus between 2.60 to 3.18 and dosage between 20% to 38.7%.

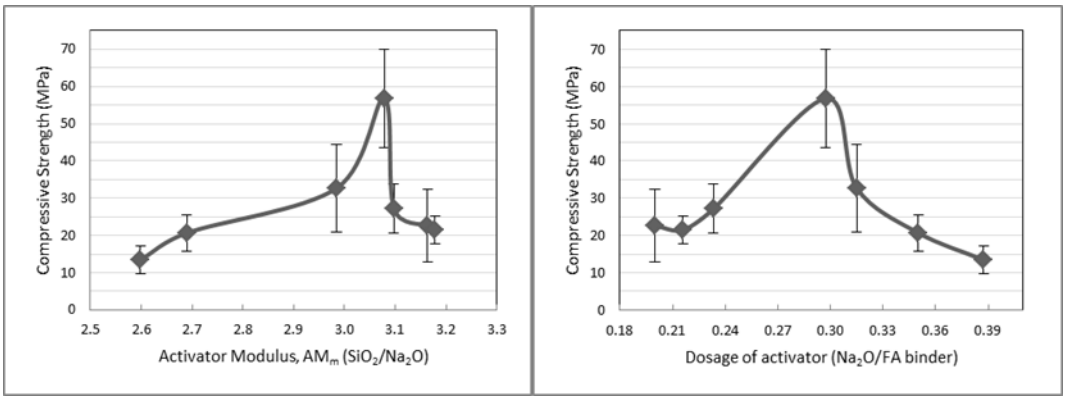

Figure 4.2 The compressive strength vs Alkali Modulus (AM_m) and Dosage of activator of Loy Yang brown coal fly ash geopolymer mortar

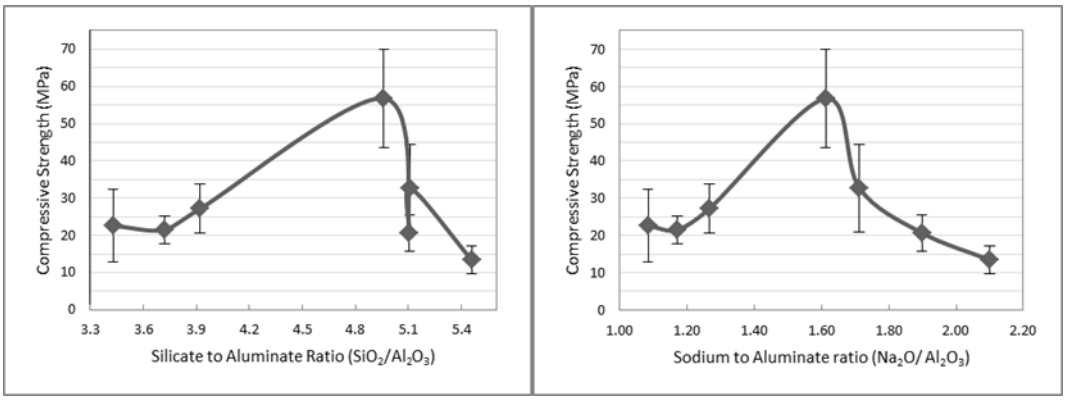

Figure 4.3 The compressive strength vs SiO_2/Al_2O_3 and Na_2O/Al_2O_3 ratios of Loy Yang brown coal fly ash geopolymer mortar

The Loy Yang brown coal fly ash geopolymer mortar compressive strength is observed to increase with increasing AM_m, to a maximum AM_m of 3.08 and increase with dosage to 29.7%, beyond which the strength falls rapidly. Indeed, the Loy Yang data shows a relatively small range of AM_m between 3.0 and 3.1, and dosage, 31.5% to 23.3%, where the compressive strength increases from 30 MPa to 50 MPa. Outside of this range the strength is less than 30 MPa, indicating

that the AM_m and dosage of activator are the key parameters in controlling the strength of the Loy Yang brown coal fly ash geopolymer mortar.

The SiO_2/Al_2O_3 and Na_2O/Al_2O_3 graphs, Figure 4.3, show slightly larger ranges, 4.2 to 5.0 and 1.3 to 1.7 where the optimum compressive strength is achieved. The maximum compressive strength corresponds to a SiO_2/Al_2O_3 ratio of 4.96 and Na_2O/Al_2O_3 ratio of 1.61. Overall the data indicates that the optimum range for the activator modulus and dosage are considerably more restrained than those that have been reported for class F fly ash geopolymers despite the relatively similar SiO_2 and Al_2O_3 content in the Loy Yang fly ash. This would suggest that other factors are also influencing the suitability and performance of the brown coal fly ash geopolymer mortar.

Figure 4.4 shows the compressive strength vs Liquid to Solid (L/S) ratio of Loy Yang brown coal fly ash geopolymer mortar. The graph shows an optimum L/S ratio of 0.48. In geopolymer water assists workability and plays the role of a reaction medium. The water will be expelled during the curing and drying stage, creating nano-pores in the matrix. These pores play a key role in the mechanical and durability performance of the geopolymer (Duxson, Provis et al. 2007, Rangan 2010). This is further examined in section 4.5.5.

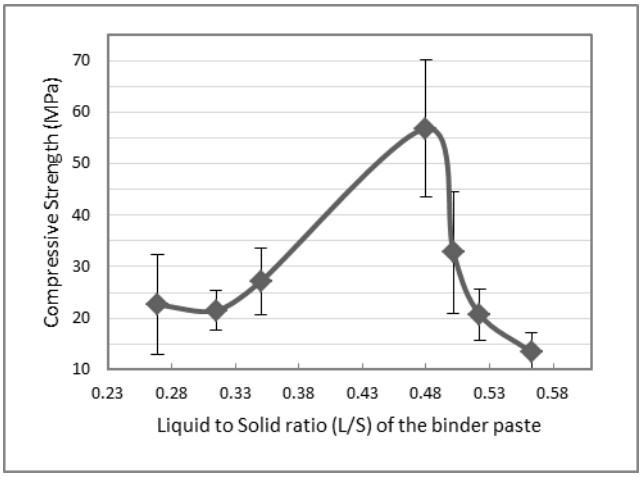

Figure 4.4 The compressive strength vs Liquid to Solid (L/S) ratio of Loy Yang brown coal fly ash geopolymer mortar

4.5.3 The compressive strength results – Hazelwood and Yallourn

The compressive strength of the Hazelwood and Yallourn brown coal fly ash geopolymer mortars are shown in Table 4.9. The compressive strengths at 7 days were less than 10 MPa, with Hazelwood mix 2 and 4 not setting, even following heat curing. The low strength of Hazelwood and Yallourn brown coal fly ash geopolymer mortars obtained are attributed to the content of aluminosilicate (SiO_2+Al_2O_3) being significantly lower, 8.72% Yallourn brown coal fly ash and 5.14% Hazelwood brown coal fly ash, compared to 64.81% Loy Yang brown coal fly ash. There is a high lime content in these materials (Yallourn brown coal fly ash 29.91% and Hazelwood brown coal fly ash 31.40%) and high lime is considered to have cementitious properties of its own. However, it appears to make little contribution to the strength of the geopolymer mortars produced. This is attributed to the lime being combined with the silica and alumina portions of the ash resulting in less of a compound reaction.

Table 4.9 The compressive strength of Hazelwood and Yallourn brown coal fly ash geopolymer mortar at 7 days

Mixture	**Compressive strength (MPa)**	
	Mean	**SD**
Hazelwood 1	9.08	0.28
Hazelwood 2	Not set	N/A
Hazelwood 3	8.81	1.10
Hazelwood 4	Not set	N/A
Hazelwood 5	5.80	0.99
Yallourn 1	9.79	1.00
Yallourn 2	6.56	2.51
Yallourn 3	9.37	1.58
Yallourn 4	5.03	0.91
Yallourn 5	7.95	0.72

The specimens also displayed relatively high standard deviations. This is attributed to the variability in the coal leading to variability in the composition of the fly ash. As noted, distinctly different chemical compositions have been reported for the brown coal fly ash (Macphee, Black et al. 1993, French and Smitham 2007, Dirgantara, Law et al. 2013).

Figure 4.5 and Figure 4.6 compare the compressive strength of Loy Yang with Hazelwood and Yallourn brown coal fly ash geopolymer mortars in relation to the AM_m, dosage of activator, SiO_2/Al_2O_3, and Na_2O/Al_2O_3 ratios. The graphs show that the key parameters of the Hazelwood and Yallourn mortar mixtures were outside the range of the Loy Yang mortar mixtures. This is due to the low aluminosilicate content of the Hazelwood and Yallourn brown coal fly ashes. Given their chemical composition it is not considered feasible to produce a viable geopolymer mix design that will fall within the optimal range of the Loy Yang brown coal fly ash geopolymer mortar.

The main component which provides the strength in geopolymerization is the aluminosilicate gel (N-A-S-H). As both the Yallourn and Hazelwood brown coal fly ashes contains significantly less aluminosilicate they would be expected to form significantly less aluminosilicate gel, though the high CaO content may be expected to form Calcium Aluminate gel (C-A-S-H) which has been reported as contributing to the strength of geopolymers. However, the compressive strength data indicates that this has not provided a significant contribution. Overall the result indicates that Hazelwood and Yallourn brown coal fly ash with their inherent chemical composition are not viable for the production of geopolymer with sufficient compressive strength to satisfy the requirements of category B1 and B2 AS3600 concretes.

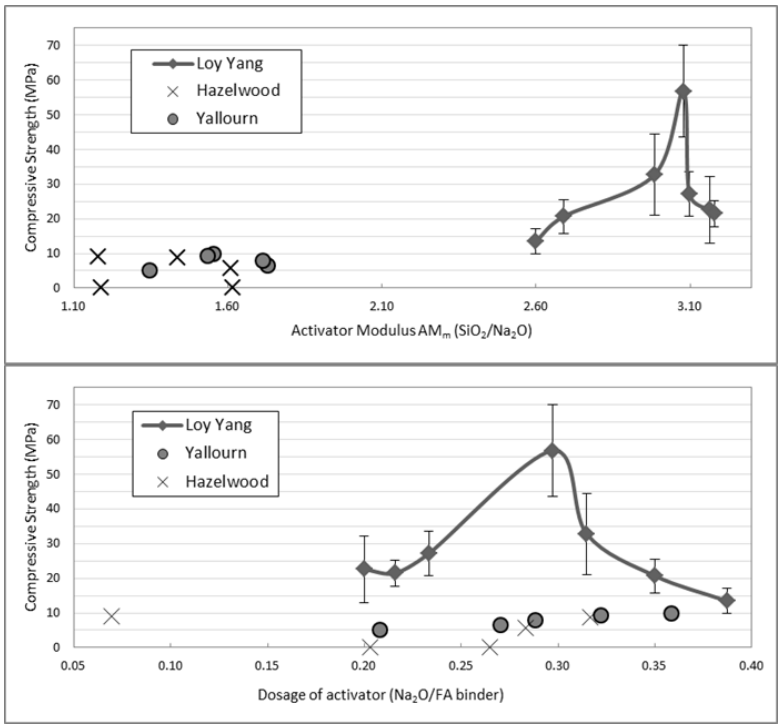

Figure 4.5 The compressive strength vs Alkali Modulus (AM_m) and Dosage of activator of Hazelwood, Yallourn and Loy Yang brown coal fly ash geopolymer mortar

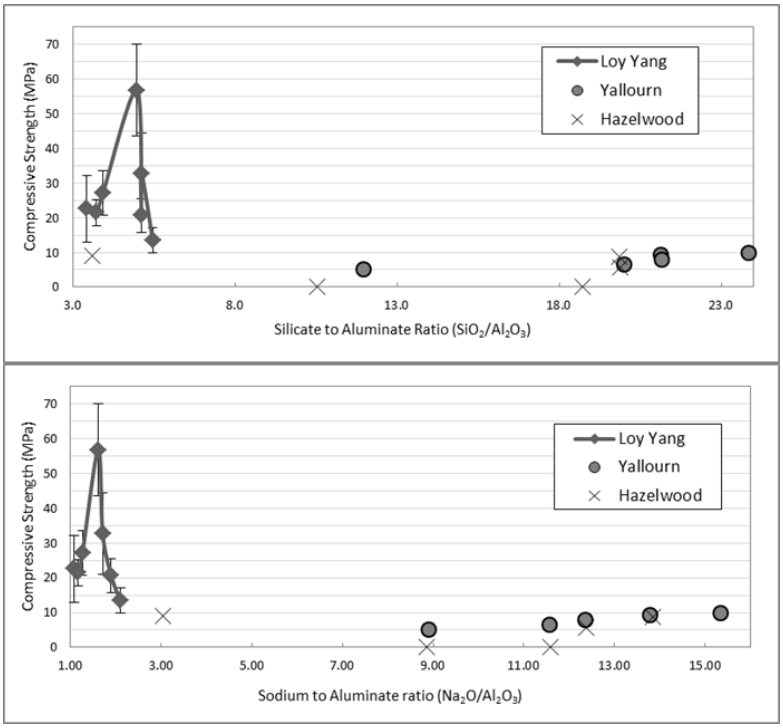

Figure 4.6 The compressive strength vs SiO_2/Al_2O_3 and Na_2O/Al_2O_3 ratios of Hazelwood, Yallourn and Loy Yang brown coal fly ash geopolymer mortar

4.5.4 Workability

The workability of the brown coal fly ash geopolymer mortar could not be obtained by the traditional slump test, due to the dryness of a number of the mixes. As such a flow table test was used to compare the workability of the mixtures. Table 4.10 and Figure 4.7 show the flow of each mix and a description of the nature of the mix. The water content of the mixture is described in two ways, Liquid to Solid (L/S) and L/S of binder. The L/S mixture is total liquid over total solid, while L/S binder is total liquid over fly ash binder (paste).

The mixture consistency varied considerably from dry to wet and friable to sticky. It is interesting to see that same L/S results in a different consistency for the different fly ashes. For example, Loy Yang 3, Hazelwood 2 and Yallourn 2 were the same L/S mixture 0.101 and L/S binder 0.480, but resulted in a wet mixture consistency of Loy Yang 3 but moist and firm mixture consistency of Hazelwood 2 and Yallourn 2. In contrast, Loy Yang 6, Hazelwood 4 and Yallourn 4 were the same L/S mixture 0.099 and L/S binder 0.350, but resulted in a wet mixture and firm consistency to Hazelwood 4 and Yallourn 4, but a moist and friable mixture consistency of Loy Yang 6. While there is a significant variation in the chemical composition of the different fly ashes it is believed that the variations in the physical properties such as particle size distribution, surface area and the amorphous and crystalline phases are also contributing factors controlling the workability.

Most of the Hazelwood and Yallourn mixes were identified as firm as a result of flash setting. The term firm refers to stable in shape not liquid or fluid during the flow table test. Flash setting is the rapid development of rigidity in a freshly mixed OPC cement paste mortar or concrete. In geopolymer concrete, a high content of CaO has been identified as increasing the reaction rate and causing rapid setting (Sindhunata 2006, Diaz, Allouche et al. 2010). Given the high CaO content of Yallourn 29.91% and Hazelwood 31.40%, it is therefore believed that

this is a contributing factor to the low workability and firm nature of the geopolymer mix produced by these fly ashes.

Table 4.10 Flow of Loy Yang, Hazelwood and Yallourn brown coal fly ash geopolymer mortar mixtures

Mixture	Flow (%)	L/S Ratio		Notes
		Mixture	Binder	
Loy Yang 1	103.25	0.102	0.315	Moist and friable mixture
Loy Yang 2	120.00	0.098	0.269	Dry and loose mixture
Loy Yang 3	5.00	0.101	0.480	Wet mixture
Loy Yang 4	33.96	0.132	0.563	Wet mixture
Loy Yang 5	23.00	0.122	0.523	Wet mixture
Loy Yang 6	108.00	0.099	0.350	Moist and friable mixture
Loy Yang 7	13.50	0.106	0.501	Wet mixture
Hazelwood 1	93.00	0.102	0.200	Dry mixture
Hazelwood 2	4.00	0.101	0.480	Moist and firm mixture
Hazelwood 3	22.50	0.122	0.523	Wet mixture
Hazelwood 4	0.00	0.099	0.350	Wet and firm mixture
Hazelwood 5	3.16	0.106	0.501	Wet and firm mixture
Yallourn 1	17.88	0.132	0.563	Wet mixture
Yallourn 2	0.00	0.101	0.480	Wet and firm mixture
Yallourn 3	29.55	0.122	0.523	Wet and sticky mixture
Yallourn 4	8.10	0.099	0.350	Wet and firm mixture
Yallourn 5	2.04	0.106	0.501	Wet and firm mixture

Figure 4.7 Image of Loy Yang, Hazelwood and Yallourn brown coal fly ash geopolymer mortar mixtures after flow table test

4.5.5 Elevated temperature curing investigation

An investigation regarding the impact of curing time was undertaken using the optimum mix design for Loy Yang brown coal fly ash geopolymer mortar, Loy Yang 3. A curing temperature of 120 °C was employed with a range of curing times from 4–14 hours.

A temperature probe was placed in the center of the specimen to monitor the temperature profile of the mortar during the heat curing, the method is described in Chapter 3 Section 3.5.4. The temperature probe was monitored through a data logger coupled with a PC.

Table 4.11 and Figure 4.8 show the curing time vs compressive strength. The compressive strength for each time regime was determined at 7 days. Figure 4.9 shows the temperature variation in the center of the mortar specimen with time.

The compressive strength data indicates that after 4 hours the mortar had achieved less than 5 MPa but by 6 hours had achieved approximately 23 MPa, 55% of the ultimate strength. By 8 hours it had achieved 33.54 MPa (80% of the strength) with little change to 33.66 at 10 hours. After 12 hours the maximum strength of 42 MPa was achieved, though by 14 hours the strength had actually decreased to 31 MPa.

Table 4.11 The compressive strength of Loy Yang brown coal fly ash geopolymer mortar at different curing times

Curing time (hours)	**Compressive strength (MPa)**	
	Mean	SD
4	4.57	1.05
6	22.97	6.76
8	33.54	6.73
10	33.66	8.17
12	42.12	5.84
14	30.99	3.56

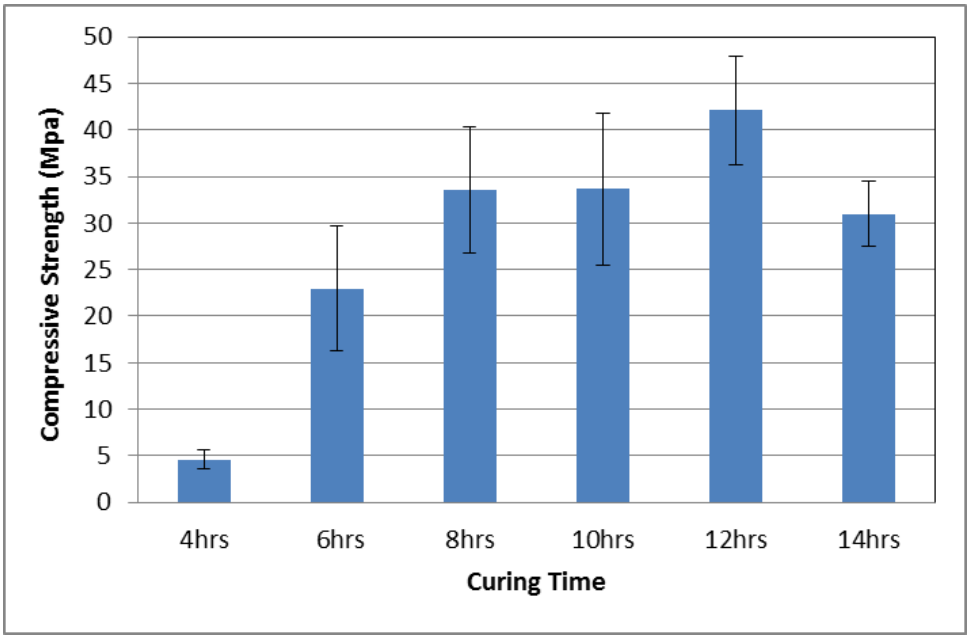

Figure 4.8 The compressive strength of Loy Yang brown coal fly ash geopolymer mortar for elevated temperature monitoring at different curing times

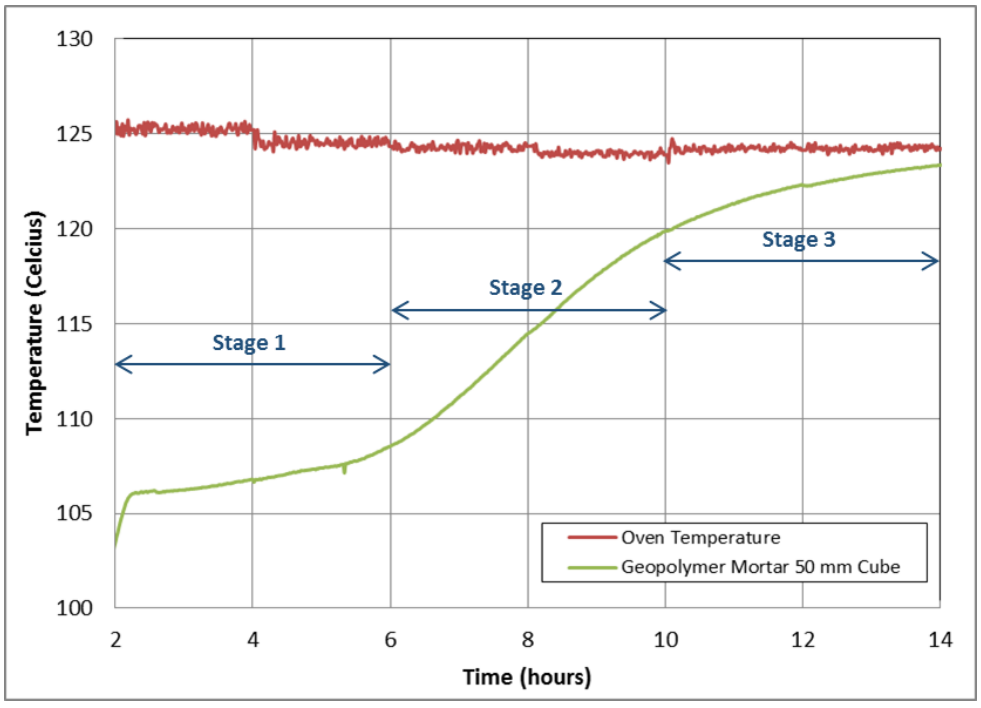

Figure 4.9 Temperature inside the oven and at the center of Loy Yang brown coal fly ash geopolymer mortar vs time

The temperature vs curing time graph in Figure 4.9 shows three distinct stages: 2–6 hours, 6–10 hours, and 10–14 hours. The temperature profile shows that by 2 hours the internal temperature had exceeded 105 °C, from 2 to 6 hours there is then a steady rise in temperature to 108 °C, from 6 to 10 hours a more rapid rise is observed to 120 °C followed by a slow rise in temperature to 14 hours where the temperature of the center of the mortar is just below the oven temperature of 125 °C.

The first stage can be identified with the period when the dissolution and speciation equilibrium steps occur as proposed by Duxson et al. (2007) in the conceptual model of geopolymerization. Gelation is also identified as commencing in this first stage. The formation of the gel is result of a complex mixture of silicate, aluminate and aluminosilicate which have been released by dissolution into the aqueous phase. Water plays the role of a reaction medium in this first stage. Dissolution consumes water which is then released during the formation of the gel, with some residual water remaining within pores in the gel (Duxson, Provis et al. 2007).

The first stage can also be related to the nucleation stage identified by Duxson et al. (2007). Nucleation is the dissolution of the aluminosilicate material and formation of polymeric species which are highly dependent on thermodynamic and kinetic parameters (Duxson, Provis et al. 2007). The temperature during this period only rise slightly from 105 to 108 °C as the nucleation uses the energy from the elevated temperature curing.

The stage after nucleation identified by Duxson et al. (2007) is growth. Growth is the condensation-crystallization phase when the nuclei reach a critical size and crystals begin to develop. This process is a structural reorganization which forms the microstructure of the material and the nano-pore distribution which is critical in determining the physical and durability properties of the geopolymer (Duxson, Provis et al. 2007, Rangan 2010). The growth period could also be identified as commencing during this first stage with the geopolymeric gel matrix

beginning to be formed, corresponding to the strength beginning to increase from less than 5 MPa at 4 hours to 23 MPa at 6 hours.

The second stage is identified as corresponding to the reorganization step in the geopolymeric process. This is where the gel formation continues, whilst the dissolution rate starts to reduce. The gel formation and reorganization steps release water during the growth stage which is then expelled and evaporated as less water is needed as dissolution decreases. During this stage, the temperature profile inside the specimen rises significantly from 108 °C at 6 hours to 120 °C at 10 hours as water is lost and dissolution ceases. The increased gel formation in this period is reflected in the compressive strength increase, to 34 MPa, observed at 8 and 10 hours.

The third stage corresponds to completion of the dissolution process and evaporation of the remaining water together with a cessation in gel formation and the reorganization step in the geopolymer formation. This is reflected in the slight rise in the temperature profile from 120 °C at 10 hours to 123 °C at 14 hours.

During this stage the aluminate matrix structure which is attributed as providing the compressive strength is created, with the maximum strength of 42 MPa achieved at 12 hours. At this point it is hypothesised that the evaporation of the remaining liquid leads to micro and macro crack formation within the matrix due to the excess heat, leading to a reduction in the strength to 32 MPa observed at 14 hours.

4.5.6 Microstructure properties

Microstructural examinations were undertaken to understand the characteristic of the brown coal fly ash raw material and geopolymer mortar and the mechanism of geopolymerization. Particle size analysis, Scanning Electron Microscopy (SEM), X-Ray Diffraction (XRD), Fourier Transform Infrared Spectroscopy (FTIR), Mercury intrusion porosimetry (MIP), and Zeta Potential

were used use to investigate the microstructure properties of brown coal fly ash and geopolymer mortar.

Particle distribution

The particle distribution of brown coal fly ash raw material is shown in Table 4.12. Figure 4.10 shows the particle size distribution curves for Loy Yang, Hazelwood and Yallourn together with specific surface areas.

Table 4.12 Particle size distribution of brown coal fly ash

Passing (%)	Loy Yang	Hazelwood	Yallourn
5µm	2.24	20.05	57.66
10µm	6.48	40.66	79.73
20µm	19.72	54.02	88.23
30µm	32.34	59.01	91.49
40µm	41.02	61.24	93.08
45µm	45.10	62.11	93.76
50µm	48.88	62.87	94.40
60µm	55.35	64.14	95.57
70µm	57.97	64.68	96.09
80µm	60.18	65.18	96.55
90µm	62.03	65.65	96.95

The data clearly demonstrates the variability in both morphology and surface area between the three brown coal fly ashes. It is interesting to note that even with a significantly lower surface area and less CaO the Loy Yang brown coal fly ash geopolymer mortar yielded a comparable compressive strength to class F and class C fly ash geopolymer concretes (Guo, Shi et al. 2009, Chindaprasirt, Chareerat et al. 2011, Law, Molyneaux et al. 2013). Conversely the Yallourn brown coal fly ash has a very high surface area with almost 90% of the particles passing the 20µm sieve The Yallourn brown coal fly ash also has almost three

times the surface area of the Hazelwood, but has a similar compressive strength. This would indicate that the surface area itself is not the principal factor in determining the suitability of a brown coal fly ash as a potential geopolymeric material.

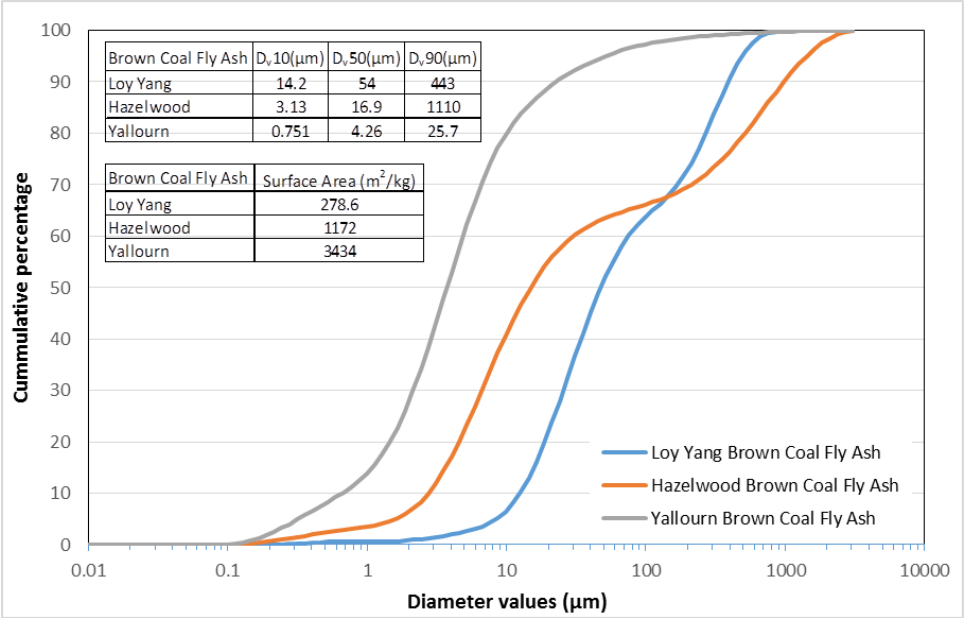

Figure 4.10 Particle distribution of brown coal fly ash

An SEM image of the raw brown coal fly ash is shown in Figure 4.11. It reflects the particle size distribution (Table 4.11). The image shows the comparison of the particle size at the same magnification. Loy Yang brown coal fly ash shows larger size particles, while Yallourn displays finer particles than Hazelwood.

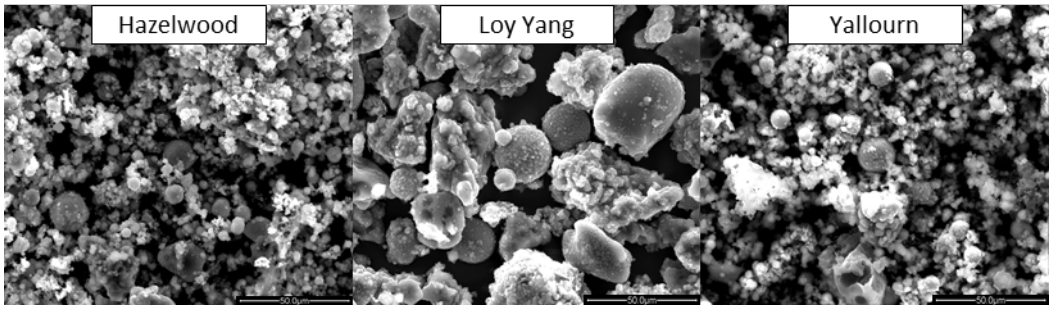

Figure 4.11 SEM image of raw brown coal fly ash

The significantly higher surface area of both Hazelwood (1172 m^2/kg) and Yallourn (3434 m^2/kg) compared to Loy Yang (278.6 m^2/kg) influence the workability variation observed (explained in this Chapter section 4.5.4). The high surface area would require more liquid content to achieve the same workability. The differences of mixture moistness and consistency for the same L/S ratio of mixture and binder (i.e Loy Yang 3, Hazelwood 2 and Yallourn 2) could be explained as a result of variation of both surface area and CaO content.

Figure 4.11 also shows fewer spherical particles in these brown coal fly ashes compared to that usually found in a typical class F fly ash. The more spherical particles of the class F fly ash give a high specific surface area providing a greater available reaction area with the calcium hydroxide (Neville 2011). This reduction in number of spherical particles is suggested as a possible reason for the lower strength of brown coal fly ash geopolymer mortar. However, despite fewer spherical particles the Loy Yang brown coal fly ash still yielded a comparable compressive strength to class F and class C fly ash geopolymer concretes (Guo, Shi et al. 2009, Chindaprasirt, Chareerat et al. 2011, Law, Molyneaux et al. 2013).

Zeta potential

As well as having a positive effect on the compressive strength CaO has been identified as influencing the zeta potential (Van Jaarsveld and Van Deventer 1999, Diaz, Allouche et al. 2010, Gunasekara, Law et al. 2014). The zeta potential is an indicator of gel formation which, in turn, determines the compressive strength. The data shows a negative zeta potential for the raw fly ash for Loy Yang and Hazelwood brown coal fly ash, and a positive potential for the Yallourn brown coal fly ash. All three materials show a negative zeta potential for the geopolymer mortar produced, Table 4.13.

Negative zeta values for the raw fly ash are attributed to the aluminates and silicates surface groups becoming deprotonated due to dissolution of CaO increasing the pH in fly ash-water system. This result in a negatively charged

surface, giving the negative zeta potential in the Loy Yang brown coal fly ash while the Hazelwood and Yallourn have high CaO content they also have a relatively low aluminosilicate content, which provides less material available to deprotonate and potentially a more positive zeta potential. It is hypothesized that the negative zeta potential of the Hazelwood mix would indicate that the aluminosilicate in the Hazelwood can be more readily deprotonated than that in the Yallourn.

Table 4.13 Zeta potential of brown coal fly ash and geopolymer mortar produced

Sample	**Zeta Potential**	
	Fly Ash	**Mortar**
Loy Yang	-14.4	-26.8
Hazelwood	-11.5	-16.0
Yallourn	+0.6	-25.0

The zeta potentials of the geopolymer mortars all gave negative zeta potentials. The Hazelwood had the smallest value, -16.0 mV, which is close to the threshold value for agglomeration. The Loy Yang and Yallourn brown coal fly ash gave similar values which would be regarded as being in the stable range for agglomeration (Riddick 1968). A small zeta potential would indicate that the geopolymer could more readily form the gel layer. This would suggest that Hazelwood brown coal fly ash should be able to readily for a geopolymer. Given the low strengths obtained this would further support the conclusion that the aluminosilicate content is insufficient to provide high strength geopolymer but could account for the ability to form a geopolymeric material despite the low aluminosilicate content. The negative zeta potentials observed for both the raw ash and the geopolymer indicate that the Loy Yang brown coal fly ash would be also expected to readily form a geopolymer. The results for the Loy Yang are consistent with those observed for class F fly ashes, giving similar strength

concrete (Gunasekara, Law et al. 2014) and further indicate that the use of Loy Yang brown coal fly ash as a geopolymeric material is feasible.

X-Ray Diffraction (XRD)

An alkaline activation is a chemical process that causes a rapid change of some partial or totally amorphous structures into compact cemented frameworks (Fernández-Jiménez and Palomo 2003). The amorphous content of fly ash has been identified as critical for the first step of the geopolymerization process as it the amorphous material that is dissolved to form the aluminosilicate gel. (Fernández-Jimenez, de la Torre et al. 2006). XRD analysis of the samples Table 4.14 shows percentages of the crystalline and amorphous phase of the different precursor brown coal fly ash materials and Figure 4.12 shows the XRF analysis.

Table 4.14 Percentage of Crystalline and Amorphous phase of XRD Analysis

Fly Ash	**Phase (%)**	
	Crystalline	**Amorphous**
Loy Yang	37.5	62.5
Hazelwood	25.6	74.4
Yallourn	13.2	86.8

The XRF shows that all of the brown coal fly ashes have different mineralogical composition. The crystalline phase of Loy Yang brown coal fly ash is dominated by Quartz (SiO_2) with only minor traces of Al_2O_3 present. However, the Hazelwood and Yallourn brown coal fly ash have no Quartz evident. Hazelwood has 31.40% of CaO, 20.59% of SO_3 and 15.85% of MgO composed of a considerable proportion of Anhydrite ($CaSO_4$) and mineral MgO, whilst Yallourn with 29.91% CaO, 19.57% of SO_3, and 15.58% of MgO contains relatively little Anhydrite. Both Hazelwood and Yallourn have similar quantities of Fe_2O_3 (16.74% and 18.20%), but only Yallourn has traces of Magnetite.

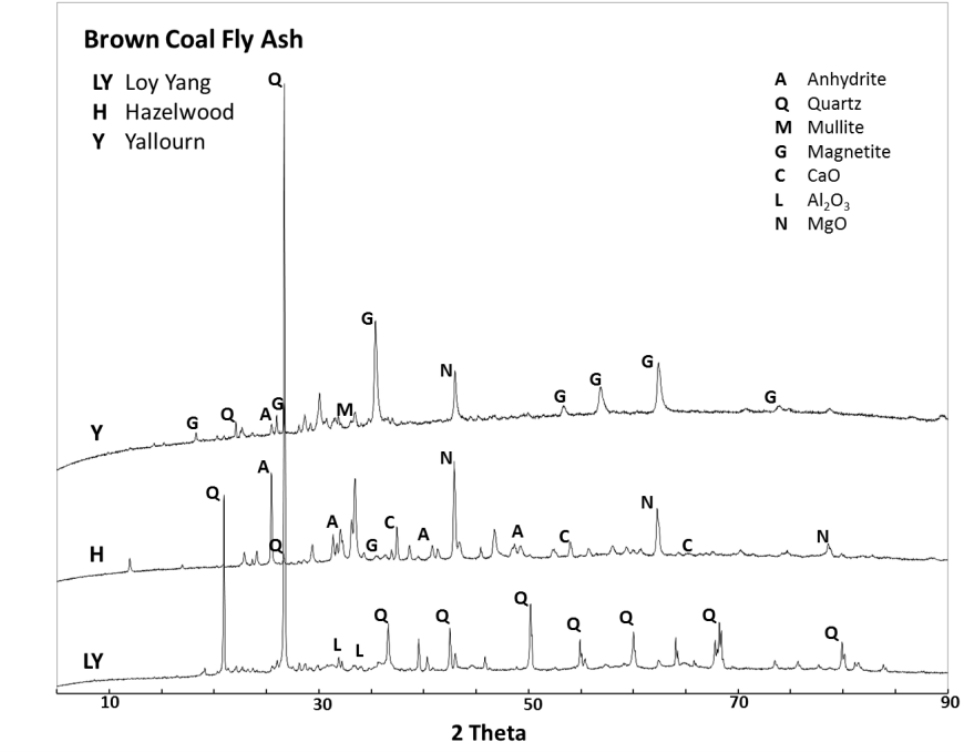

Figure 4.12 XRF analysis of brown coal fly ash

The XRD analysis of the samples also identifies the percentages of the crystalline and amorphous phase of the different precursor brown coal fly ash materials. The percentages of the crystalline phase are 37.5%, 25.6% and 13.2% respectively for Loy Yang, Hazelwood and Yallourn. This gives an amorphous percentage of 62.5%, 74.4% and 86.8% respectively for Loy Yang, Hazelwood and Yallourn. Despite having the lowest amorphous content the Loy Yang has the highest compressive strength. Overall the data indicates that the total amorphous content is not a critical factor in determining the compressive strength obtained. Rather the mineralogical composition and reactivity of the brown coal fly ash appears to have a crucial bearing on the performance.

Fourier Transform Infrared Spectroscopy (FTIR)

The presence of different mineralogical phases and the reactivity of the precursor ash and corresponding geopolymer were analysed using FTIR (Zhang, Wang et al. 2012, Valcke, Pipilikaki et al. 2015).

Fourier transform infrared (FTIR) absorption spectra were captured in the range 4000-500 cm^{-1} and recorded at a spatial resolution of 4 cm^{-1} and a scan speed of 0.2 cm/s. The FTIR spectrum which illustrates the major reaction zones of Si-O and Al-O of the precursor fly ashes and their corresponding geopolymer mortar are shown in Figure 4.13 and Figure 4.14. The corresponding geopolymers were from the optimum mix of each brown coal fly ash which are Loy Yang 3, Hazelwood 1 and Yallourn 1.

The presence of aluminium-silicate bonds and the degree of incorporation aluminium into the gel matrix after the geopolymerization are significant factors in strength development. Previous studies have reported that the aluminium-silicates peaks in the FTIR spectrum can be found in the range 1300 to 700 cm^{-1}, with the higher wavenumber peaks (1300–000 cm^{-1}) relating to a lower concentration of glassy (aluminium low) silicates and the lower wavenumber (900–700 cm^{-1}) peaks to a higher quantity of glassy (aluminium high) silicates (Zhang, Wang et al. 2012, Valcke, Pipilikaki et al. 2015).

All three brown coal fly ashes have broad peaks in the 1100–1200 cm^{-1} range, with Yallourn having two sharp peaks around 1000 cm^{-1} and Hazelwood one sharp peak around 850 cm^{-1}. This would indicate that the majority of the raw fly ash in all materials is (low) aluminium silicates. The broad peaks in this range are attributed to T-O asymmetric stretching (T = Al or Si) and overlapping peaks from the crystalline phases quartz, mullite and anhydrite (Zhang, Wang et al. 2012, Valcke, Pipilikaki et al. 2015). As such these peaks are identified as a combination of active bonds from the glassy aluminosilicates and inactive bonds from the crystalline quartz, mullite and anhydrite. The sharp peaks are identified as being from active bonds associated with (medium) aluminium silicates.

Following geopolymerization the peaks have broadened and reduced in intensity for all of the materials and generally shifted to lower frequencies, over the range 1200 to 950 cm^{-1}. The Yallourn now has a single sharp peak at approximately 875 cm^{-1} and the Hazelwood a single sharp peak at 850 cm^{-1}. All three geopolymers also have two sharp peaks at approximately 800 cm^{-1}. During geopolymerization

shifts to lower frequencies is seen as indicative of incorporation of aluminium into the silicate backbone (Phair and Van Deventer 2002).

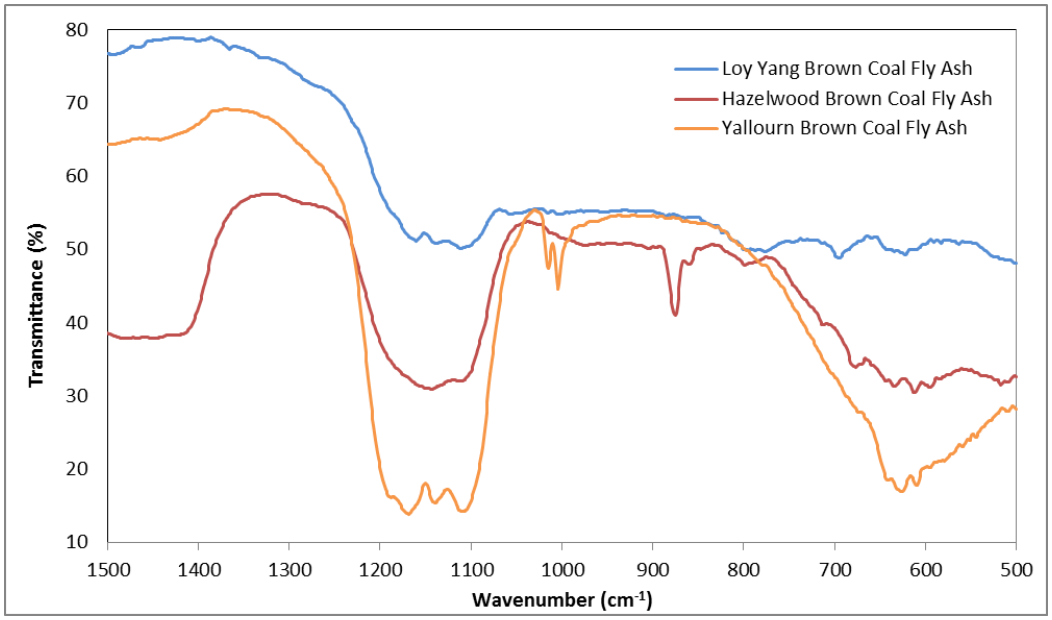

Figure 4.13 FTIR spectra of the precursor brown coal fly ash

The broadening and reduction of the peaks in the range 1200 to 950 cm^{-1} is hypothesized as being due to the reaction of the glassy aluminosilicates leading to a shift to lower frequencies, indicative of incorporation of alumina into the gel matrix. This reaction leads to the observed shift to lower frequencies for the reacted species and the reduction in intensity observed. This reaction is also associated with the sharp peaks observed for all three geopolymers noted at 800 cm^{-1} and 700 cm^{-1}. The peaks for the crystalline material remain unaltered at the same wavenumber, hence the broadening in the peak due to the overlap of the unreacted crystalline material and the reacted glassy material. The shift of the sharp peaks is in the Hazelwood and Yallourn is identified as the (aluminium medium) silicates reacting and being incorporated into the silicate backbone.

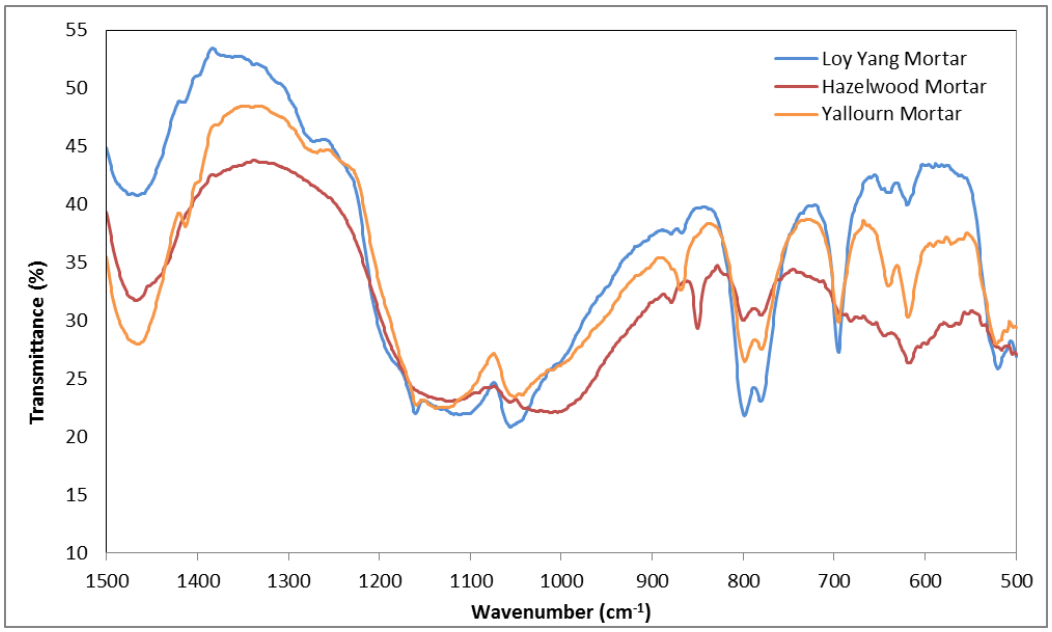

Figure 4.14 FTIR spectra of the brown coal fly ash geopolymer mortar

It is interesting to note that the most intense peak for the geopolymers at 800 cm^{-1} is for the Loy Yang brown coal fly ash geopolymer mortar which would indicate a high degree of reactivity in the fly ash and of considerable incorporation of the aluminium into the silicate backbone. The results are indicative of a high rate of release of aluminium in the case of the Loy Yang mix which has been identified as being critical (Tennakoon, Nazari et al. 2014). The rapid release of aluminium will lead to the production of a gel with a uniform composition and structure. This in turn is expected to lead to a geopolymer with higher strength, as observed for the Loy Yang brown coal fly ash geopolymer mortar.

Mercury Intrusion Porosimetry (MIP)

Porosity distribution analysis of Loy Yang brown coal fly ash geopolymer mortar was undertaken using Auto pore IV 9500 (V1.09) Micrometrics mercury intrusion porosimeter. Micrometrics MIP provides a wide range of information on the pore properties, such as pore size distribution, the total pore volume or porosity, the skeletal and apparent density, and the specific surface area of a sample (Webb

and Orr 1997). Pore size distribution of Loy Yang brown coal fly ash geopolymer mortar based on dV/dlogD pore volume and cumulative pore volume showed in Figure 4.15.

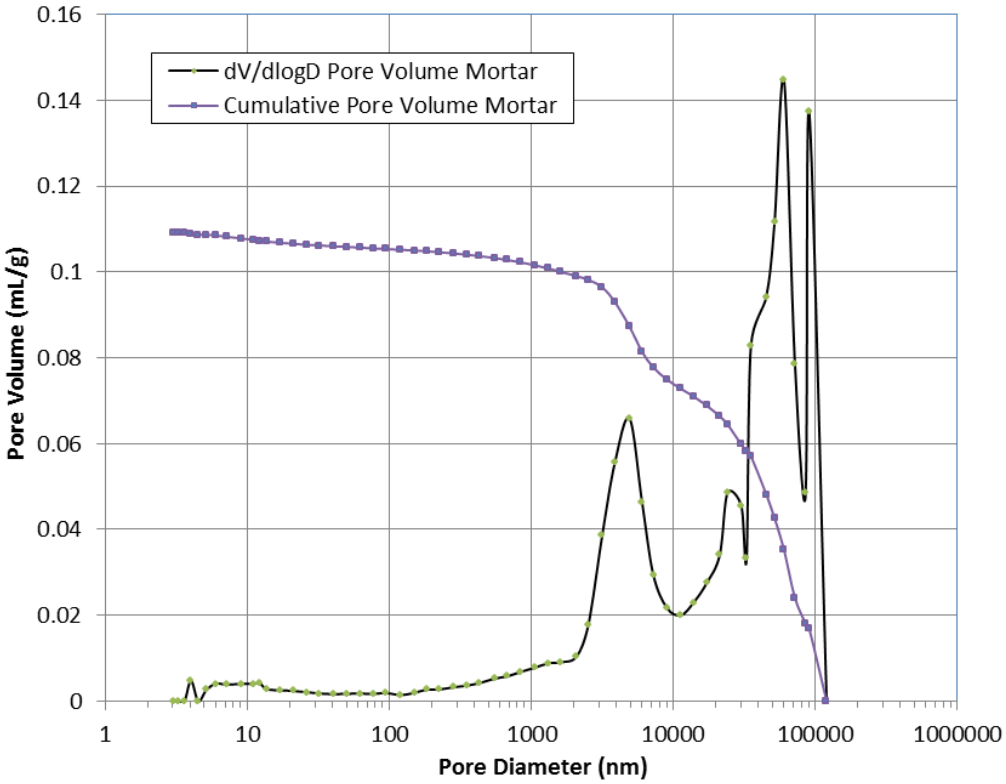

Figure 4.15 Pore size distribution of Loy Yang brown coal fly ash geopolymer mortar

Loy Yang brown coal fly ash geopolymer mortar showed a multi pore size distribution. The pore sizes measured ranged between 3 nm to 100,000 nm.

According to Sindhunata (2006), the pore structures could be divided into three groups based on the pore diameter i.e mesopores (3.6–50 nm), macropores (50–200 nm) and pores larger than 200 nm. He reported that macropores (50-200 nm) are formed during the early stage of reaction, as gel continues to form, transforming macropores into mesopores. Macropores are apparent in the fly ash based geopolymers that are cured at 'medium' temperature (50 °C). The presence of pore sizes larger than 200 nm is characteristic of less reacted

geopolymers. There are two systems which show pores larger than 200 nm: (i) geopolymers that are synthesized with alkali hydroxide solutions and (ii) geopolymers that are synthesized at low temperature (30 °C) (Sindhunata 2006). On the other hand, research on class F fly ash geopolymers has shown that the mesopores are typical pores between geopolymer phases, while micropores exist within the gel network. The macropores fills the gaps between unreacted fly ash particles (Zheng, Wang et al. 2010).

The Loy Yang brown coal fly ash geopolymer mortar shows a peak in mesopores at 4 nm, and four further peaks of pores larger than 200 nm between 1,000–100,000 nm i.e around 5,000 nm, at 24,000, 60,000 and 90,000 nm. The pores identified are principally in the macropores region, corresponding to gaps between unreacted fly ash grains and between aggregate. This would suggest that little refinement of the pore matrix has occurred within the Loy Yang brown coal fly ash geopolymer materials. While, the SEM images and the compressive strengths would indicate that some degree of refinement has occurred, the SEM micrographs do show the presence of large macropores in the matrix, correlating with the MIP data.

Elevated temperature investigation phase mapping

Quanta SEM apparatus was used to investigate the microstructural behaviour and strength evolution of Loy Yang brown coal fly ash geopolymer mortar at different curing times. The research utilised SEM with secondary electron (SE) and backscattered electron (BSE) detectors using unpolished and flat-polished epoxy impregnated specimens. Unpolished specimens from fractured or sawn surfaces used SE mode to examine the morphological nature of the surface, while polished specimen were used to identify and quantify various phases of the cementitious material using BSE mode and EDX spectroscopy (Kjellsen, Monsøy et al. 2003, Scrivener 2004).

Figure 4.16 show the microstructure image of unpolished Loy Yang brown coal fly ash geopolymer mortar specimens at 8, 10, 12 and 14 hours curing times and

Figure 4.17 the polished specimens. At 8 hours the image displays an open porous structure with a large number of unreacted fly ash grains present. A reduced number of unreacted grains was observed at 10 hours. The images at 10, 12 and 14 hours also show a more compact structure with more homogeneous structure at 12 and 14 hours.

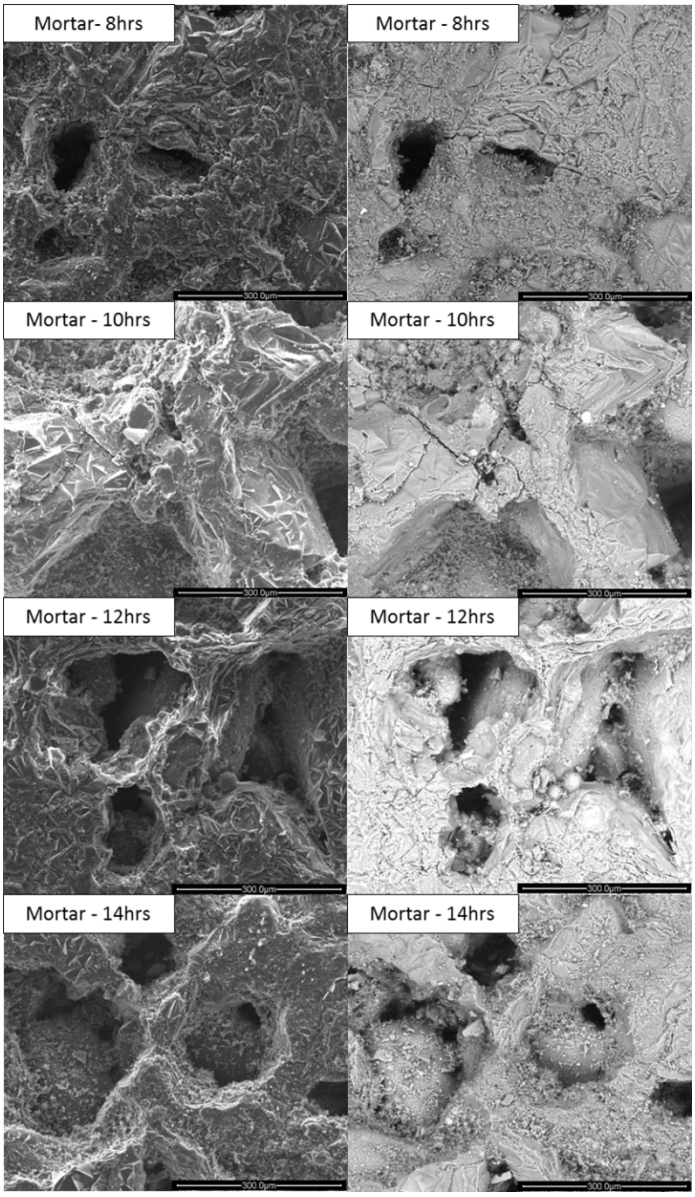

Figure 4.16 SEM unpolished specimen images of Loy Yang brown coal fly ash geopolymer mortar of different curing times at 200x magnification (left image using Secondary Electron-SE and right image using Backscattered Electron-BSE)

The SEM images correlate well with the temperature profile observed (Figure 4.9). The rapid rise in temperature observed between 6 to 10 hours corresponds to the second stage, a period of gel formation and reorganization, with the matrix going from an open porous nature to the denser homogenous structure seen at 10 hours. The reduction in the temperature rise between 10 to 14 hours corresponds to the period where an increase in the micro cracking is observed in third stage, supporting the assertion that this corresponds to evaporation of the remaining water which causes micro cracking (Brinker and Scherer 1990, Sindhunata 2006).

Figure 4.17 shows the microstructure of the specimen which is characterised by reasonably homogeneous gel structure and micro cracks. The homogeneous gel structure is attributed to the high reactivity resulting from elevated temperature curing.

The SEM images again correlate well with the temperature profile observed in Figure 4.9. At 8 hours the geopolymer displays an open porous structure with a large number of unreacted fly ash grains present. The images at 10, 12 and 14 hours show a more compact homogeneous structure, though a number of macropores are observed throughout. Some unreacted fly ash grains are still observed at 10 hours, but by 12 and 14 hours few are observed, indicating that the gelation process has reached a conclusion. Micro cracking is also observed at 10, 12 and 14 hours, with a significant increase in the number and size of the micro cracks at 14 hours.

The back scattered electron imaging and X-ray imaging (mapping) were performed on a Quanta SEM. The elemental and map phasing analysis were undertaken using an Oxford Aztec EDS attached to the SEM. The key elements in geopolymerization i.e SI, Al, and Na, in addition to the intrinsic elements of brown coal fly ash Ca and S were determined in this examination. Figure 4.18 shows the element distribution map of Loy Yang brown coal fly ash geopolymer mortar under different curing durations.

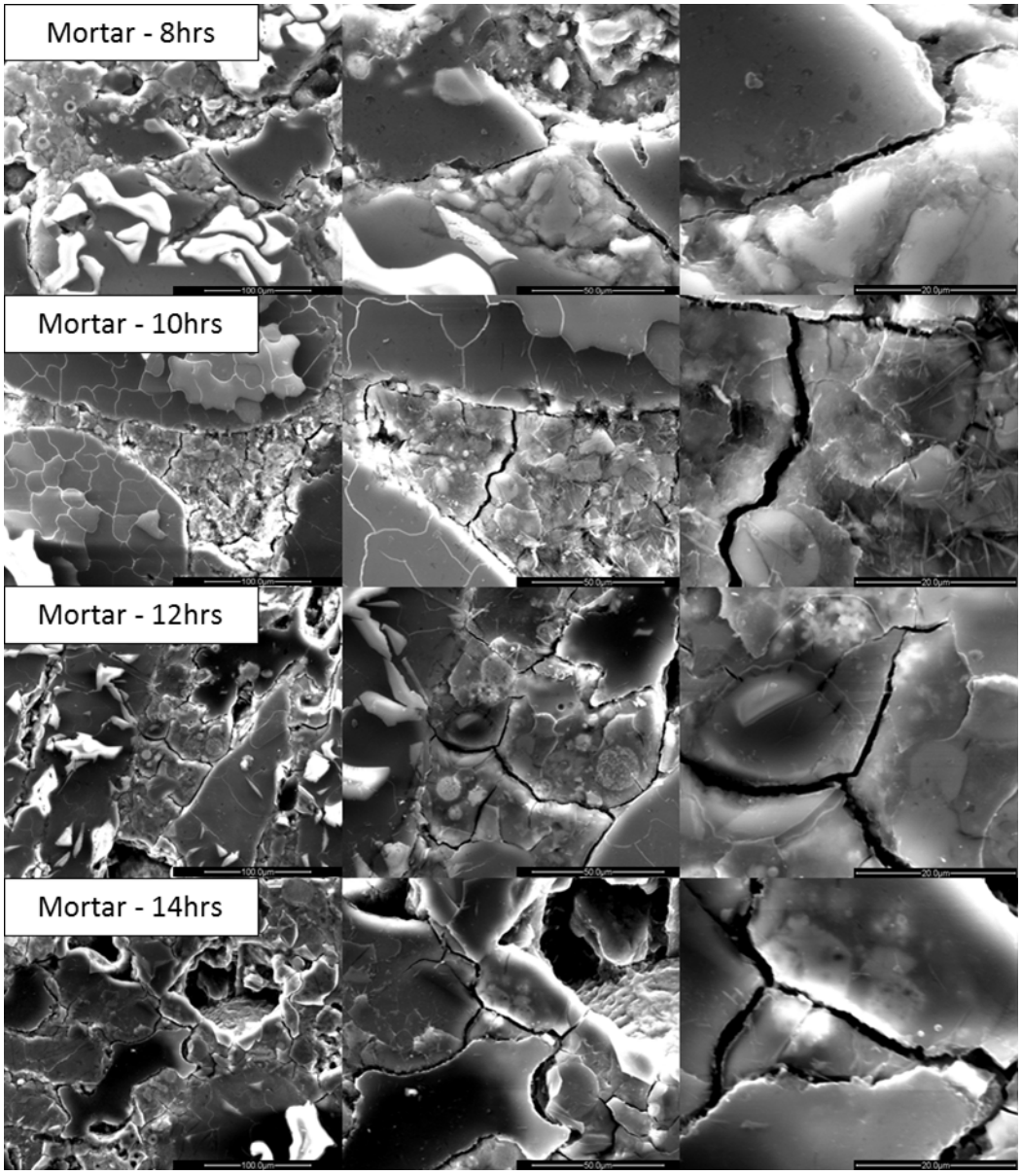

Figure 4.17 SEM Polished specimen images of Loy Yang brown coal fly ash geopolymer mortar of different curing times using Secondary Electron-SE (left side 400x magnification, middle 1000x, and right side 3000x)

Phase identification was undertaken for each sample for each curing time i.e 8, 10, 12 and 14 hours curing time. All sample exhibited an geopolymeric phase following the elevated temperature curing. A single SiAlO geopolymeric phase was observed at 8, 10 and 12 hours, while two geopolymeric phases was observed only at 14 hours. The geopolymeric phases identified, fraction, oxide

content i.e SiO_2, Al_2O_3, Na_2O, CaO and ratio are shown in Table 4.15. An example of the geopolymer phases detected is given in Figure 4.19 for a specimen after 14 hours elevated curing.

The major phase identified, with a 90.31% fraction, at 8 hours curing time was SiAlO, comprising SiO_2 52.7% and Al 24.2% corresponding to an SiO_2/Al_2O_3 ratio of 2.2. At 10 hours the major phase was identified as an 84.10% fraction and an SiO_2/Al_2O_3 ratio of 1.9 and at 12 hours having a 98.97% fraction and an SiO_2/Al_2O_3 ratio of 2.4. The SiAlO geopolymeric phase at 8, 10 and 12 hours are identified as a mixture of polysialate-siloxo (Si-O-Al-O-Si) and polysialate-disiloxo (-Si-O-Al-O-Si-O-Si-O-). The two geopolymeric phases observed at 14 hours had SiO_2/Al_2O_3 ratios of 1.6 and 1.7. As such both phases are identified as polysialate-siloxo (Si-O-Al-O-Si).

The phase analysis identification can be correlated with the stages observed in the elevated temperature profile analysis (Figure 4.9). The 8 hours curing time specimen shows three other phases i.e AlO, SiO and NaSiO. These phases are associated with the formation of the gel. Gelation has been reported as a complex mixture of silicate, aluminate and alumina silicate species formed when the species released by dissolution into the aqueous phase (Duxson, Provis et al. 2007). The NaSiO fraction is associated with the step prior to the geopolymer precursor, when the alkali silicates or hydroxides provide sodium (Na^+) ions to be incorporated into the matrix. The geopolymer precursor is identified as first step to orthosialate in the geopolymerization process (Davidovits 1994d, Rangan 2010).

The rapid rise of temperature observed at the second stage between 6 to 10 hours curing is identified as corresponding to the on-going geopolymerization process, with reduced dissolution, on-going gel formation and growth and re-organisation within the geopolymer matrix. This is reflected in the variation in SiO_2/Al_2O_3 ratio between 2.2 at 8 hours, 1.9 at 10 hours and 2.4 at 12 hours.

The decrease of the SiO_2/Al_2O_3 ratio at 14 hours is indicative of incorporation of aluminium into the silicate backbone. The incorporation of aluminium into the silicate backbone was observed for the Loy Yang brown coal fly ash geopolymer mortar in the FTIR study (described in the previous sub section of this Chapter). The results are indicative of a high rate release and incorporation of aluminium that will lead to the production of a gel with a more uniform composition and structure (Tennakoon, Nazari et al. 2014), as observed in the SEM images. This corresponds to the increase in strength observed (to the 42 MPa maximum) at 12 hours. However, at 14 hours the reduction in strength and micro-cracking observed indicate that although there has been incorporation of Al into the matrix backbone, the micro cracking has resulted in a reduction of strength.

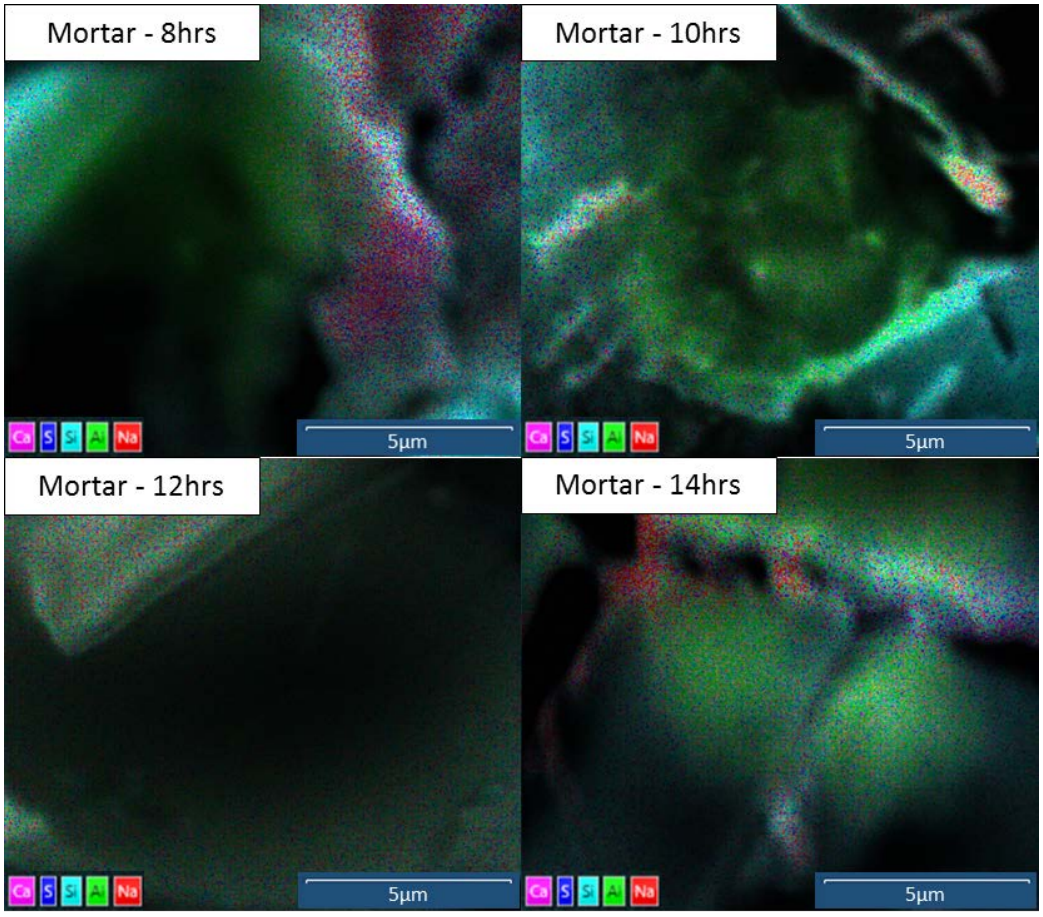

Figure 4.18 Element distribution map of Loy Yang brown coal fly ash geopolymer mortar at different elevated temperature curing time

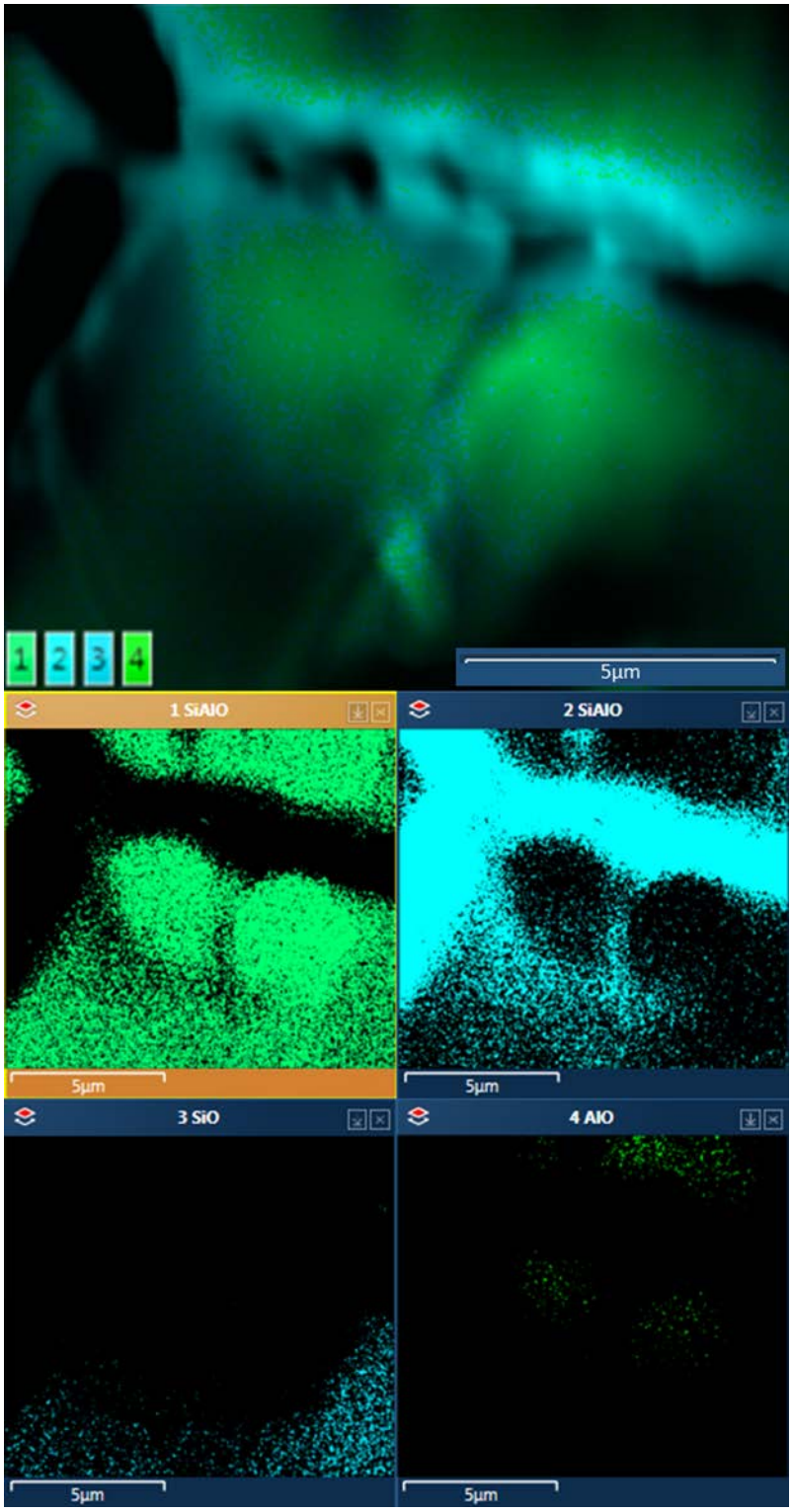

Figure 4.19 Phase mapping analysis of Loy Yang brown coal fly ash geopolymer mortar at 14 hours elevated temperature curing

Table 4.15 Geopolymer phase fraction, composition and ratio of Loy Yang brown coal fly ash geopolymer concrete from different curing time duration

Sample	Phases Fraction		Oxide (%)				SiO_2/Al_2O_3	Al_2O_3/Na_2O
	Name	(%)	SiO_2	Al_2O	Na_2	CaO		
8 hours	1 SiAlO	90.31	52.	24.2	7.4	1.5	2.2	3.3
	2 AlO	6.13	17.	66.7	-	0.9	0.3	-
	3 SiO	2.47	96.	3.3	-	-	29.3	-
	4 NaSiO	0.23	38.	5.1	37.6	-	7.5	0.1
10 hours	1 SiAlO	84.19	52.	27.8	5.7	1.3	1.9	4.9
	2 SiO	7.75	88	6.4	2.2	0.6	13.8	2.9
	3 AlSiO	7.08	25.	58.3	3.4	1.8	0.4	17.1
12 hours	1 SiAlO	98.97	51.	21.3	10.9	1.8	2.4	2.0
14 hours	1 SiAlO	48.75	47.	28.4	4.9	1.2	1.7	5.8
	2 SiAlO	46.36	41.	25.4	8.3	2.0	1.6	3.1
	3 SiO	3.37	80.	5.7	6.9	1.5	14.2	0.8
	4 AlO	0.67	14.	59.0	2.9	1.2	0.3	20.3

4.6. Summary of chapter 4

Chapter 4 on brown coal fly ash geopolymer mortar could be summarised as follows:

1) The strengths obtained from Loy Yang brown coal fly ash geopolymer mortars are comparable to those obtained from previous research on class F and class C fly ash. The strengths are indicative that brown coal fly ash geopolymer can produce compressive strengths acceptable for use in the construction industry.
2) The high CaO content of the Hazelwood and Yallourn brown coal fly ash was observed to contribute little to the strength. Coupled with the low

aluminosilicate content the compressive strength results indicate neither are feasible to use for geopolymer concrete.

3) Modified Activator Modulus (AM_m) and dosage of activator are the key parameters in determining the strength of Loy Yang brown coal fly ash geopolymer mortar.
4) Loy Yang brown coal fly ash geopolymer mortar shows a restricted range for the AM_m and dosage in order to achieve optimum compressive strength.
5) The optimum compressive strength was achieved under a curing regime of 120 °C for 12 hours following a 24 hours post mixing rest at room temperature.
6) The surface area of the fly ash influences the moistness and consistency of the mix and hence affects the workability.
7) The negative zeta potentials observed for both the raw ash and the geopolymer of Loy Yang brown coal fly ash indicate that the use of Loy Yang brown coal fly ash as a geopolymeric material is feasible.
8) The Fourier transform infrared (FTIR) analysis of Loy Yang brown coal fly ash geopolymer mortar indicates a high degree of reactivity in the fly ash and of considerable incorporation of the aluminium into the silicate backbone. This is attributed as the primary reason for the high compressive strengths observed for the Loy Yang brown coal fly ash geopolymer mortar.
9) The porosity distribution analysis of Loy Yang brown coal fly ash geopolymer mortar identified pores principally in the macropores region correlating with the SEM micrograph.

The temperature profile of elevated temperature curing could be divided into three stages which correlated well with the geopolymeric reaction mechanism reported from previous studies, and reflected appropriately with SEM microstructural analysis and the phase mapping investigation.

References

AS3600 (2001). Concrete Structures. AS3600. Sydney, Australia, Australian Standard

Bakharev, T. (2005). "Geopolymeric materials prepared using Class F fly ash and elevated temperature curing." Cement and Concrete Research 35(6): 1224-1232.

Brinker, C. J. and G. W. Scherer (1990). Sol-gel science : the physics and chemistry of sol-gel processing. Boston, Academic Press.

Chindaprasirt, P., T. Chareerat, S. Hatanaka and T. Cao (2011). "High-Strength Geopolymer Using Fine High-Calcium Fly Ash." Journal of Materials in Civil Engineering 23(3): 264-270.

Chindaprasirt, P., T. Chareerat and V. Sirivivatnanon (2007). "Workability and Strength of coarse high calcium fly ash geopolymer." Cement and Concrete Composites 29(3): 224-229.

Davidovits, J. (1994d). Properties of geopolymer cements. First international conference on alkaline cements and concretes.

Diaz, E., E. Allouche and S. Eklund (2010). "Factors affecting the suitability of fly ash as source material for geopolymers." Fuel 89(5): 992-996.

Dirgantara, R., D. Law, T. Molyneaux and D. Kong (2013). Brown coal fly ash geopolymer mortar. ACMSM 22, Sydney, CRC Press.

Duxson, P., A. Provis, J. L. Lukey, G. C. Van Deventer, A. Fernández-Jiménez and J. S. J. Palomo (2007). "Geopolymer technology: The current state of the art." Journal of Materials Science 42(9): 16.

Fernández-Jimenez, A., A. G. de la Torre, A. Palomo, G. López-Olmo, M. M. Alonso and M. A. G. Aranda (2006). "Quantitative determination of phases in the alkali activation of fly ash. Part I. Potential ash reactivity." Fuel 85(5–6): 625-634.

Fernández-Jiménez, A. and A. Palomo (2003). "Characterisation of fly ashes. Potential reactivity as alkaline cements." Fuel 82(18): 2259-2265.

Fernández-Jiménez, A. and A. Palomo (2005). "Composition and microstructure of alkali activated fly ash binder: Effect of the activator." Cement and Concrete Research 35(10): 1984-1992.

French, D. and J. Smitham (2007). Fly Ash Characteristics and Feed Coal Properties. Pullenvale, Qld 4069, Australia, Cooperative Research Centre for Coal in Sustainable Development.

Gunasekara, C., D. Law and S. Setunge (2014). Effect of composition of fly ash on compressive strength of fly ash based geopolymer mortar. 23rd Australasian Conference on the Mechanics of Structures and Materials (ACMSM23), Byron Bay.

Gunasekara, C., D. W. Law, S. Setunge and J. G. Sanjayan (2015). "Zeta potential, gel formation and compressive strength of low calcium fly ash geopolymers." Construction and Building Materials 95: 592-599.

Guo, X., H. Shi, L. Chen and W. A. Dick (2009). Performance and Mechanism of Alkali-Activated Complex Binders of High-Ca Fly Ash and other Ca-Bearing Materials. 2009 World Of Coal Ash (WOCA) Conference. Lexington, KY, USA.

Hardjito, D. and B. V. Rangan (2005). Development and Properties of Low-Calcium Fly Ash-Based Geopolymer Concrete, Research Report GC 1. Perth, Australia, Curtin University of Technology.

Hardjito, D., S. E. Wallah, D. M. Sumajouw and B. V. Rangan (2004). "On the development of fly ash-based geopolymer concrete." ACI Materials Journal-American Concrete Institute 101(6): 467-472.

Ivan Diaz-Loya, E., E. N. Allouche and S. Vaidya (2011). "Mechanical Properties of Fly-Ash-Based Geopolymer Concrete." ACI Materials Journal 108(3).

Kjellsen, K., A. Monsøy, K. Isachsen and R. Detwiler (2003). "Preparation of flat-polished specimens for SEM-backscattered electron imaging and X-ray microanalysis—importance of epoxy impregnation." Cement and Concrete Research 33(4): 611-616.

Law, D. W., T. K. Molyneaux, A. Wardhono, R. Dirgantara and D. Kong (2013). The Use Brown Coal Fly Ash To Make Geopolymer Concrete. ACCTA 2013, Johannesburg.

Li, X., X. Ma, S. Zhang and E. Zheng (2013). "Mechanical Properties and Microstructure of Class C Fly Ash-Based Geopolymer Paste and Mortar." Materials 6(4): 1485-1495.

Macphee, D. E., C. J. Black and A. H. Taylor (1993). "Cements Incorporating Brown Coal Fly Ash from The Latrobe Valley Region of Victoria, Australia." Cement and Concrete Research 23(3): 507-517.

Neville, A., M. (2011). Properties of Concrete. England, Pearson Education Limited.

Palomo, A., M. W. Grutzeck and M. T. Blanco (1999). "Alkali-activated fly ashes: A cement for the future." Cement and Concrete Research 29(8): 1323-1329.

Phair, J. and J. Van Deventer (2002). "Effect of the silicate activator pH on the microstructural characteristics of waste-based geopolymers." International Journal of Mineral Processing 66(1): 121-143.

Rangan, B. V. (2010). Fly Ash-Based Geopolymer Concrete. The International Workshop on Geopolymer Cement and Concrete, Mumbai, India.

Riddick, T. M. (1968). "Control of colloid stability through zeta potential." Blood 10(1).

Scrivener, K. L. (2004). "Backscattered electron imaging of cementitious microstructures: understanding and quantification." Cement and Concrete Composites 26(8): 935-945.

Sindhunata (2006). A Conceptual Model of Geopolymerisation. PhD, The University of Melbourne.

Sindhunata, J. Van Deventer, G. Lukey and H. Xu (2006). "Effect of curing temperature and silicate concentration on fly-ash-based geopolymerization." Industrial & Engineering Chemistry Research 45(10): 3559-3568.

Skavara, F., L. Kopecky, J. Nemecek and Z. Bittnar (2006). "Microstructure of Geopolymer Materials Based on Fly Ash." Ceramics − Silikáty 50(4): 7.

Tennakoon, C., A. Nazari, J. G. Sanjayan and K. Sagoe-Crentsil (2014). "Distribution of oxides in fly ash controls strength evolution of geopolymers." Construction and Building Materials 71(0): 72-82.

Valcke, S. L., P. Pipilikaki, H. R. Fischer, M. H. Verkuijlen and E. R. van Eck (2015). "FT-IR and 29Si-NMR for evaluating aluminium–silicate precursors for geopolymers." Materials and Structures 48(3): 557-569.

Van Jaarsveld, J. and J. Van Deventer (1999). "Effect of the alkali metal activator on the properties of fly ash-based geopolymers." Industrial & Engineering Chemistry Research 38(10): 3932-3941.

Wang, K., S. P. Shah and A. Mishulovich (2004). "Effects of curing temperature and NaOH addition on hydration and strength development of clinker-free CKD-fly ash binders." Cement and concrete research 34(2): 299-309.

Webb, P. A. and C. Orr (1997). Analytical methods in fine particle technology, Micromeritics Instrument Corp.

Zhang, Z., H. Wang and J. L. Provis (2012). "Quantitative study of the reactivity of fly ash in geopolymerization by FTIR." Journal of Sustainable Cement-Based Materials 1(4): 154-166.

Zheng, L., W. Wang and Y. Shi (2010). "The effects of alkaline dosage and Si/Al ratio on the immobilization of heavy metals in municipal solid waste incineration fly ash-based geopolymer." Chemosphere 79(6): 665-671.

CHAPTER 5

BROWN COAL FLY ASH GEOPOLYMER CONCRETE

5.1. Overview

This chapter presents research on Loy Yang brown coal fly ash geopolymer concrete. The research presented in this chapter uses brown coal fly ash from Loy Yang power plant in Victoria, Australia. The Loy Yang brown coal fly ash geopolymer concretes were produced based on the optimum mix from Loy Yang brown coal fly ash geopolymer mortar specimens, Chapter 4. The mechanical properties, durability and factors affecting these properties were examined for the Loy Yang brown coal fly ash geopolymer concrete.

5.2. Materials, mix design and proportions

Brown coal fly ash from Loy Yang power station was used, and the properties of Loy Yang brown coal fly ash are described in Chapter 3 Section 3.2.1.

The solution used as alkaline activator is a combination of sodium hydroxide (NaOH) and sodium silicate (Na_2SiO_3). The properties of sodium silicate and sodium hydroxide are presented in Chapter 3 Section 3.2.2.

The combined aggregates used for the Loy Yang brown coal fly ash geopolymer concrete were combination of fine aggregate (sand), coarse aggregates 7 mm and 10 mm. The aggregates used for the mixes were in an oven dried condition. Typical grading of the fine aggregate and coarse aggregate are shown in Table 3.5 in Chapter 3 Section 3.2.4.

The mix design for Loy Yang brown coal fly ash geopolymer concrete is based on the optimum mix composition Loy Yang 3 mortar (Table 4.3 in Chapter 4 Section 4.3.1). Using the Loy Yang 3 mix the fine aggregate (sand) proportion was substituted by a combination of aggregates: 43% of fine aggregate, 38% of 10 mm and 19% of 7 mm coarse aggregates (Table 3). The percentages of combined

aggregates were adopted from previous research at RMIT with same source of the aggregates (Adam 2009). The mix design proportions of Loy Yang brown coal fly ash geopolymer concrete in mass (kg) per m^3 mix is given in Table 5.1. Table 5.2 shows the proportion of combined aggregates.

Table 5.1 Mix design of Loy Yang brown coal fly ash geopolymer concrete, Mass (kg) per m^3 mix

Mixture	Fly Ash	Aggregates	Na_2SiO_3	NaOH
Loy Yang 3	279.0	1677.3	363.1	21.0

Table 5.2 Mix design with aggregates proportion of Loy Yang brown coal fly ash geopolymer concrete, Mass (kg) per m^3 mix

Mixture	Fly Ash	Aggregates			Na_2SiO_3	NaOH
		Fine	7mm	10mm		
Loy Yang 3	279.0	721.2	318.7	637.4	363.1	21.0

5.3. Mixing, curing and testing

The mixing was as described in Chapter 3 Section 3.5.2. Elevated temperature curing was applied to the specimens as described in Chapter 3 Section 3.5.3. Compressive strength measurements of concrete were performed on a Universal Testing Machine with initial stroke of 1 mm/min in accordance with AS 1012.9 standard (AS-1012.9 1999). Three cubes were tested at 28 days after casting.

5.4. The compressive strength results and variability

The compressive strength of Loy Yang brown coal fly ash geopolymer concrete obtained ranges from 52.08 MPa at 56 days to 60.38 MPa at 90 days (Table 5.3). The maximum strengths of geopolymer concrete obtained are equivalent to those obtained from geopolymer mortar using the same composition of Loy Yang brown coal fly ash (Loy Yang 3 mixture). The strengths of geopolymer concrete

are also consistent with those specified in AS 3600 for exposure category B1 and B2 which are indicative that Loy Yang brown coal fly ash can produce geopolymer concrete with compressive strengths acceptable for use in the construction industry (AS3600 2001).

Table 5.3 The compressive strength of Loy Yang brown coal fly ash geopolymer mortar

Mixture	**Compressive strength (MPa)**						
	7 days		**56 days**		**90 days**		**Average**
	Mean	SD	Mean	SD	Mean	SD	
Loy Yang	59.59	3.49	52.08	3.88	60.38	0.46	57.35

The results show minimal variation of geopolymer concrete between 7 and 90 days, which would be expected due to the elevated curing temperatures applied. This is consistent with the variation observed for geopolymer mortar specimen (Chapter 4 Section 4.5.1), and similar findings have been reported by other authors (Palomo, Grutzeck et al. 1999, Bakharev 2005, Sindhunata, Van Deventer et al. 2006).

However, a wide variation of strength was observed when the volume of mix was increased and a second batch of fly ash supplied from the Loy Yang power plant was used. Table 5.4 shows the variation of strength of Loy Yang brown coal fly ash geopolymer concrete.

A significant variation in the chemical composition between the two batches and within the second batch was found, despite the materials being from the same source (Table 5.5). The data shows significant variations with the SiO_2 content varying from 47.52% (Loy Yang Batch 1) to 67.53% (Loy Yang Batch 2 sample D), the Al_2O_3 content varying from 17.29% (Loy Yang Batch 1) to 8.53% (Loy Yang Batch 2 sample D) and the total SiO_2 + Al_2O_3 content varying from 76.06% (Loy Yang Batch 2 sample D) to 63.2% (Loy Yang Batch 2 sample B).

Table 5.4 The compressive strength of Loy Yang brown coal fly ash (from different batch) geopolymer concrete at 28 days

Mixture	Compressive strength (MPa)		Mass (kg)
	Mean	SD	
Loy Yang Batch 1	43.81	4.31	26.881
Loy Yang Batch 2 – A	29.38	6.62	53.884
Loy Yang Batch 2 – B	23.76	2.73	61.581
Loy Yang Batch 2 – C	31.41	7.72	34.488
Loy Yang Batch 2 – D	13.29	4.43	29.569

Table 5.5 Chemical composition of Loy Yang brown coal fly ash from different batch and package

Oxide %	Loy Yang Brown Coal Fly Ash				
	Batch 1	Batch 2			
		A	B	C	D
SiO_2	47.52	51.92	49.66	52.96	67.53
Al_2O_3	17.29	12.42	13.54	12.69	8.53
Fe_2O_3	5.98	6.84	7.05	7.06	4.54
CaO	2.25	2.47	2.57	2.35	1.23
MgO	4.63	4.13	4.34	4.06	2.28
K_2O	0.50	0.51	0.46	0.48	0.51
Na_2O	6.26	5.24	5.29	5.50	3.63
TiO_2	1.26	1.23	1.17	1.21	1.15
P_2O_5	0.74	0.71	0.58	0.47	0.82
SO_3	13.03	13.86	14.73	12.42	9.09
Cl_2O	0.44	0.54	0.51	0.73	0.56
Mn_2O	0.10	0.15	0.09	0.10	0.14

Using the chemical composition variation of Loy Yang brown coal fly ash batch 2 (Table 3.1), the key parameter in controlling the strength of the Loy Yang brown

coal fly ash geopolymer mortar such as AM_m, dosage of activator, SiO_2/Al_2O_3, and Na_2O/Al_2O_3 were calculated (Table 5.6).

Table 5.6 Activator modulus, dosage of activator, SiO_2/Al_2O_3, and Na_2O/Al_2O_3 ratios of Loy Yang brown coal fly ash (from different batch) geopolymer concrete mixture

Mixture	Activator		Ratio	
	Modulus (AM_m)	Dosage (%)	SiO_2/Al_2O_3	Na_2O/Al_2O_3
Loy Yang Batch 1	3.078	0.297	4.961	1.611
Loy Yang Batch 2 – A	3.359	0.283	7.260	2.161
Loy Yang Batch 2 – B	3.269	0.284	6.493	1.986
Loy Yang Batch 2 – C	3.366	0.287	7.188	2.136
Loy Yang Batch 2 – D	4.192	0.262	12.401	2.958

Figure 5.1 – Figure 5.4 compare the compressive strength of Loy Yang brown coal fly ash geopolymer mortar and concrete graphs in relation to the AM_m, dosage of activator, SiO_2/Al_2O_3, and Na_2O/Al_2O_3.

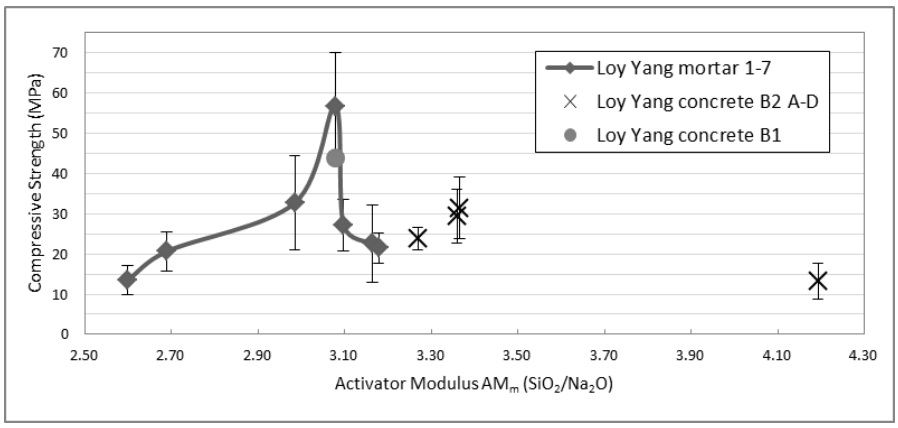

Figure 5.1 The compressive strength vs Alkali Modulus (AM_m) of Loy Yang brown coal fly ash geopolymer mortar and concrete

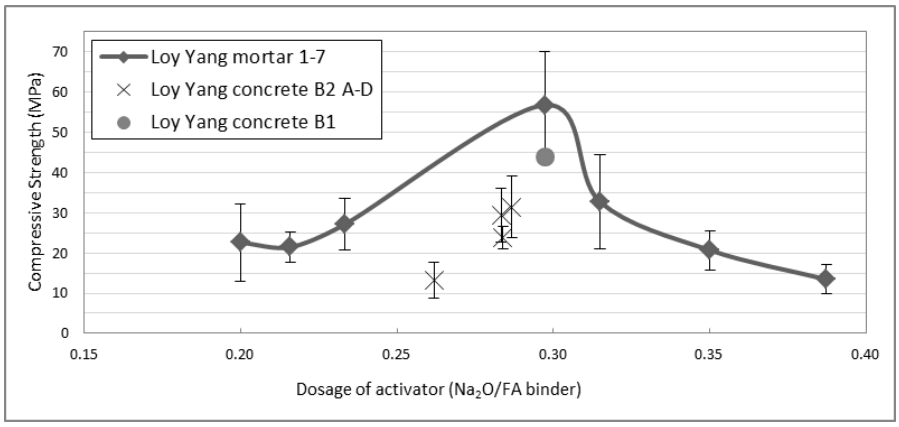

Figure 5.2 The compressive strength vs Dosage of activator of Loy Yang brown coal fly ash geopolymer mortar and concrete

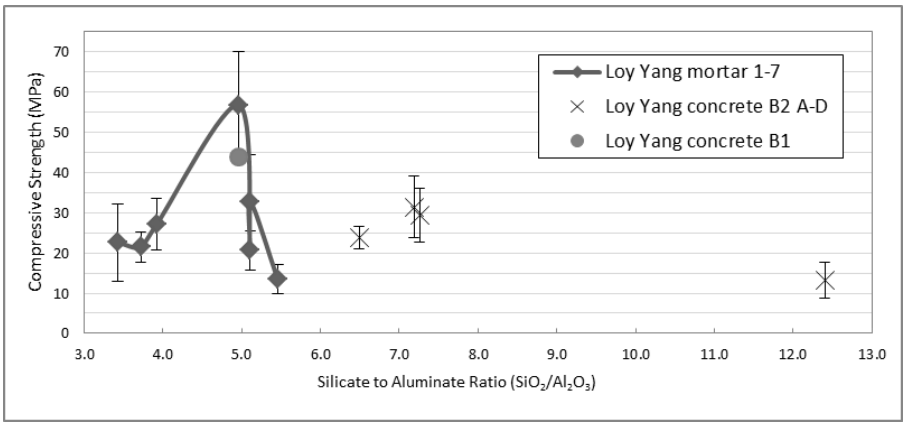

Figure 5.3 The compressive strength vs SiO_2/Al_2O_3 ratio of Loy Yang brown coal fly ash geopolymer mortar and concrete

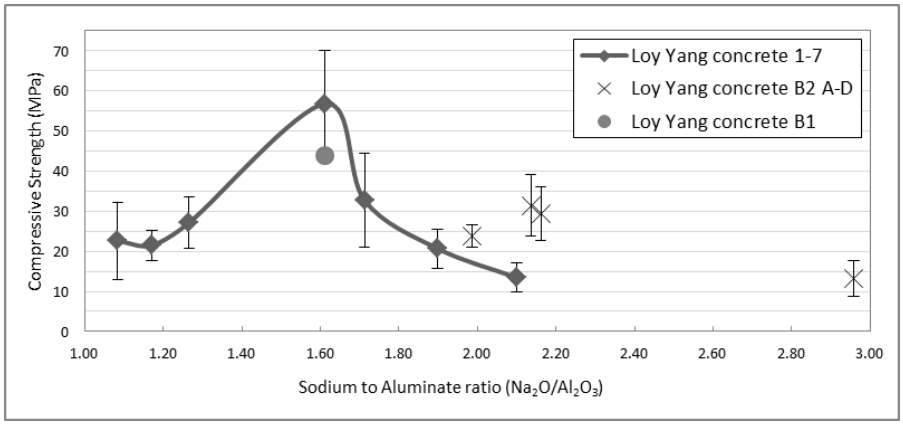

Figure 5.4 The compressive strength vs Na_2O/Al_2O_3 ratio of Loy Yang brown coal fly ash geopolymer mortar and concrete

The results demonstrate that the compressive strength of geopolymer concrete produced from Batch 1 (geopolymer mortar) is significantly higher than that produced from Batch 2. In particular Figure 5.1 shows that the AM_m of the Loy Yang Batch 2 mixes were outside the range identified as optimal for the Loy Yang brown coal fly ash geopolymer mortar mixes. Similarly the SiO_2/Al_2O_3 and Na_2O/Al_2O_3 for Batch 2 falls outside the range of the mortar samples, though two ratios of Na_2O/Al_2O_3 do fall within the range studied for the mortar. This would suggest that the AM_m and SiO_2/Al_2O_3 are influential in the performance but that the Na_2O/binder and Na_2O/Al_2O_3 do not have as such a significant influence on the strength of geopolymer produced.

Overall the data illustrate how the inherent variations in the material composition can affect the properties of the geopolymer produced. In particular the effect they can have on the AM_m. Only the lowest value of AM_m of the specimens (mix Loy Yang Batch 1) is in the region corresponding to compressive strength above 40 MPa.

Two possible alternative methods to address this variation are suggested;

1. Treatment of the raw fly ash such as refining the material prior to adoption in the geopolymerization. This could be employed to ensure that the composition of the fly ash remained within the parameters identified for the optimised mix design.
2. Optimisation of the mix design based on the chemical composition of the raw fly ash supplied.

Both alternatives however have drawbacks. In option one it may not be feasible to produce an acceptable material using refining due to the distribution of the chemical elements within the fly ash grains. In option 2 it may not be feasible to produce an optimised mix design given that the data has shown that the geopolymer is highly sensitive to the AM_m, which may be difficult to achieve. In

both cases the cost and time may affect the commercial viability of the production.

It is further hypothesized that the increase in volume of the sample sizes has contributed to the variations in strength observed. Table 5.4 shows that the smallest mix Loy Yang Batch 1 provided the highest compressive strength of above 40MPa. The small volume may enable better mixing of the materials. In particular given the relatively large size of the Loy Yang brown coal fly ash particles intimate contact between the activator solution and the fly ash would be anticipated to enable efficient dissolution of the fly ash particles. In a larger mix this may not be achieved to such a high degree.

Another factor that may influence the geopolymerization is the curing temperature. Previous research has shown that a curing temperature of 120 ^{o}C is required to optimise the compressive strength, with significantly lower strength achieved at 80 ^{o}C (Law, Molyneaux et al. 2013). Temperature profiles in the 50 mm cube specimens had shown that a temperature in excess of 100 ^{o}C was achieved within 2 hours, however in significantly larger concrete specimens it may be that the internal temperature is not sufficient to promote the geopolymerization.

5.5. Elevated temperature curing investigation

To investigate the effect of curing duration on compressive strength, similar testing to that for 50 mm cubes geopolymer mortar and concrete specimens were undertaken for 100, 200 and 300 mm cubes. A temperature probe was set up at a range of depths along the center line of the specimen to monitor the temperature profile of the specimen during the heat curing, the method is described on Chapter 3 Section 3.5.4. The temperature probe was monitored through a data logger coupled with a PC.

Figure 5.5 shows the temperature variation in the center of the 50 mm cubes concrete specimen with time compared to mortar specimens (described on

Chapter 4 Section 4.5.5). There was slight difference of temperature profile between mortar and concrete specimens. Both profiles show that by 2 hours the internal temperature had exceeded 100 °C, followed a steady rise to 110 °C at 6 hours, then a more rapid rise to 120 °C between 6 to 10 hours and followed by a slow rise in temperature to just below 125 °C at 14 hours. The profile of 50 mm cube concrete specimen reflected the geopolymerization process hypothesised for mortar specimens. That is the initial rise in temperature corresponds with the dissolution process with little gel formation, then as the internal temperature exceeds 100 °C this corresponds with gelation which is accelerated by the heat curing. As the gel forms the solution is reduced due to evaporation which corresponds to a more rapid rise in temperature within the mortar up to 12 hours, when the maximum strength is achieved. At this point, the geopolymer matrix has been established and gel formation reduced. As the time progresses the evaporation of the remaining liquid leads to crack formation within the matrix due to the excess heat, leading to a reduction in the strength at 14 hours.

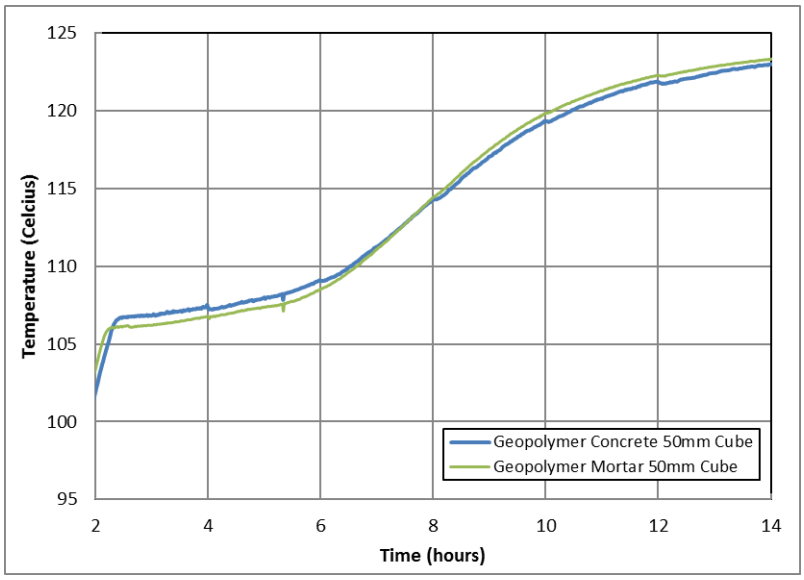

Figure 5.5 Temperature at the center of 50 mm cubes Loy Yang brown coal fly ash geopolymer concrete and mortar vs time.

It was observed that the temperature profile of 50 mm cubes mortar and concrete specimens were very different to profile of the larger size specimen. Figure 5.6 shows the temperature profile at the center of 100, 200 and 300 mm cubes specimens over a 24 hour curing period compared to 50 mm cube specimen.

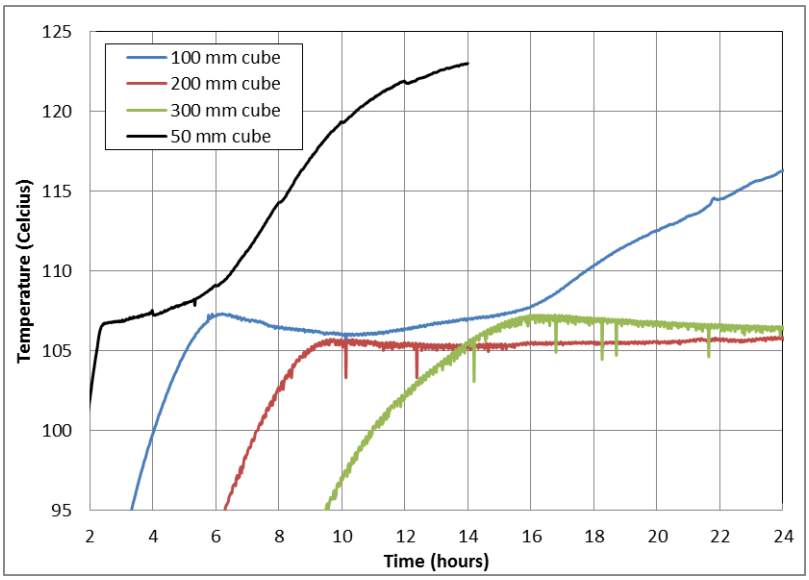

Figure 5.6 Temperature at center of the 50, 100, 200 and 300 mm cubes specimens of Loy Yang brown coal fly ash geopolymer concrete vs time

The temperature profiles of Figure 5.6 show the internal temperature exceeded 100 °C at different times e.g. 4 hours for 100 mm cube, 7 hours for 200 mm cube and 11 hours for 300 mm cube. All specimens subsequently rose to above 105 °C. While the 50 mm cube continued to rise slowly till 6 hours and then displayed a rapid rise. The 100, 200 and 300 mm cubes all showed a slight drop in temperature of 1–2 °C before remaining constant in the 105 to 107 °C range. The 100 mm cube displayed a steady rise in temperature from 16 hours until 24 hours, the temperature exceeding 115 °C at this point. Both the 200 and 300 mm cubes maintained a constant temperature until 24 hours.

The temperature profiles would suggest that the gelation, matrix forming process, is still underway in the larger sized specimens, suggesting that the geopolymerization process is not complete at the center even after 24 hours heat curing at 120 °C. This could account for the lower compressive strengths observed. In addition failure of some of the 200x200x100 mm^3 and 300x300x100 mm^3 specimens were observed on demoulding, again indicative that geopolymerization is not complete (Figure 5.7), as structural integrity was not achieved.

Figure 5.7 Broken specimen Loy Yang brown coal fly ash geopolymer concrete when demoulded

Figure 5.8 – Figure 5.10 show the temperature profile at different locations within the 100, 200 and 300 mm cubes specimens over a 24 hour curing period.

Figure 5.8 shows temperature profiles of 100 mm cube specimen of Loy Yang brown coal fly ash geopolymer concrete at 25, 50 (center) and 75 mm depths. The profiles show the internal temperature exceeded 100 °C at around 4 hours.

The profile of 100 mm cube is similar to the 50 mm cube concrete specimen, with longer duration before a cessation in gel formation between 14–16 hours. A similar profile is observed at all depths.

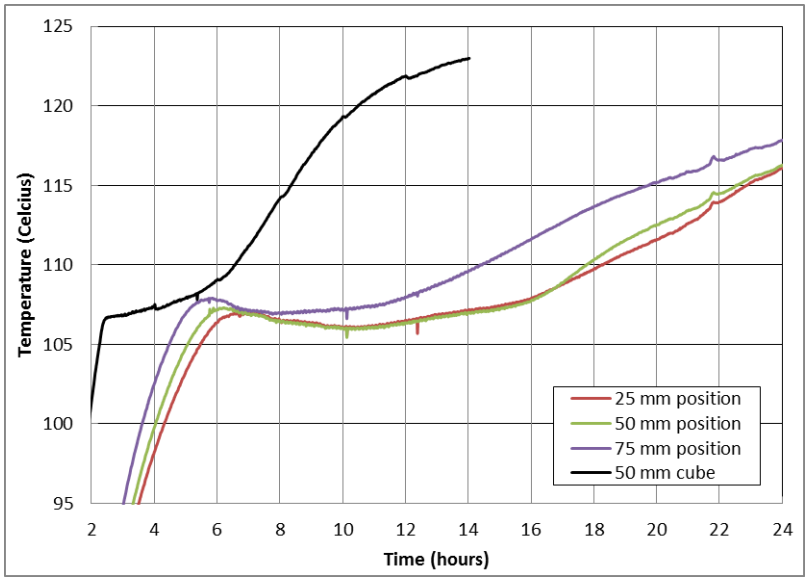

Figure 5.8 Temperature at 25, 50 and 75 mm position, Loy Yang brown coal fly ash 100 mm cube geopolymer concrete vs time.

Figure 5.9 and Figure 5.10 show the temperature profiles of 200 and 300 mm cubes specimens of Loy Yang brown coal fly ash geopolymer concrete at 25 mm depth increments.

The profiles show the internal temperature exceeded 100 °C after 8 hours for 200 mm cube and 11 hours for 300 mm cube. The 200 mm cube profile shows a drop followed by a slight steady rise in temperature between 105 and 110 °C up to 24 hours, for all locations other than at 25 mm which show a constant steady rise throughout. In the 300 mm cube all the probes show a slight drop in temperature, other than the 50 mm measurement which shows a steady rise (Note no 25 mm data available for this specimen). Both profiles indicate that other than at the surface of the mix the temperature remains constant or falls slightly, remaining in the 105 – 107 ^{o}C range.

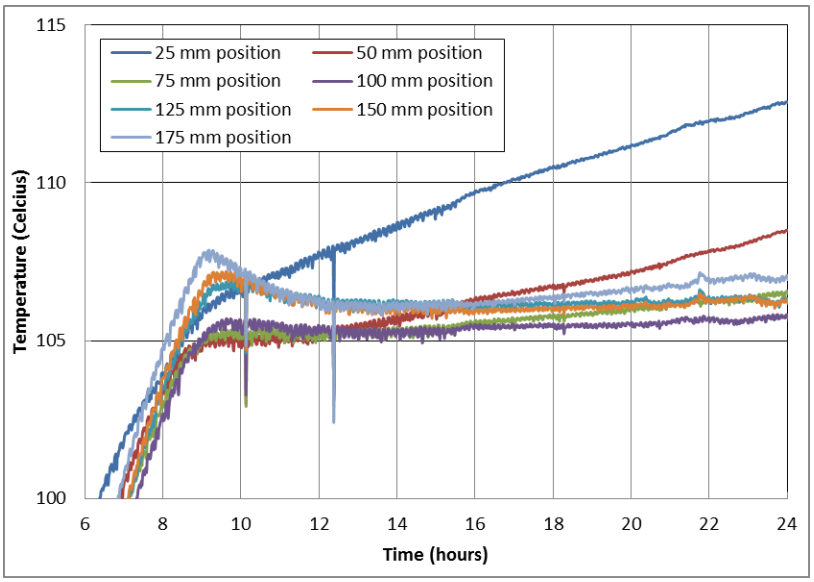

Figure 5.9 Temperature at different position Loy Yang brown coal fly ash 200 mm cube geopolymer concrete vs time.

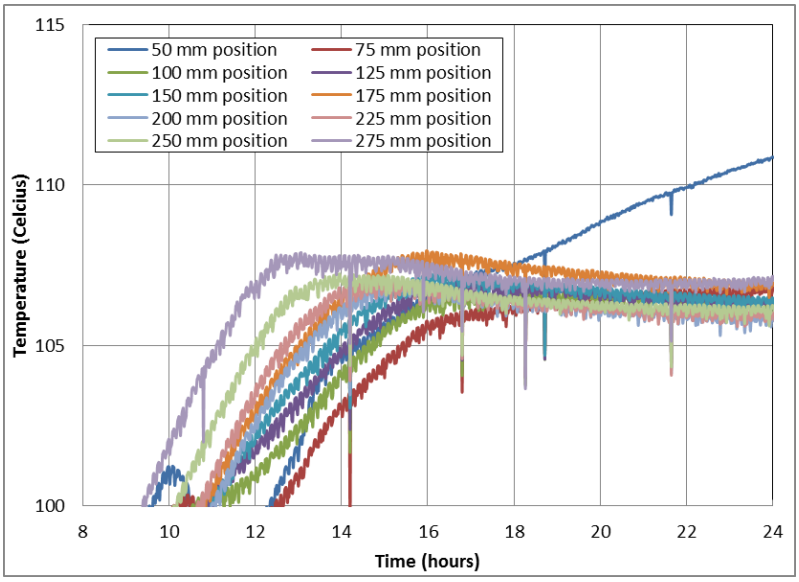

Figure 5.10 Temperature at different position Loy Yang brown coal fly ash 300 mm cube geopolymer concrete vs time.

That would support the hypothesis that gelation has not been completed within the larger mixes and the geopolymerization is still on going. This is further supported by analysis of a cross-section of 300x300x100 mm^3 specimen which

showed unreacted material at the center of the specimen (Figure 5.11). Figure 5.11 also shows macropores in the geopolymer structures (discussed in Section 5.6). This unreacted material would account for the failure in the specimens when demoulded and indicate that for large mixes longer curing times may be required.

Figure 5.11 Cross section of 300x300x100 mm^3 specimen of Loy Yang brown coal fly ash geopolymer concrete.

5.6. Microstructure properties

Using Quanta SEM apparatus the microstructure of Loy Yang brown coal fly ash geopolymer concrete at different curing durations were examined for 50 mm cube specimens. The analysis utilises secondary electrons (SE) to observe the morphological nature of the polished surface of sawn specimens (Kjellsen, Monsøy et al. 2003).

Figure 5.12 shows the image of polished Loy Yang brown coal fly ash geopolymer concrete specimens at 8, 10, 12 and 14 hour curing times. At 8 hours the geopolymer displays an open porous structure with a large number of unreacted

fly ash grains present. The images at 10, 12 and 14 hours show a more compact homogeneous structure, though a number of macropores are observed throughout. Some unreacted fly ash grains are still observed at 10 hours, but by 12 and 14 hours few are observed, indicating that the gelation process has reached a conclusion. Micro cracking is also observed at 10, and 12 hours, with a significant increase in the number and size of the micro cracks at 14 hours.

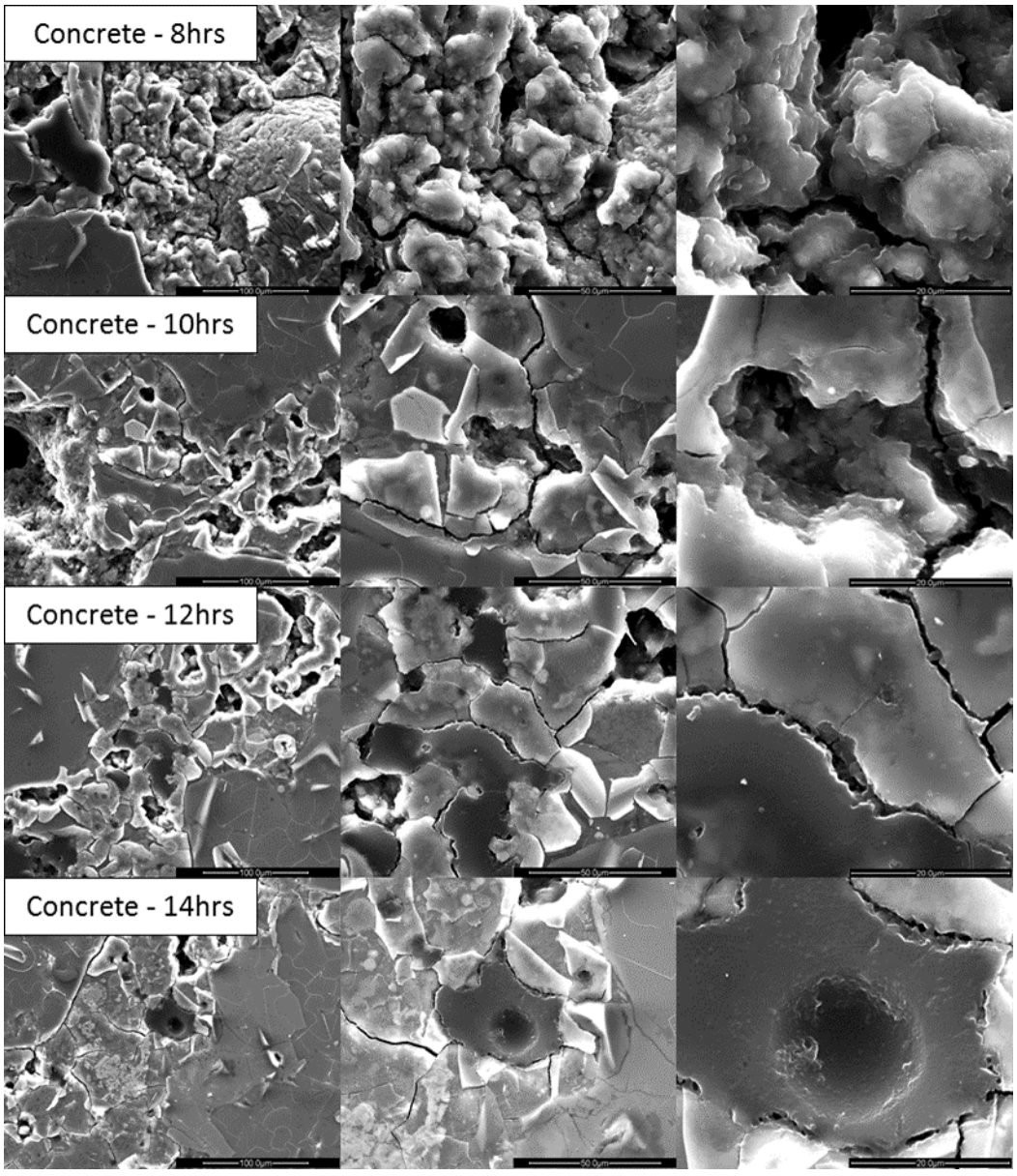

Figure 5.12 SEM Polished specimen image of Loy Yang brown coal fly ash geopolymer concrete of different curing time using Secondary Electron-SE (left side 400x magnification, middle 1000x, and right side 3000x)

The SEM images correlate well with the temperature profile observed for the mortar specimens (described in Chapter 4 Section 4.5.5). The rapid rise in temperature observed between 6 to 10 hours (Figure 4.9 in Chapter 4) is identified as corresponding to the second stage of gel formation and reorganization, with the matrix going from an open porous structure with a large number of unreacted fly ash grains present at 8 hours to the denser homogenous image seen at 10 hours. The reduction in the temperature rise between 10 to 14 hours corresponds to a period where there is an increase in the micro cracking, analogous with the third stage in the mortar where evaporation of the remaining water in hypothesised as causing micro cracking (Brinker and Scherer 1990, Sindhunata 2006).

The quantity of the gel formed is dependent on the degree of geopolymerization. Gel fills the cavities between unreacted fly ash particles, aggregate and pore space in the matrix, thus refining the size of the pores. In order to identify the pore-structure after geopolymerization, mercury intrusion porosimetry (MIP) was also undertaken on the Loy Yang brown coal fly ash geopolymer concrete.

Analysis was undertaken on 50 mm cube specimens, where the temperature profile data has indicated that geopolymerization would have occurred uniformly throughout, comparable to 50 mm cube mortar specimens. The pore size distribution of both Loy Yang brown coal fly ash geopolymer concrete and mortar were compared based on dV/dlogD pore volume and cumulative pore volume, and shown in Figure 5.13.

Figure 5.13 shows the variation of pore properties of both specimens. Both Loy Yang brown coal fly ash geopolymer concrete and mortar showed a multi pore size distribution. The pores can be divided into three groups based on the pore diameter mesopores (3.6–50 nm), macropores (50–200 nm) and pores larger than 200 nm (Sindhunata 2006). Research on class F fly ash geopolymers has shown that the mesopores are typical pores between geopolymer phases, while

micropores exist within the gel network. The macropores fill the gaps between unreacted fly ash particles (Zheng, Wang et al. 2010).

Both the mortar and concrete show a peak in macropores around 4,000 – 5,000 nm, with the mortar showing three further peaks between 10,000 and 100,000 nm at 24,000, 60,000 and 90,000 nm. The concrete however, has two much smaller peaks around 85,000 – 90,000 nm. The mortar shows a peak in mesopores at 4 nm.

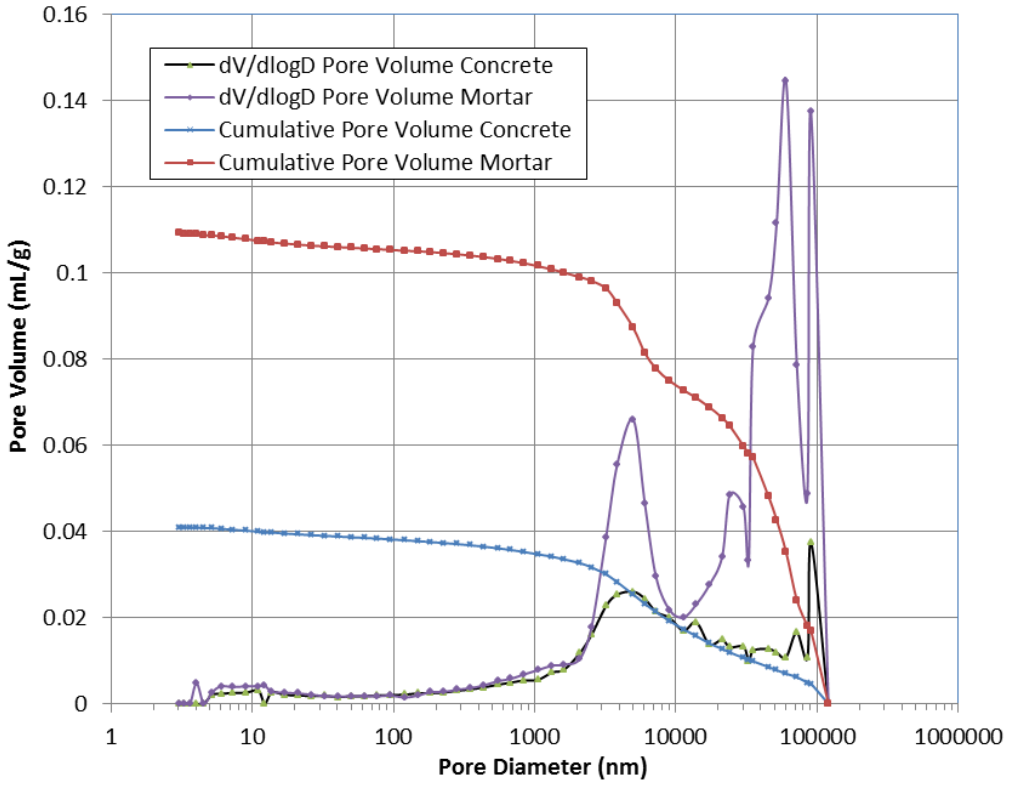

Figure 5.13 Pore size distribution of Loy Yang brown coal fly ash geopolymer mortar and concrete specimens

The pores identified for both the mortar and the concrete are principally in the macropores region, corresponding to gaps between unreacted fly ash grains and between aggregate. This would suggest that little refinement of the pore matrix has occurred within the Loy Yang brown coal fly ash geopolymer materials. While, the SEM images and the compressive strengths would indicate that some

degree of refinement has occurred, the SEM micrographs do show the presence of large macropores in the matrix, correlating with the MIP data.

Loy Yang brown coal fly ash geopolymer concrete has a lower cumulative pore volume compared to the geopolymer mortar. This does not imply that geopolymer concrete has fewer pores than the mortar, rather than geopolymer concrete has more macropores of a lower diameter size.

Figure 5.14 shows the optical macro image of the sawn surface of both geopolymer mortar and concrete specimens. Loy Yang brown coal fly ash geopolymer concrete shows larger and more interconnected pores compared to geopolymer mortar. The optical image was taken with different focuses to expose the depth and the pore network, in particular in the geopolymer concrete.

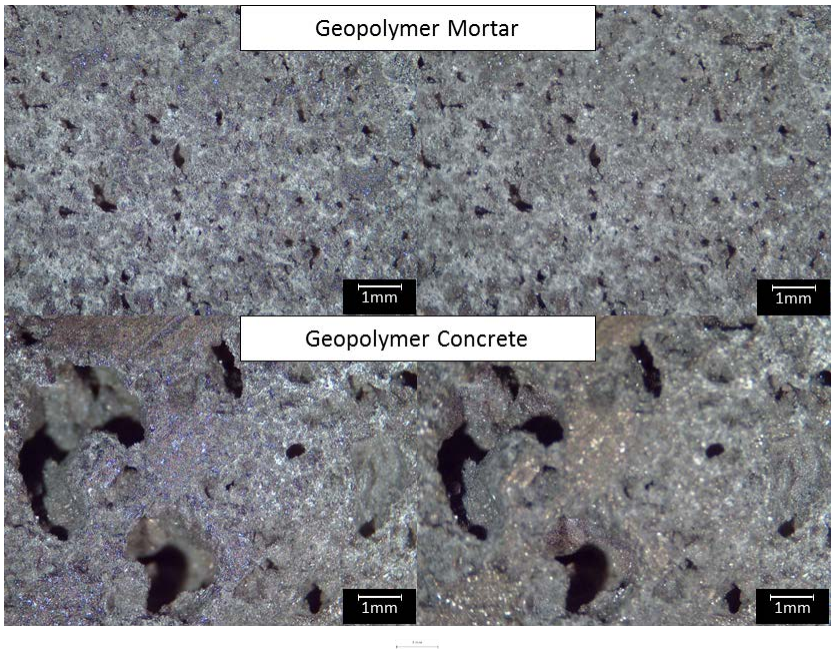

Figure 5.14 Optical image of the sawn surface specimen of Loy Yang brown coal fly ash geopolymer mortar and concrete

The different porosity profile of both Loy Yang brown coal fly ash geopolymer mortar and concrete could also be interpreted as result of different aggregate

sizes used within the mixes. The aggregate size in the mix could affect the geometric structure formed, with the larger coarse aggregate in the geopolymer concrete resulting in the larger pores observed in the concrete specimen.

5.7. Macroscopic investigation

According to Provis (2013) the fundamental aim of research and development in the area of alkali-activation is the production of highly durable concrete (Provis 2013). A series of standard concrete durability tests were applied to Loy Yang brown coal fly ash geopolymer concrete to investigate a number of the mechanical properties and durability characteristic of the geopolymer concrete. This section presents experimental results of the macroscopic investigation and Non Destructive Test (NDT) for durability properties of Loy Yang brown coal fly ash geopolymer concrete. Testing was undertaken on the initial batch (Batch 1) of the Loy Yang brown coal fly ash.

5.7.1 Schmidt Rebound Hammer

The Schmidt Rebound Hammer measures the rebound of a spring-loaded mass impacting against the surface of the sample. The hammer impacts the concrete at a defined energy with its rebound dependent on the hardness of the concrete, this hardness is measured by the test equipment. The test was conducted using a Schmidt Type N hammer in according to ASTM standard (ASTM-C805-02 2003). Striking points were uniformly distributed to reduce the influence of coarse aggregates distribution and averages of the rebound value calculated. Two cuboid Loy Yang brown coal fly ash geopolymer concrete specimens of 300 mm width x 300 mm length x 100 mm height were tested at 28 and 90 days after casting and average values for each data point was considered (Batch 1 – (i) and (ii)).

Table 5.7 shows the rebound indexes of Loy Yang brown coal fly ash geopolymer concrete and OPC concrete as control. The results do not give a direct

measurement of the strength of the concrete i.e the values can only use as an indication based on surface properties. The OPC concrete control specimens show a small increase in the index at 90 days, while the geopolymer concrete a slight decrease. However, based on the standard deviation this variation is not statistically significant, indicating that the strength remained constant from 28 to 90 days for both materials. However, a significant variation was observed between the two geopolymer specimens, compared with the two concrete specimens. This would indicate a degree of variability in the geopolymer produced, even though they are from the same mix.

Table 5.7 Rebound indexes of Loy Yang brown coal fly ash geopolymer concrete at 28 and 90 days

Sample	**Rebound index**				***Compressive Strength (MPa) at 28 days***
	28 days		**90 days**		
	Mean	**SD**	**Mean**	**SD**	
Loy Yang Batch 1-(i)	11.3	1.04	10.8	0.88	43.79
Loy Yang Batch 1-(ii)	16.8	2.99	16.7	2.39	
OPC Control A	23.8	2.99	24.4	2.12	53.38
OPC Control B	24.3	3.67	25.7	3.04	

5.7.2 Electrical resistivity

Once corrosion of the reinforcing steel of the concrete is induced by chloride attack, the electrical resistivity is an effective parameter to evaluate the corrosion rate. A concrete material with high resistivity will show a lower corrosion rate compare to a concrete with a low resistivity (Morris, Vico et al. 2002). The resistivity test results are shown in Table 5.8.

Table 5.8 shows the resistivity of the specimen at 28 and 90 days of age in accordance with IAEA (2002). The Loy Yang brown coal fly ash geopolymer concrete standard deviation was significantly higher compared to OPC concrete.

The high standard deviation of geopolymer concrete result shows more variability of the data compared to OPC concrete. The raw data (Appendix B, Table B.2) shows that low resistivity were found clustered around center of the cuboid, and implies inhomogeneous bulk properties of the specimen. This is consistent with the elevated curing data (Section 5.5) which indicates that the geopolymerization is not complete at the centre of the specimen. It is hypothesised that the lower resistivities measured at the centre are due to residual moisture and possibly excess activator both of which would lead to a lower resistivity. The higher resistivities at the edge would be consistent with the zone where geopolymerization is complete and the excess moisture has been lost.

Table 5.8 Resistivity of Loy Yang brown coal fly ash geopolymer concrete at 28 and 90 days

Sample	**Resistivity (kΩcm)**			
	28 days		**90 days**	
	Average	SD	Average	SD
Loy Yang Batch 1-(i)	15.5	16.18	13.5	10.29
Loy Yang Batch 1-(ii)	22.1	17.95	16.5	10.16
OPC Control A	7.0	2.26	6.8	2.34
OPC Control B	7.1	1.97	7.3	2.16

While the result for geopolymer concrete might not represent the average resistivity of the sample, taking this as a reference allows comparison with OPC concrete (Table 5.8) and previous results on class F fly ash geopolymer concrete (Wardhono 2015) (Table 5.9). Table 5.8 shows that the Loy Yang brown coal fly ash geopolymer concrete demonstrates a “Low/Moderate” to “Negligible” corrosion risk with resistivity valued from 13.5 – 22.1 kΩcm compared to “High” corrosion risk of OPC concrete with resistivity valued between 6.8 – 7.3 kΩcm (IAEA 2002).

While the 28 day results are similar for the class F and Loy Yang brown coal fly ash geopolymers, the Loy Yang brown coal fly ash geopolymer concrete does not show the increase in resistivity with age that was shown in the class F fly ash geopolymer results (Wardhono 2015).

Table 5.9 Resistivity of Loy Yang brown coal fly ash geopolymer concrete and other class F fly ash geopolymer concrete at 28 and 90 days

Test	**Resistivity (kΩcm)**		
	Loy Yang		**Wardhono[1]**
	Batch 1-(i)	**Batch 1-(ii)**	**G15-1.00**
28 days	15.5	22.1	8.0
90 days	13.5	16.5	38.9

[1]Wardhono (2015)

In addition to the inhomogeneity observed further possible reasons for the continued low resistivity (at the center of the specimen) for Loy Yang brown coal fly ash geopolymer concrete could be the alkali activator i.e dosage of activator Na_2O. A higher dosage of activator could lead to an increase in the ion concentration in the pore fluid of the specimen. An increase of ionic concentration would lead higher conductivity and hence cause the low resistivity values measured. Finally, the low resistivity could also an aspect of the high porosity and permeability present in the Loy Yang brown coal fly ash geopolymer concrete specimens. High porosity could lead to a high concentration of ions and moisture in the pore structure, which would allow the electrical current easily passes through the specimen. It has been previously reported that the conductivity of saturated concrete is influenced by the extent of connected capillary porosity and the ionic concentration in the pore structure (McCarter, Starrs et al. 2000).

The Loy Yang brown coal fly ash geopolymer concrete pores identified are principally macropores, corresponding to gaps between unreacted fly ash grains and between aggregate. Hence they provided connected capillary porosity. Given that similar activator concentrations are used in the Loy Yang brown coal and class F fly ash geopolymer materials, but that the Loy Yang brown coal fly ash geopolymer concrete has a more open pore structure is it judged more likely that the Loy Yang brown coal fly ash geopolymer concrete lower resistivity at 90 days is due to a combination of the inhomogeneity due to the incomplete curing and the high porosity and permeability of the concrete produced.

The resistivities around center of the cuboid are very low as some of the values were below 5 kΩcm. Resistivity less than 5 kΩcm demonstrates a “Very High” corrosion risk (IAEA 2002). The result could interpreted that overall (taken as a whole of the experiment specimen) the Loy Yang brown coal fly ash geopolymer concrete exhibits a “Very High” corrosion risk.

5.7.3 Ultrasonic Pulse Velocity (UPV)

The ultrasonic sonic pulse velocity (UPV) test is a technique to determine the bulk property of concrete. The pulse velocity depends on the elastic properties and density that are related to the quality and strength of the concrete specimen. The test also identifies possible cavities, cracks or defects within the concrete.

The velocity test results of Loy Yang brown coal fly ash geopolymer concrete at 28 and 90 days of age are shown in Table 5.10 (with calculation spreadsheet in Appendix B, Table B.3). Geopolymer concrete exhibits “Very Poor” to “Poor” quality compare to OPC concrete which shows “Good” quality in accordance with IAEA (2002). The longitudinal pulse velocity of geopolymer concrete varied from 1.7 to 2.1 km/s while OPC concrete varied from 4.4 to 4.4 km/s. The quality of the geopolymer concrete correlates well with the high degree of macropores found in the MIP analysis. The macropores would reduce the density of the

geopolymer concrete, which would cause the reduction in the velocity of the UPV signal observed.

No significant change was found between 28 and 90 days of age for both concrete types, which implies that the bulk properties and quality of both concretes had not changed over time. This is consistent with the previous observation on compressive strength, rebound hammer and resistivity.

Table 5.10 Velocity of Loy Yang brown coal fly ash geopolymer concrete at 28 and 90 days

Sample	**Velocity (m/s)**			
	28 days		**90 days**	
	Average	SD	Average	SD
Loy Yang Batch 1-(i)	1723.6	997.36	1737.0	864.55
Loy Yang Batch 1-(ii)	2052.3	987.48	1982.5	882.94
OPC Control A	4435.9	97.63	4401.7	64.57
OPC Control B	4380.9	106.70	4349.5	106.51

Table 5.10 also shows a significantly higher standard deviation for Loy Yang brown coal fly ash geopolymer concrete compared to OPC concrete. Again the high standard deviation of geopolymer concrete results infers variability in the geopolymer matrix. The raw data of UPV test results (Appendix B, Table B.3) shows that lower velocities were found in centre of the specimen. The lower velocity found in the centre of the specimen indicates the more porous area of the specimen. This would support the temperature profile data analysis (discussed in Section 5.5) that suggests the geopolymeric reaction had not concluded in the center of the large scale specimens.

5.7.4 Air permeability and water absorption (sorptivity)

The autoclam air permeability and water absorption (sorptivity) tests were performed as a rapid analysis of the air and water absorption of the concrete

surface by a non-destructive method. Commonly, concrete deterioration is caused by the infiltration of aggressive elements e.g. chloride, sulphate and CO_2, into the concrete. These elements first will alter the surface layer of concrete by forming a micro environment and then penetrate into the concrete. The quality of the concrete can be estimated by determining the resistance of the surface to infiltration of aggressive species into the concrete.

Both samples of Loy Yang brown coal fly ash geopolymer concrete failed the air permeability test. The pressure decayed rapidly after priming at 500mBar, and reach zero before 5 minutes. As a reference the air permeability test was undertaken for one OPC concrete specimen at 28 days (Appendix B, Table B.5).

A sorptivity test was performed instead of a water permeability test given the failure of the air permeability test, as the test pressure for sorptivity is 20mBar compared to 500mBar for water permeability test.

The sorptivity index was measured by plotting the flow of water recorded against the square root of time for the 15 minute test duration. The data points between 5 and 15 minutes were used for analysis as the points before 5 minutes are generally found to be unstable. The selected data points were fitted by a regression line and the slope was determined as the sorptivity index of the specimen (Amphora-NDT 2014). The slope obtained using Microsoft Excel (SLOPE function) (Henderson, Basheer et al. 2004, Torrent and Luco 2007). The sorptivity test results, represented by the autoclam sorptivity index, are shown in Table 5.11. The detailed raw data are presented in Appendix B Table B.4.

Table 5.11 shows a significant variation of sorptivity index (at 28 days) of Loy Yang brown coal fly ash geopolymer concrete. Sample Batch 1-(i) displays a high sorptivity index of 116.75 $m^3 \times 10^{-7}/\sqrt{min}$ compared to 63.87 $m^3 \times 10^{-7}/\sqrt{min}$ of sample Batch 1-(ii). Moreover, samples Batch 1-(i) failed at 90 days.

The reference OPC concrete demonstrates a “Very Good” protective quality based on Autoclam air permeability index 0.045 Ln (pressure)/min, and also

shows a “Very Good” protective quality based on Autoclam sorptivity index valued 0.061 $m^3 \times 10^{-7}/\sqrt{min}$ (Amphora-NDT 2014).

Table 5.11 Autoclam air permeability and sorptivity index of Loy Yang brown coal fly ash geopolymer concrete at 28 and 90 days

Autoclam Index		**Loy Yang**		**OPC Control**
		Batch 1-(i)	**Batch 1-(ii)**	
Sorptivity ($m^3 \times 10^{-7}/\sqrt{min}$)	28 days	116.75	63.87	0.061
	90 days	*Failed*	157.56	*NA*
Air Permeability Ln(Pressure)/min	28 days	*Failed*	*Failed*	0.045

The high sorptivity index of Loy Yang brown coal fly ash geopolymer concrete, Batch 1-(ii) 63.87 $m^3 \times 10^{-7}/\sqrt{min}$ at 28 days, 157.56 $m^3 \times 10^{-7}/\sqrt{min}$ at 90 days, and unsuccessful test of sample Batch 1-(i) at 90 days (Figure 5.15), indicates a poor quality material. A high permeability index indicates a low quality in the surface layer which can lead to a poor durability for the concrete. It also indicates the ease with which water penetrates into the concrete. In the case of this Loy Yang brown coal fly ash geopolymer concrete, the poor performance is attributed to the high porosity due to the large quantity of macropores present in the material. Indeed the interconnected pores in the specimen provided a route for the water to leak at points on the surface adjacent to the test, as shown on Figure 5.15.

Figure 5.15 Surface pore water leaking during water absorption (sorptivity) test Loy Yang brown coal fly ash geopolymer concrete sample Batch 1-(i)

5.7.5 Chloride diffusion

A chloride ponding test was undertaken to obtain chloride diffusion data for Loy Yang brown coal fly ash geopolymer concrete. The experimental detail is described in Chapter 3 Section 3.7.2. Table 5.12 shows the chloride content in % weight of the sample of the specimen.

The Chloride diffusion coefficient (D_a) and the surface concentration (C_s) are estimated by plotting the chloride data profiles and determining the best fitted curve using Fick's 2nd Law as suggested by Crank (Crank 1979). The C_s value is the value derived from curve fitting to incremental chloride contents with extrapolation to the surface value (Bamforth 1998). Figure 5.16 shows the best-fit curve of chloride profile obtained using Microsoft Excel (SOLVER function).

Table 5.12 Chloride content by weight of sample (%) of Loy Yang brown coal fly ash geopolymer concrete

Specimen	Depth (mm)	Chloride (Cl^-) content % by mass sample
Loy Yang Batch 1	0–20	0.05743
	20–40	0.04564
	40–100	0.00841

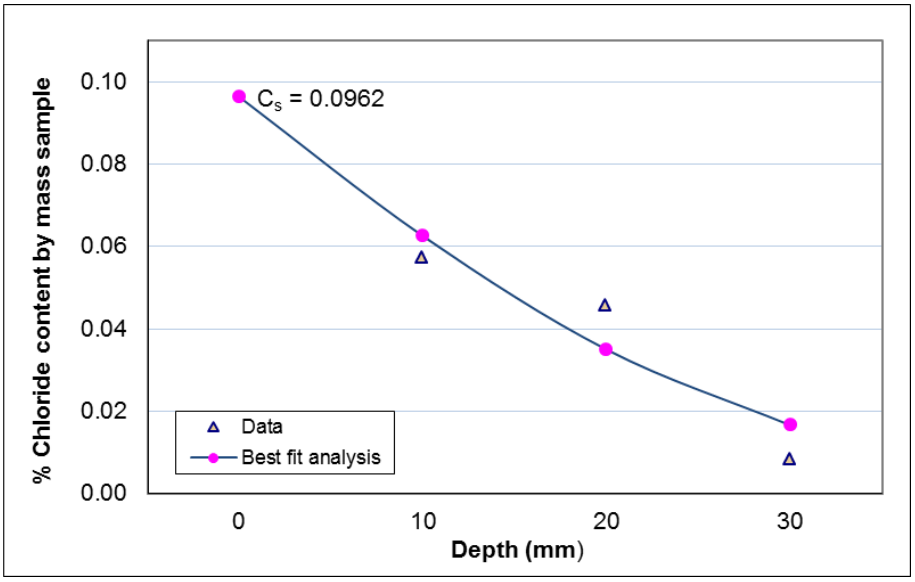

Figure 5.16 Chloride profile and best fit curve of Loy Yang brown coal fly ash geopolymer concrete specimen

Table 5.13 shows surface chloride content and the chloride diffusion of Loy Yang brown coal fly ash geopolymer concrete. The surface chloride content (C_s) of Loy Yang brown coal fly ash geopolymer concrete gave a value of 0.0962% which is low compared to the predictive value for blended cement reported by Bamforth (1998). The predictive typical average value for blended cement (with fly ash or ground granulated blast furnace slag) is normally between 0.25 and 0.3% with 0.5% when subjected to ideal curing condition (Bamforth 1998, Liu, Tang et al. 2014). Bamforth (1998) also described a model for predicting chloride ingress. The predictive apparent diffusion coefficient (D_{ca}) value for fly ash blended

cement at 90 days using Bamforth's model is 6-7x10^{-11} m^2/s comparable to the chloride coefficient value 3.11x10^{-11} m^2/s of Loy Yang brown coal fly ash geopolymer concrete.

Table 5.13 Surface chloride content and the chloride diffusion of Loy Yang brown coal fly ash geopolymer concrete

Specimen	Chloride diffusion coefficient (D_a) (m^2/s)	Surface chloride content (C_s) (%)
Loy Yang Batch 1	3.11x10^{-11}	0.0962

The Loy Yang brown coal fly ash geopolymer concrete chloride coefficient value of 3.11x10^{-11} m^2/s is high compared to that reported in the literature for OPC and blended cements, generally of the order of 1x10^{-12} m^2/s to 1x10^{-13} m^2/s (Duracrete 1998), and also high compared to class F or C fly ash geopolymer concrete, which is of the order 1x10^{-11} m^2/s to 1x10^{-12} m^2/s (Kupwade-Patil and Allouche 2012) or indeed alkali activated slag concrete, 1x10^{-12} m^2/s to 5x10^{-12} m^2/s (Ma, Nanukuttan et al. 2015). This would suggest a high porosity and permeability in the Loy Yang brown coal fly ash geopolymer concrete, which is consistent with the air permeability and water absorption (sorptivity) data and the MIP analysis. The high porosity and permeability provide a route for the chloride ions to penetrate the concrete through the interconnected pores.

Table 5.14 compares the chloride diffusion coefficient and surface chloride content of Loy Yang brown coal fly ash geopolymer concrete to other geopolymer concrete reported research. The chloride rate of diffusion of this study (3.11x10^{-11} m^2/s) is comparable to Wardhono (2015) (79.6x10^{-11} m^2/s) and Adam (2009) (3.10x10^{-11} m^2/s) geopolymer concretes. The relatively high chloride diffusion coefficients of these geopolymers might be attributable to the elevated temperature curing employed. Both Wardhono (2015) and Adam (2009) geopolymer concrete applied 24 hours curing at elevated temperature of 80 °C and reported comparable chloride rate of diffusion result of the order of 1x10^{-10}

to $1x10^{-11}$ m^2/s, opposed to a lower diffusion coefficient of $3.7x10^{-12}$ m^2/s reported by Chindaprasirt and Chalee (2014) for geopolymer concrete and $1x10^{-12}$ m^2/s to $5x10^{-12}$ m^2/s of Ma et al. (2015) for alkali activated slag concrete, which were air cured (Adam 2009, Chindaprasirt and Chalee 2014, Ma, Nanukuttan et al. 2015, Wardhono 2015). The geopolymers cured at elevated temperatures have shown evidence of micro cracking. The micro cracking has been attributed to the elevated curing and is hypothesized as providing a mechanism for chloride ions to diffuse into the concrete, hence leading to the observation of the higher diffusion coefficient.

Table 5.14 Comparison of chloride diffusion of Loy Yang brown coal fly ash, other geopolymer concrete and alkali activated slag concrete reported research

Component	**Loy Yang Batch 1**	**Wardhono[1] G15-1.00**	**Adam[2] G7.5-1.00**	**Chinda-prasirt[3] 14 M**	**Ma[4] AAS**
C_s (%)	0.0962	0.29	0.17	NA	NA
D_a (m^2/s)	$3.11x10^{-11}$	$79.6x10^{-11}$	$3.10x10^{-11}$	$3.7x10^{-12}$	$1\text{-}5x10^{-12}$
CaO (%)	2.25	0.18	3.47	18.75	NA
SiO_2 (%)	47.52	70.30	49.45	32.10	NA
Na_2O (%)	21.6	15	7.5	0.69	NA
SiO_2/Al_2O_3	2.75	3.04	1.67	1.61	NA

[1]Wardhono (2015), [2]Adam (2009), [3]Chindaprasirt and Chalee (2014), [4]Ma, Nanukuttan et al. (2015)

In OPC concrete, the chloride diffusion is affected by C-S-H gel formed during hydration. Some chloride ions are retained and bound to the C-S-H gel, referred to as chloride binding (Luping and Nilsson 1993). The free chloride ions which are not bound are able to diffuse through the concrete pores and induce corrosion on the reinforcing bars. Researchers have reported that for geopolymer concrete, chloride ions can be bound by NaOH and CaO (Chindaprasirt and Chalee 2014). A higher NaOH concentration binds more chloride ions while a

high content of CaO reacts with silicate compounds to form similar C-S-H cement gel of the OPC concrete, which can bind chlorides. The NaOH concentration coupled with the CaO content will increase the chloride binding capacity and reduce the chloride diffusion coefficient. The Loy Yang brown coal fly ash has a relatively low CaO, 2.25%, Table 3.1, comparable to a low CaO Class F Fly Ash, and as such this is not expected to contribute significantly to any chloride binding.

5.7.6 Carbonation

An accelerated carbonation chamber was used to assess the carbonation depth ingression of the specimens for set durations. The specimens were exposed to three variables i.e CO_2 dosage of 2% ± 1%, temperature at 20 °C ± 1 °C, and humidity 70% ± 1% RH.

Figure 5.17 shows the image of the specimens after 7, 14 and 28 days in the accelerated carbonation chamber along with a control specimen stored outside the chamber in the laboratory environment, at 7 days and previously reported data (Adam 2009, Wardhono 2015).

The Loy Yang control sample at 7 days shows no carbonation, displaying a pale pink coloration caused by the phenolphthalein indicator, though some duller areas are noted. The Loy Yang sample exposed to CO_2 at 7 days shows a dull pink/colourless area throughout the inner part of the specimen and a pale pink colour only at the outer layer next to the epoxy surface. The 14 and 28 days sample display similar profiles. As such the dull pink/colourless zone is identified as having been carbonated. The similarity in the profiles at 7, 14 and 28 days indicates carbonation had fully occurred by 7 days.

It was also noted that the colour of non-carbonated Loy Yang brown coal fly ash geopolymer concrete after it was sprayed with phenolphthalein indicator was a paler pink compared to clear pink of geopolymer specimen and OPC control specimen previously reported (Adam 2009, Wardhono 2015). This implies that the pH of the pore solution of Loy Yang brown coal fly ash geopolymer concrete

is lower. Following carbonation the minimal change in pink colouration in both the brown coal and class F fly ash geopolymers would suggest that the pH in geopolymer concrete is not significantly affected by the CO_2.

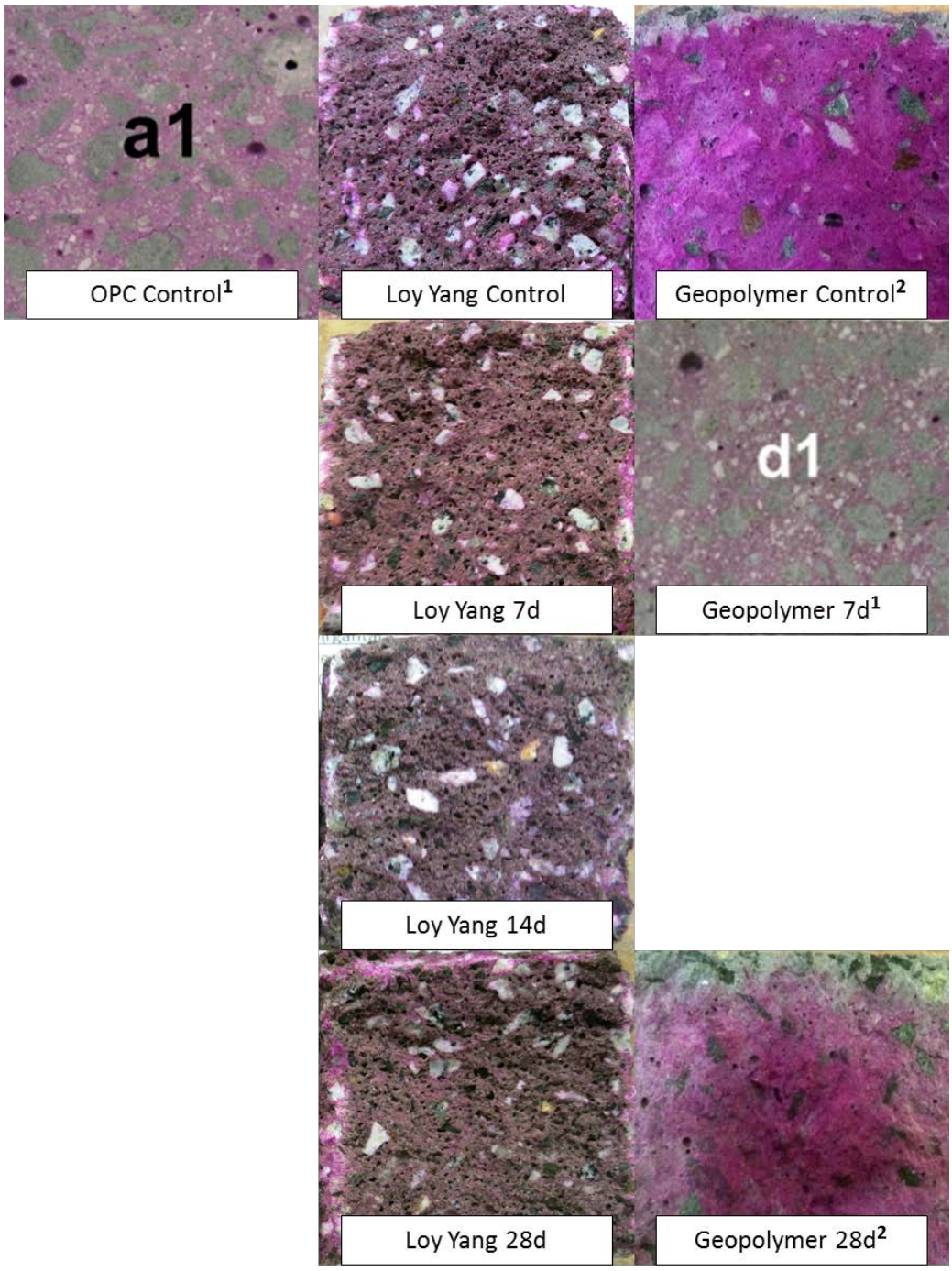

Figure 5.17 Carbonation of Loy Yang brown coal fly ash geopolymer concrete, other previous research reported and control specimen after certain days in the accelerated carbonation chamber [1]Wardhono (2015), [2]Adam (2009).

It has been proposed that the carbonation process in the geopolymer is different to that of OPC concrete. According to Davidovits (2005) the carbonation products of geopolymer concrete are sodium carbonate or potassium carbonate which have a minimum pH of 10–10.5 (Davidovits 2005). This pH is much higher that the pH from the calcium carbonate produced by the carbonation of OPC concrete, which can have pH lower than 9. This variation in pH would explain the colour difference among the geopolymer and OPC specimens after phenolphthalein indicator is sprayed post carbonation.

Furthermore, the carbonation of geopolymer concrete was different from OPC concrete, in that there was no clear border between the coloured and colourless area. As such it is not easily possible to measure the penetration depth using a phenolphthalein indicator as the carbonation 'front' was not clear. According to Neville (2011), sometimes when the partial carbonation occurs, the carbonation 'front' cannot be seen clearly. In the case of geopolymer concrete, it is suggested that the partial carbonation is the carbonation of NaOH, where the NaOH reacts with CO_2 forming Na_2CO_3 and releasing water. This partial carbonation is different to a full carbonation in OPC concrete, whereas the carbonation front advances the CO_2 reacts to form both $Ca(OH)_2$ and C-S-H (Neville 2011).

The fundamental factor of the carbonation is the diffusivity process which depends on the function of the pore system of the specimen (Neville 2011). The carbonation of OPC concrete is carbonation of $Ca(OH)_2$, while in the case of geopolymer concrete as $Ca(OH)_2$ is not available, the constituent that can be carbonated is NaOH. The high rate of carbonation of fly ash geopolymer concrete might be affected by (1) the low content of CaO to react with CO_2, (2) the high dosage of NaOH, and (3) the high porosity and permeability.

Table 5.15 shows the particular constituent of different fly ash geopolymer concretes. The relatively low quantity of CaO results in there being less material available to react with the CO_2, hence leading to a faster carbonation process. In

addition, the high porosity and permeability observed in the Loy Yang brown coal fly ash geopolymer concrete increase the rate of penetration of CO_2.

Table 5.15 Comparison of particular constituent of different fly ash geopolymer concrete

Components	Loy Yang Batch 1	Wardhono[1] G15-1.00	Adam[2] G7.5-1.00
CaO (%)	2.25	0.18	3.47
Na_2O (%)	21.6	15	7.5

[1]Wardhono (2015), [2]Adam (2009)

Overall the Loy Yang brown coal fly ash geopolymer concrete demonstrates a higher rate of carbonation compared to OPC concrete, though the pH following carbonation would appear to be higher than that of OPC concrete. The results are attributed to the high porosity and permeability of the specimen coupled with a lack of $Ca(OH)_2$ and C-S-H resulting in a lower initial pH for the geopolymer concrete and a different carbonation process resulting in a higher pH post carbonation.

5.8. Summary of chapter 5

Chapter 5 on Loy Yang brown coal fly ash geopolymer concrete could be summarised as follows:

1) The strengths obtained from Loy Yang brown coal fly ash geopolymer concrete are comparable to those obtained from Loy Yang brown coal fly ash geopolymer mortar previously. The strengths are indicative that Loy Yang brown coal fly ash geopolymer can produce compressive strengths acceptable for use in the construction industry.
2) The AM_m and SiO_2/Al_2O_3 are influential in the performance but the Na_2O/binder and Na_2O/Al_2O_3 do not have a significant influence on the strength of geopolymer produced.

3) The increase in volume of the sample sizes has contributed to the variations in strength. A smaller volume may enable better mixing of the materials. In particular enabling intimate contact between the activator solution and the fly ash to provide efficient dissolution of the fly ash particles. In a larger mix this may not be achieved to such a high degree.
4) Elevated temperature curing at 120 °C for 12 hours may not be sufficient for a significantly large concrete specimen as this may not achieve the internal temperature required to complete geopolymerization.
5) The aggregate size in the mix could affect the geometric structure formed, with larger coarse aggregate in the geopolymer concrete resulting in the larger pores observed in the concrete specimen.
6) The porosity distribution analysis of Loy Yang brown coal fly ash geopolymer mortar and concrete identified pores principally in the macropores region. The Loy Yang brown coal fly ash geopolymer concrete showing larger and more interconnected pores compared to geopolymer mortar.
7) The Schmidt Hammer rebound indexes show minimal variation between 28 and 90 days compressive strength. However, a degree of variability of the geopolymer produced from the same mix was observed.
8) The resistivity readings of Loy Yang brown coal fly ash geopolymer concrete specimen shows values from below 5 kΩcm to over 20 kΩcm. Taking the lower value as a threshold, Loy Yang brown coal fly ash geopolymer concrete exhibits “Very High” corrosion risk. The low resistivity of Loy Yang brown coal fly ash geopolymer concrete is hypothesized as being due to the inhomogeneity in the concrete caused by incomplete curing resulting in the high porosity and permeability of the concrete produced.
9) The low ultrasonic pulse velocity (UPV) of Loy Yang brown coal fly ash geopolymer concrete suggests “Very Poor” to “Poor” quality of the concrete. The low velocity correlates with the high degree of macropores

found in the specimen. The macropores would reduce the density of the geopolymer concrete, which would cause the reduction in the velocity of the UPV signal observed.

10) A high porosity due to the large quantity of macropores present in the material combined with the interconnected pores in the specimen is responsible for the failed air permeability test and high sorptivity index of Loy Yang brown coal fly ash geopolymer concrete, and indicates a poor performance which can lead to an inadequate durability.
11) The high chloride coefficient implies a high porosity and permeability, which is consistent with the air permeability, water absorption results and the MIP analysis. High porosity, permeability and micro cracking attributable to the elevated temperature curing provide a route for the chloride ions to penetrate the concrete through the interconnected pores.
12) Loy Yang brown coal fly ash geopolymer concrete demonstrates a higher rate of carbonation compare to OPC concrete. The results are again attributed to the high porosity and permeability of the specimen coupled with a different carbonation process occurring due to a lack of $Ca(OH)_2$ and C-S-H.

References

Adam, A. (2009). Strength and durability properties of alkali activated slag and fly ash-based geopolymer concrete. PhD, RMIT University.

Amphora-NDT (2014). Autoclam Permeability System, Operating Manual. Belfast, Northern Island, Amphora Technologies Ltd.

AS3600 (2001). Concrete Structures. AS3600. Sydney, Australia, Australian Standard

AS-1012.9 (1999). Methods of testing concrete. Method 9, Determination of the compressive strength of concrete specimens. North Sydney, N.S.W, Standards Australia: 1-12.

ASTM-C805-02 (2003). ASTM C805-02. Standard Test Method for Rebound Number of Hardened Concrete. USA, ASTM International.

Bakharev, T. (2005). "Geopolymeric materials prepared using Class F fly ash and elevated temperature curing." Cement and Concrete Research 35(6): 1224-1232.

Bamforth, P. (1998). "Guide for Prevention of Corrosion in Reinforced Concrete Exposed to Salt." Technology Division, Taywood Engineering.

Brinker, C. J. and G. W. Scherer (1990). Sol-gel science : the physics and chemistry of sol-gel processing. Boston, Academic Press.

Chindaprasirt, P. and W. Chalee (2014). "Effect of sodium hydroxide concentration on chloride penetration and steel corrosion of fly ash-based geopolymer concrete under marine site." Construction and Building Materials 63: 303-310.

Crank, J. (1979). The mathematics of diffusion. England, Oxford university press.

Davidovits, J. (2005). Geopolymer chemistry and sustainable Development. The Poly(sialate) terminology: a very useful and simple model for the promotion and understanding of green-chemistry. Geopolymers, Green Chemistry and Sustainable Development Solutions. J. Davidovits. Saint-Quentin, France, Institut Géopolymère: 9-15.

Duracrete (1998). Modelling of Degradation, Probabilistic Performance Based Durability Design of Concrete Structures Report, EU-Project(Brite Euram III) No. BE95-1347.

Henderson, G., P. Basheer, A. Long, V. Malhotra and N. Carino (2004). "Pull-off test and permeation tests." Handbook on Nondestructive Testing of Concrete: 6.1-6.12.

IAEA (2002). Guidebook on non-destructive testing of concrete structures. Vienna, Austria, International Atomic Energy Agency.

Kjellsen, K., A. Monsøy, K. Isachsen and R. Detwiler (2003). "Preparation of flat-polished specimens for SEM-backscattered electron imaging and X-ray microanalysis—importance of epoxy impregnation." Cement and Concrete Research 33(4): 611-616.

Kupwade-Patil, K. and E. N. Allouche (2012). "Examination of chloride-induced corrosion in reinforced geopolymer concretes." Journal of Materials in Civil Engineering 25(10): 1465-1476.

Law, D. W., T. K. Molyneaux, A. Wardhono, R. Dirgantara and D. Kong (2013). The Use Brown Coal Fly Ash To Make Geopolymer Concrete. ACCTA 2013, Johannesburg.

Liu, J., K. Tang, D. Pan, Z. Lei, W. Wang and F. Xing (2014). "Surface chloride concentration of concrete under shallow immersion conditions." Materials 7(9): 6620-6631.

Luping, T. and L.-O. Nilsson (1993). "Chloride binding capacity and binding isotherms of OPC pastes and mortars." Cement and concrete research 23(2): 247-253.

Ma, Q., S. V. Nanukuttan, P. M. Basheer, Y. Bai and C. Yang (2015). "Chloride transport and the resulting corrosion of steel bars in alkali activated slag concretes." Materials and Structures: 1-15.

McCarter, W., G. Starrs and T. Chrisp (2000). "Electrical conductivity, diffusion, and permeability of Portland cement-based mortars." Cement and Concrete Research 30(9): 1395-1400.

Morris, W., A. Vico, M. Vazquez and S. De Sánchez (2002). "Corrosion of reinforcing steel evaluated by means of concrete resistivity measurements." Corrosion Science 44(1): 81-99.

Neville, A., M. (2011). Properties of Concrete. England, Pearson Education Limited.

Palomo, A., M. W. Grutzeck and M. T. Blanco (1999). "Alkali-activated fly ashes: A cement for the future." Cement and Concrete Research 29(8): 1323-1329.

Provis, J. L. (2013). "Geopolymers and other alkali activated materials: why, how, and what?" Materials and Structures 47(1-2): 15.

Sindhunata (2006). A Conceptual Model of Geopolymerisation. PhD, The University of Melbourne.

Sindhunata, J. Van Deventer, G. Lukey and H. Xu (2006). "Effect of curing temperature and silicate concentration on fly-ash-based geopolymerization." Industrial & Engineering Chemistry Research 45(10): 3559-3568.

Torrent, R. and L. F. Luco (2007). Report 40: Non-Destructive Evaluation of the Penetrability and Thickness of the Concrete Cover-State-of-the-Art Report of RILEM Technical Committee 189-NEC, RILEM publications.

Wardhono, A. (2015). The Durability of Fly Ash Geopolymer and Alkali-Activated Slag Concretes. PhD, RMIT University.

Zheng, L., W. Wang and Y. Shi (2010). "The effects of alkaline dosage and Si/Al ratio on the immobilization of heavy metals in municipal solid waste incineration fly ash-based geopolymer." Chemosphere 79(6): 665-671.

CHAPTER 6

GENERAL DISCUSSION

Currently there are numerous supplementary cementing materials (SCM) or pozzolanic materials (PM) available, primarily by-products or waste material from industrial processes. Substituting the major part of Portland cement by PM or SCM is potentially the most effective way of decreasing both energy consumption and the production of greenhouse gases from cement production, as well as providing a beneficial use for the fly ash by-product from coal fired power stations. This by-product can be interground or blended with the cement at the cement plant, or substituted for cement at the batch plant. The levels of substitution can be 20-70% of the Portland cement or even a 100% replacement in geopolymer concretes. Fly ash as an industrial by-product contains silicate materials is included among a range of other materials that are classed as SCM and PM e.g. ground granulated blast furnace slag, metakaolin, and natural pozzolans (Papadakis and Tsimas 2002, Malhotra 2005, Naik 2008, Aïtcin and Mindess 2011, Law, Molyneaux et al. 2013, Thomas 2013, Tennakoon, Sagoe-Crentsil et al. 2014).

Activation of fly ash involving using a highly alkaline solution will form an inorganic binder, known as geopolymer, with several commercial products recently coming on to the market (Duxson, Provis et al. 2007, Davidovits 2011). The silicate materials (silicon and aluminium oxides) in the fly ash react with alkaline liquid (alkaline activator) and become soluble reactants which form geopolymer paste that binds the aggregates and other unreacted materials to form concrete. Geopolymer concrete gives similar strength to both ordinary Portland (OP) cement and blended cements concretes. The compressive strength and the workability of geopolymer concrete are influenced by the proportions and properties of the constituent materials that make the geopolymer paste (Rangan 2010).

Geopolymer concrete has been reported as having a significant impact in reducing CO_2 emissions, though the level of reduction reported has varied considerably, from over 80% to only 9% (Habert, d'Espinose de Lacaillerie et al. 2011, McLellan, Williams et al. 2011, Turner and Collins 2013, Davidovits 2015). However, regardless of the CO_2-e (carbon dioxide equivalent) emission of geopolymer concrete being only 9% less than of concrete with 100% OP cement (Turner and Collins 2013), fly ash has an important advantage as it is a by-product which would otherwise be a waste product to be disposed of with the associated costs (Meyer 2009). Worldwide, fly ash production was 900 million tonnes per year in 2005 and it is anticipated to increase up to about 2000 million tonnes in 2020 (Malhotra 2008). In 2005 Australia produced around 13 million tonnes of fly ash with only around 4 million tonnes being sold or used in a beneficial manner, the remainder being deposited into ponds or landfill mixed with bottom ash (ADAA 2007, Keyte 2009). Existing stockpiles of fly ash and bottom ash will be enough to produce alkali-activated fly ash geopolymer concrete for centuries to come.

Australia's brown coal recoverable EDR (Economic Demonstrated Resources) is approximately 23% of the world's recoverable resources, with 93% deposited in the Latrobe Valley-Victoria and considered as one of the largest single brown coal fields in the world. Australian brown coal is currently considered to be unsuitable for export and is used exclusively to generate electricity in domestic power stations (Geoscience Australia and ABARE 2014). The majority of the brown coal fly ash produced (estimated 15% of total production Australian coal production in 2011-2012) is stored in ponds or sent to landfill (Geoscience Australia and ABARE 2014). Presently brown coal fly ash is not used as a binder in concrete as it tends to show little geopolymer reaction and is more likely to be classified a non- reactive filler (Macphee, Black et al. 1993, CIA 2011).

The activation process for geopolymer concretes is attributable to the activation of the aluminosilicate by high concentration alkali, consequently a higher proportion of silica (SiO_2) and/or the sum of SiO_2 and alumina (Al_2O_3) are needed

to ensure that sufficient potential reactive constituent is present in the fly ash. At present class F fly ash is the most commonly used binder material in the synthesis of alkali-activated binder (Sindhunata 2006, Guo, Shi et al. 2010). Earlier research on geopolymer mortar using an unblended high aluminosilicate brown coal fly ash as 100% replacement of OP cement demonstrated compressive strength comparable to those obtained from OP cement mortar (Law, Molyneaux et al. 2013, Tennakoon, Sagoe-Crentsil et al. 2014). This demonstrated the potential to produce geopolymer concrete using Australia-Victoria brown coal fly ash and could result in utilization of by-product produced from coal burning power stations presently disposed of directly into the environment. The silicate and aluminate content within fly ash are the main contributors to the geopolymer reaction, while a high content CaO could potentially affected the workability, the rate of reaction and cause rapid setting (Diaz, Allouche et al. 2010). The suitability of brown coal fly ash as a binder will depend on its inherent physical and chemical properties. To date little research has been undertaken on the feasibility of using brown coal fly ash as a waste product (Bankowski, Zou et al. 2004, Škvára, Kopecký et al. 2009).

This study investigated brown coal fly ash from three power plants in the La Trobe Valley, Australia, Loy Yang, Yallourn and Hazelwood. Curing temperature, curing time and curing condition have been identified as influencing the compressive strength of geopolymer concrete. Elevated temperature or heat curing assists the geopolymerization reaction. Temperature significantly affects the structural transition from the amorphous to the crystalline, while the curing condition will also affect the micro and nano structure of geopolymers (Hardjito, Wallah et al. 2004, Wang, Shah et al. 2004, Bakharev 2005, Sindhunata 2006, Chindaprasirt, Chareerat et al. 2007, Criado, Fernández-Jiménez et al. 2010, Lloyd and Rangan 2010). A 24 hours curing period at room temperature prior to heat curing has been reported as beneficial for strength development (Bakharev 2005), while a longer curing time will produce dehydration and excessive shrinkage as the gel contracts without transforming to a more semi-crystalline

form (van Jaarsveld, van Deventer et al. 2002). In addition curing at a relative humidity of over 90% in which the pastes are kept in air-tight containers has been reported as resulting in a dense and compact material, while curing at a relative humidity of 40-50% with the paste in direct contact with the atmosphere produces a granular, porous material (Criado, Fernández-Jiménez et al. 2010). Previous research on brown coal fly ash geopolymer concrete has identified that curing at an elevated temperature of 120 ^{o}C for 24 hours gave the optimum compressive strength (Law, Molyneaux et al. 2013). As such the curing conditions adopted were 24 hours curing at room temperature prior to elevated temperature curing at 120 ^{o}C for duration of 12 hours (Chapter 3). The specimens were wrapped with heat resistant cling film to reduce evaporation.

Loy Yang brown coal fly ash geopolymer mortar strengths above 40 MPa were obtained (Chapter 4) and are comparable to those obtained from previous research on class F and class C fly ash (Chindaprasirt, Chareerat et al. 2007, Ivan Diaz-Loya, Allouche et al. 2011, Gunasekara, Law et al. 2015). The results show minimal variation with time, indicating that the elevated curing had resulted in the activation of the brown coal fly ash and completion of the geopolymeric reaction. This is in agreement with findings reported by other authors for elevated curing of fly ash geopolymers (Palomo, Grutzeck et al. 1999, Bakharev 2005, Sindhunata, Van Deventer et al. 2006). Hazelwood and Yallourn brown coal fly ash geopolymer mortars gave compressive strengths less than 10 MPa. Due to their inherent chemical composition it is considered that these two fly ashes are not viable for the production of geopolymer with sufficient compressive strength to satisfy the requirements of category B1 and B2 AS3600 concretes. The low strength of Hazelwood and Yallourn brown coal fly ash mortars is attributed to the low aluminosilicate content. Though there is a high lime content in these materials which is considered to have cementitious properties of its own, it makes little contribution to the strength of the geopolymer mortars produced. This is attributed to the lime being combined with the silica and alumina portions of the ash resulting in less of a compound reaction. All specimens displayed

relatively high standard deviations attributed to the variability in the coal leading to variability in the composition of the fly ash. As noted, distinctly different chemical compositions have been reported for the brown coal fly ash (Macphee, Black et al. 1993, French and Smitham 2007, Dirgantara, Law et al. 2013).

The maximum strength of the geopolymer concrete obtained (Chapter 5) is equivalent to those obtained from geopolymer mortar with the Loy Yang brown coal fly ash. The compressive strength of Loy Yang brown coal fly ash geopolymer concretes obtained are consistent with those specified in AS 3600 for exposure category B1 and B2 which are indicative that brown coal fly ash can produce geopolymer concrete with compressive strengths acceptable for use in the construction industry (AS3600 2001). However, it has been observed that there is a significant strength variation of geopolymer concrete produced from different batches of Loy Yang brown coal fly ash. Overall, the data illustrate how the inherent variations in the material composition can affect the properties of the geopolymer produced. It is further believed that the increase in volume of the sample sizes has contributed to the variations in strength observed, with the smallest mix providing the highest compressive strength. A small volume may enable better mixing of the materials, however in a larger mix this may not be achieved to such a high degree. It was also observed that in the relatively larger specimens, the curing conditions might not be sufficient to promote gopolymerization throughout the specimen. Distinctly different temperature profiles were observed in the 50 mm cubes Loy Yang brown coal fly ash geopolymer mortar and concrete specimens compared to the 100, 200 and 300 mm cubes concrete specimens and between the edges of the 200 and 300 mm cubes concrete specimens and the centre of these specimens.

Workability has been identified as a key factor affecting geopolymer properties, with the particle size distribution, surface area and CaO content of the fly ash noted as factors influencing the workability (Chindaprasirt, Chareerat et al. 2007, Gunasekara, Law et al. 2015). Within this study different consistencies were found for different fly ashes with same Liquid to Solid ratio (L/S). The mixture

consistency varied considerably from a wet, to a moist and to a firm consistency. The variation in the particle size distribution, the surface area and CaO content is hypothesised as the reason for this variation.

The performance of geopolymer concrete depends on the polymerization process in the geopolymer binder (Chapter 4), identified as being due to a number of factors, the alkali modulus of the activator, the SiO_2/Al_2O_3, Na_2O/binder and Na_2O/Al_2O_3 ratio's, the particle size distribution, surface area, the amorphous content and zeta potential (Hardjito, Wallah et al. 2004, Duxson, Provis et al. 2005, Duxson, Lukey et al. 2006, Fernandez-Jimenez, Palomo et al. 2006, Duxson, Mallicoat et al. 2007, Gunasekara, Law et al. 2015). The performance of Loy Yang brown coal fly ash geopolymer mortar has been observed to be significantly influenced by AM_m and SiO_2/Al_2O_3, and to a lesser degree by the Na_2O/binder and Na_2O/Al_2O_3 (Chapter4). The optimum ranges are considerably more restrained than those that have been reported for class F fly ash geopolymers despite the relatively similar SiO_2 and Al_2O_3 content. Variability in both the morphology and surface area of brown coal fly ash have been identified affecting the reactivity but are not considered as the main parameters in determining the suitability of a brown coal fly ash as a potential geopolymeric material (Fernández-Jiménez and Palomo 2003, Tennakoon, Nazari et al. 2014). The negative zeta potential of Loy Yang brown coal fly ash further suggests that the use of Loy Yang brown coal fly ash as a geopolymeric material is feasible, while the XRD and XRF analysis of the samples suggest that the total amorphous content is not a critical factor in determining the compressive strength rather the mineralogical composition and reactivity of the brown coal fly ash, which appears to have a crucial bearing on the performance. The FTIR analysis indicates a high degree of reactivity in the Loy Yang brown coal fly ash geopolymer mortar, and considerable incorporation of the aluminium into the silicate backbone. The results are indicative of a high rate of release of aluminium which has been identified to lead to a geopolymer with high strength (Tennakoon, Nazari et al. 2014).

Monitoring of the elevated curing was used to investigate the geopolymeric reaction mechanism of the Loy Yang brown coal fly ash geopolymer mortar (Chapter 4) and concrete (Chapter 5). The temperature profile of the elevated curing agreed with the geopolymeric reaction mechanism reported from previous studies (Duxson, Provis et al. 2007) and correlated well with the SEM microstructural analysis and the phase mapping investigation.

Three distinct stages were identified during the elevated curing investigation. The first stage was identified as involving the dissolution and speciation equilibrium steps followed by gelation. The first stage also related to the thermodynamic nucleation stage which involves the dissolution of the aluminosilicate material and formation of polymeric species, followed by growth when the nuclei reach a critical size and crystals begin to develop. This process is a structural reorganization to form the microstructure which is critical in determining the physical and durability properties of the geopolymer (Duxson, Provis et al. 2007, Rangan 2010). The SEM analysis identified three phases i.e AlO, SiO and NaSiO, associated with the formation of the gel, which has been reported as a complex mixture of silicate, aluminate and alumina silicate species formed when the species released by dissolution into the aqueous phase (Duxson, Provis et al. 2007). The NaSiO fraction is associated with the step prior to the geopolymer precursor, when the alkali silicates or hydroxides provide sodium (Na^+) ions to be incorporated into the matrix.

The second stage corresponds to the reorganization step in the geopolymeric process, where the gel formation continues and the dissolution rate starts to reduce. During this stage, the temperature inside the specimen rises significantly as water is lost and dissolution ceases. The increased gel formation in this period is reflected in the increase of the compressive strength. The SEM image taken of at the beginning of this stage showed the geopolymer with an open porous structure with a large number of unreacted fly ash grains present. At the conclusion of this stage the geopolymer displays a more compact homogeneous structure with a number of macropores and a reduced number of unreacted fly

ash grains observed. These processes are reflected in SiO_2/Al_2O_3 ratio variation during this stage.

The third stage corresponds to the completion of the dissolution process and evaporation of the remaining water together with a cessation in gel formation and the reorganization step in the geopolymer formation. This is reflected in the slight rise of the temperature profile. During this stage the aluminate matrix of the structure, responsible for providing the compressive strength, is created. From this point the evaporation of the remaining liquid leads to micro and macro crack formation within the matrix due to the excess heat leading to a reduction in the strength. It has been observed in the SEM images and phase analysis that the gelation process has reached a conclusion. Micro cracking is observed in the early period of this stage with a significant increase in the number and size with time. The decrease in the SiO_2/Al_2O_3 is indicative of incorporation of aluminium into the silicate backbone, corresponding with the increase in strength observed. However, ultimately the micro cracking has results in a reduction of strength at the end of the elevated curing period.

It has been stated that durability properties of concrete are influenced and controlled by the number, type, size and distribution of pores present in the paste and the aggregate constituents, and the bond between them, whilst permeability is influenced by the pore size distribution and continuity (Basheer, Kropp et al. 2001, Lloyd, Provis et al. 2009, Bernal, Bílek et al. 2014). The durability testing conducted on the Loy Yang brown coal fly ash geopolymer concrete indicated that the geopolymer concrete was generally of a poor quality with a high level of porosity, due to a large quantity of macropores and an interconnected pore structure (Chapter 5). A degree of variability in the Schmidt Hammer rebound indexes of the geopolymer produced was observed. The electrical resistivity of the Loy Yang brown coal fly ash geopolymer concrete specimen displayed a similar variation, which is attributed to a combination of the inhomogeneity due to the incomplete curing, coupled with high porosity and permeability of the concrete. The ultrasonic pulse velocity of Loy Yang brown

coal fly ash geopolymer concrete correlated well with the high quantity of macropores. The data also showed a high rate of chloride diffusion, a high index of water absorption (sorptivity) and a high rate of carbonation. Good durability is a major factor for success of concrete as a construction material and ensuring the design and service life of a structure is achieved (Papadakis, Vayenas et al. 1991, ACI.201.2R-08 2008, Provis 2013).

A further consideration is the high sulphate content (13.03%) of the Loy Yang brown coal fly ash coupled with a high MgO content (4.63%). It has been reported that sulphate tends to reduce the reaction rate and the high Mg content together with the Na present from the activator could also lead to the formation of crystalline compounds such as $MgSO_4$ and Na_2SO_4 which could be unstable in water leading to durability issues and a reduction in compressive strength (Macphee, Black et al. 1993, Criado, Fernández-Jiménez et al. 2010).

Thus while the investigation showed that it was feasible to produce a geopolymer concrete with a compressive strength of over 40MPa from brown coal fly ash, the microstructural and durability studies raise concerns over the long term performance and commercial viability. As such further studies in the area of alkali-activation are needed to assess durability in order to produce a highly durable geopolymer concrete.

References

ACI.201.2R-08 (2008). Guided to Durable Concret : Reported by ACI Commitee 201. Michigan, USA, American Concrete Institute.

ADAA (2007). Coal Combustion Products Handbook, Ash Development Association of Australia, Cooperative Research Centre for Coal in Sustainable Development.

Aïtcin, P.-C. and S. Mindess (2011). Sustainability of Concrete. Abingdon, Oxon, CRC Press.

AS3600 (2001). Concrete Structures. AS3600. Sydney, Australia, Australian Standard

Bakharev, T. (2005). "Geopolymeric materials prepared using Class F fly ash and elevated temperature curing." Cement and Concrete Research 35(6): 1224-1232.

Bankowski, P., L. Zou and R. Hodges (2004). "Reduction of metal leaching in brown coal fly ash using geopolymers." Journal of Hazardous Materials 114(1–3): 59-67.

Basheer, L., J. Kropp and D. J. Cleland (2001). "Assessment of the durability of concrete from its permeation properties: a review." Construction and building materials 15(2): 93-103.

Bernal, S. A., V. Bílek, M. Criado, A. Fernández-Jiménez, E. Kavalerova, P. V. Krivenko, M. Palacios, A. Palomo, J. L. Provis and F. Puertas (2014). Durability and testing–degradation via mass transport. Alkali Activated Materials, Springer: 223-276.

Chindaprasirt, P., T. Chareerat and V. Sirivivatnanon (2007). "Workability and Strength of coarse high calcium fly ash geopolymer." Cement and Concrete Composites 29(3): 224-229.

CIA (2011). Recommended Practice Geopolymer Concrete. Sydney, Concrete Institute of Australia.

Criado, M., A. Fernández-Jiménez and A. Palomo (2010). "Alkali activation of fly ash. Part III: Effect of curing conditions on reaction and its graphical description." Fuel 89(11): 3185-3192.

Davidovits, J. (2011). Geopolymer Chemistry and Applications 3rd edition, Institut Géopolymère.

Davidovits, J. (2015). False Values on CO2 Emission for Geopolymer Cement/Concrete published in Scientific Papers. Technical paper #24, Geopolymer Institute Library.

Diaz, E., E. Allouche and S. Eklund (2010). "Factors affecting the suitability of fly ash as source material for geopolymers." Fuel 89(5): 992-996.

Dirgantara, R., D. Law, T. Molyneaux and D. Kong (2013). Brown coal fly ash geopolymer mortar. ACMSM 22, Sydney, CRC Press.

Duxson, P., G. C. Lukey and J. S. J. van Deventer (2006). "Thermal evolution of metakaolin geopolymers: Part 1 – Physical evolution." Journal of Non-Crystalline Solids 352(52–54): 5541-5555.

Duxson, P., S. Mallicoat, G. Lukey, W. Kriven and J. Van Deventer (2007). "The effect of alkali and Si/Al ratio on the development of mechanical properties of metakaolin-based geopolymers." Colloids and Surfaces A: Physicochemical and Engineering Aspects 292(1): 8-20.

Duxson, P., A. Provis, J. L. Lukey, G. C. Van Deventer, A. Fernández-Jiménez and J. S. J. Palomo (2007). "Geopolymer technology: The current state of the art." Journal of Materials Science 42(9): 16.

Duxson, P., J. L. Provis, G. C. Lukey, S. W. Mallicoat, W. M. Kriven and J. S. Van Deventer (2005). "Understanding the relationship between geopolymer

composition, microstructure and mechanical properties." Colloids and Surfaces A: Physicochemical and Engineering Aspects 269(1): 47-58.

Fernández-Jiménez, A. and A. Palomo (2003). "Characterisation of fly ashes. Potential reactivity as alkaline cements." Fuel 82(18): 2259-2265.

Fernandez-Jimenez, A. M., A. Palomo and C. Lopez-Hombrados (2006). "Engineering properties of alkali-activated fly ash concrete." ACI Materials Journal 103(2): 106-112.

French, D. and J. Smitham (2007). Fly Ash Characteristics and Feed Coal Properties. Pullenvale, Qld 4069, Australia, Cooperative Research Centre for Coal in Sustainable Development.

Geoscience Australia and ABARE (2014). Australian Energy Resource Assessment. Canberra, Commonwealth of Australia (Geoscience Australia).

Gunasekara, C., D. W. Law, S. Setunge and J. G. Sanjayan (2015). "Zeta potential, gel formation and compressive strength of low calcium fly ash geopolymers." Construction and Building Materials 95: 592-599.

Guo, X., H. Shi, L. Chen and W. A. Dick (2010). "Alkali-activated complex binders from class C fly ash and Ca-containing admixtures." Journal of Hazardous Materials 173(1–3): 480-486.

Habert, G., J. B. d'Espinose de Lacaillerie and N. Roussel (2011). "An environmental evaluation of geopolymer based concrete production: reviewing current research trends." Journal of Cleaner Production 19(11): 1229-1238.

Hardjito, D., S. E. Wallah, D. M. Sumajouw and B. V. Rangan (2004). "On the development of fly ash-based geopolymer concrete." ACI Materials Journal-American Concrete Institute 101(6): 467-472.

Ivan Diaz-Loya, E., E. N. Allouche and S. Vaidya (2011). "Mechanical Properties of Fly-Ash-Based Geopolymer Concrete." ACI Materials Journal 108(3).

Keyte, L. M. (2009). 2. Fly Ash Glass Chemistry and Inorganic Polymer Cements. Geopolymers - Structure, Processing, Properties and Industrial Applications. J. L. Provis and J. S. J. van Deventer, Woodhead Publishing.

Law, D. W., T. K. Molyneaux, A. Wardhono, R. Dirgantara and D. Kong (2013). The Use Brown Coal Fly Ash To Make Geopolymer Concrete. ACCTA 2013, Johannesburg.

Lloyd, N. A. and B. V. Rangan (2010). Geopolymer Concrete with Fly Ash. Second International Conference on Sustainable Construction Materials and Technologies. Universita Politecnica delle Marche, Ancona, Italy.

Lloyd, R. R., J. L. Provis and J. S. van Deventer (2009). "Microscopy and microanalysis of inorganic polymer cements. 1: remnant fly ash particles." Journal of materials science 44(2): 608-619.

Macphee, D. E., C. J. Black and A. H. Taylor (1993). "Cements Incorporating Brown Coal Fly Ash from The Latrobe Valley Region of Victoria, Australia." Cement and Concrete Research 23(3): 507-517.

Malhotra, V. (2005). Global warming, and role of supplementary cementing materials and superplasticisers in reducing greenhouse gas emissions from the manufacturing of portland cement. The 1st Panhellenic Conference on the Utilization of industrial by-products in Construction, Thessaloniki, Greece, EVIPAR.

Malhotra, V. (2008). "Role of fly ash in reducing greenhouse gas emissions during the manufacturing of portland cement clinker." Advances in Concrete Technologies in the Middle East: 19-20.

McLellan, B. C., R. P. Williams, J. Lay, A. van Riessen and G. D. Corder (2011). "Costs and carbon emissions for geopolymer pastes in comparison to ordinary portland cement." Journal of Cleaner Production 19(9–10): 1080-1090.

Meyer, C. (2009). "The greening of the concrete industry." Cement and Concrete Composites 31(8): 601-605.

Naik, T. R. (2008). "Sustainability of concrete construction." Practice Periodical on Structural Design and Construction 13(2): 98-103.

Palomo, A., M. W. Grutzeck and M. T. Blanco (1999). "Alkali-activated fly ashes: A cement for the future." Cement and Concrete Research 29(8): 1323-1329.

Papadakis, V. and S. Tsimas (2002). "Supplementary cementing materials in concrete: Part I: efficiency and design." Cement and Concrete Research 32(10): 1525-1532.

Papadakis, V. G., C. G. Vayenas and M. N. Fardis (1991). "Physical and Chemical Characteristics Affecting the Durability of Concrete." ACI Materials Journal 8(2): 11.

Provis, J. L. (2013). "Geopolymers and other alkali activated materials: why, how, and what?" Materials and Structures 47(1-2): 15.

Rangan, B. V. (2010). Fly Ash-Based Geopolymer Concrete. The International Workshop on Geopolymer Cement and Concrete, Mumbai, India.

Sindhunata (2006). A Conceptual Model of Geopolymerisation. PhD, The University of Melbourne.

Sindhunata, J. Van Deventer, G. Lukey and H. Xu (2006). "Effect of curing temperature and silicate concentration on fly-ash-based geopolymerization." Industrial & Engineering Chemistry Research 45(10): 3559-3568.

Škvára, F., L. Kopecký, V. Šmilauer and Z. Bittnar (2009). "Material and structural characterization of alkali activated low-calcium brown coal fly ash." Journal of Hazardous Materials 168(2–3): 711-720.

Tennakoon, C., A. Nazari, J. G. Sanjayan and K. Sagoe-Crentsil (2014). "Distribution of oxides in fly ash controls strength evolution of geopolymers." Construction and Building Materials 71(0): 72-82.

Tennakoon, C., K. Sagoe-Crentsil, J. G. Sanjayan and A. Shayan (2014). Early Age Properties of Alkali Activated Brown Coal Fly Ash Binders. Advanced Materials Research, Trans Tech Publ.

Thomas, M. (2013). Supplementary cementing materials in concrete, CRC Press.

Turner, L. K. and F. G. Collins (2013). "Carbon dioxide equivalent (CO2-e) emissions: A comparison between geopolymer and OPC cement concrete." Construction and Building Materials 43(0): 125-130.

van Jaarsveld, J. G. S., J. S. J. van Deventer and G. C. Lukey (2002). "The effect of composition and temperature on the properties of fly ash- and kaolinite-based geopolymers." Chemical Engineering Journal 89(1–3): 63-73.

Wang, K., S. P. Shah and A. Mishulovich (2004). "Effects of curing temperature and NaOH addition on hydration and strength development of clinker-free CKD-fly ash binders." Cement and concrete research 34(2): 299-309.

CHAPTER 7

CONCLUSION

This research contributes to the knowledge of environmentally friendly binders synthesized from waste by-product material, specifically brown coal fly ash. More specifically, this study undertook novel research on the potential use of La Trobe Valley-Victoria brown coal fly ash as a binder in the manufacture of geopolymer concrete. Geopolymer mortar from brown coal fly ash from three power plants, Loy Yang, Yallourn and Hazelwood, was assessed. The results indicated that while compressive strengths over 40 MPa could be achieved from the Loy Yang brown coal fly ash geopolymer mortar, strengths of less than 10 MPa were found for the Yallourn and Hazelwood. Based on the results of the mortar specimens the research addressed the feasibility of producing Loy Yang brown coal fly ash geopolymer concrete, specifically investigating a range of mix designs, looking at the effect of the AM, SiO_2/Al_2O_3, Na_2O/binder and Na_2O/Al_2O_3 ratios, workability, zeta potential, compressive strength and a range of durability properties. The research used a range of techniques including, SEM, XRD, XRF and FTIR to determine the mechanical and durability properties and to provide an understanding of the geopolymerization process and the mechanical and durability characteristics. The results of the research provide a fundamental understanding of the geopolymerization mechanism for Loy Yang brown coal fly ash geopolymer mortar and concrete and present an opportunity for potentially diverting a waste stream into a useful material.

7.1. General Conclusion

The principal conclusions of the PhD research are:

1) The fly ash used could not be classified as either class C or class F due to the high sulphur content (Loy Yang) and the low aluminosilicate content (Yallourn and Hazelwood) as such the term brown coal fly ash is applied.

2) The strengths obtained from Loy Yang brown coal fly ash geopolymer concrete are indicative that brown coal fly ash geopolymer can produce compressive strengths acceptable for use in the construction industry. Whilst the strengths obtained for Hazelwood and Yallourn brown coal fly ash indicate that they are not feasible to use as geopolymer concrete.
3) The low aluminosilicate content of the Hazelwood and Yallourn brown coal fly ash are identified as the key reason for the low strength obtained with the high CaO content observed to contribute little to the strength.
4) The Modified Activator Modulus (AM_m) and SiO_2/Al_2O_3 ratio are the key parameters in determining the strength of Loy Yang brown coal fly ash geopolymer concrete.
5) Loy Yang brown coal fly ash geopolymer mortar demonstrated a restricted range for the AM_m and dosage in which the optimum compressive strength could be achieved.
6) Negative zeta potentials are observed for both the raw ash and the geopolymer of Loy Yang brown coal fly ash. Negative zeta potentials indicate a good ability to form geopolymeric material.
7) The FTIR analysis of Loy Yang brown coal fly ash and mortar indicates a high degree of reactivity in the brown coal fly ash and of considerable incorporation of the aluminium into the silicate backbone.
8) The MIP analysis identified that the porosity distribution of the Loy Yang brown coal fly ash concrete were principally in the macropores region, which was confirmed by the SEM analysis, which also showed that the structure contained a high number of interconnected pores and considerable inhomogeneity.
9) The temperature profile of elevated temperature curing could be divided into three stages which correlated well with the geopolymeric reaction mechanism reported from previous studies, and reflected appropriately with the SEM microstructural and phase mapping investigation.

10) The optimum compressive strength was achieved under a curing regime of 120 °C for 12 hours following a 24 hour delay post mixing at room temperature. However, these curing conditions may not be sufficient for large scale specimen as the internal temperature required to complete geopolymerization may not be achieved.
11) Variability in performance was observed between batches of the Loy Yang brown coal fly ash, attributed to variation in the chemical composition of the ash. Variability in performance was also observed in larger mixes attributed to a combination of the chemical variation in the ash and the curing process.
12) The durability properties measured (Schmidt Hammer, electrical resistivity, UPV, air permeability, water absorption, chloride diffusion and carbonation) were all consistent with a poor quality concrete. This was attributed to the high porosity and the number of interconnected pores present in the geopolymer matrix.

7.2. Future Prospects

The Loy Yang brown coal fly ash geopolymer concrete displayed compressive strengths acceptable for use in the construction industry concrete, whilst the Hazelwood and Yallourn brown coal fly ash gave mortar strengths considered not feasible to use for geopolymer concrete, due to the low aluminosilicate content. In addition to the compressive strengths the FTIR and zeta potential data showed that the Loy Yang brown coal fly ash has the potential to enable the manufacture of a geopolymer concrete that could be used as a construction material. However the durability data coupled with the variability in the chemical composition within the ash and the high sulphur content raise concerns over the consistency of the concrete produced and the long term performance. As such a number of outstanding issues remain which require further research and investigation.

Overall the data illustrate how the inherent variations in the material composition can affect the properties of the geopolymer produced. There are two possible alternative methods proposed to address this. The first is treatment of the raw brown coal fly ash, such as refining the material prior to adoption in the geopolymerization, to ensure that the composition of the brown coal fly ash remains within the parameters identified for the optimised mix design. The second is to investigate optimisation of the mix design based on the chemical composition of the raw brown coal fly ash supplied. There is also a need to consider the effect of the high sulphur content on the geopolymer produced and whether the refining process can reduce or remove the sulphur present and if mix optimisation can overcome any detrimental effects from sulphate salts potentially produced.

The inhomogeneity in a large volume sample sizes of geopolymer concrete attributed to insufficient mixing and insufficient temperature curing also needs to be investigated. The next stage of development should consider curing techniques which are capable of promoting the complete geopolymerization to improve strength and more importantly the long term mechanical and durability characteristics. A deeper understanding of curing process is also required. Curing is known to play a key role in the micro and nano structural development of the geopolymer reaction products. This can contribute to a granular and porous material being produced and to micro cracking. The high (interconnected) porosity, permeability and micro cracking observed could be avoided by applying the right curing condition. Finally, the bonding mechanism, together with the effect of the interactions between porosity, permeability and micro cracking on the performance of brown coal fly ash geopolymer concrete need to be fully understood in order to produce a highly durable geopolymer concrete.

APPENDICES

Appendix A : The Compression Strength Results

Appendix B : The Durability Properties

Appendix A The Compression Strength Results

Table A.1 Loy Yang Brown Coal Fly Ash Geopolymer Mortars Curing Time Results

No.	Mixture	Days Test	No.	Result					
				Max Force (kN)	Area(mm^2)		Compressive Strength (MPa)		
					L(mm)	W(mm)	Sample	Average	Std Dev
1	Loy Yang 8hrs	7	1	21.9297	50	50	8.77	8.97	1.15
2	Loy Yang 8hrs	7	2	19.8281	50	50	7.93		
3	Loy Yang 8hrs	7	3	25.5078	50	50	10.20		
4	Loy Yang 10hrs	7	1	51.0078	50	50	20.40	19.16	1.08
5	Loy Yang 10hrs	7	2	46.1953	50	50	18.48		
6	Loy Yang 10hrs	7	3	46.4844	50	50	18.59		
7	Loy Yang 12hrs	7	1	70.1250	50	50	28.05	26.38	1.95
8	Loy Yang 12hrs	7	2	60.5703	50	50	24.23		
9	Loy Yang 12hrs	7	3	67.1172	50	50	26.85		
10	Loy Yang 14hrs	7	1	57.3828	50	50	22.95	24.98	2.84
11	Loy Yang 14hrs	7	2	70.5781	50	50	28.23		
12	Loy Yang 14hrs	7	3	59.3906	50	50	23.76		

Table A.2 Loy Yang Brown Coal Fly Ash Geopolymer Mortars Testing Results

No.	Mixture	Days Test	No.	Result					
				Max Force (kN)	Area(mm^2)		Compressive Strength (MPa)		
					L(mm)	W(mm)	Sample	Average	Std Dev
1	Loy Yang 1	7	1	53.0313	50	50	21.21	21.49	3.84
2	Loy Yang 1	7	2	63.6484	50	50	25.46		
3	Loy Yang 1	7	3	44.4766	50	50	17.79		
4	Loy Yang 2	7	1	33.7266	50	50	13.49	22.63	9.67
5	Loy Yang 2	7	2	54.0703	50	50	21.63		
6	Loy Yang 2	7	3	81.8906	50	50	32.76		
7	Loy Yang 3	7	1	178.0254	50	50	71.21	56.81	13.22
8	Loy Yang 3	7	2	135.0195	50	50	54.01		
9	Loy Yang 3	7	3	113.0229	50	50	45.21		
10	Loy Yang 4	7	1	44.0234	50	50	17.61	13.44	3.65
11	Loy Yang 4	7	2	29.6719	50	50	11.87		
12	Loy Yang 4	7	3	27.0703	50	50	10.83		
13	Loy Yang 5	7	1	37.8047	50	50	15.12	20.68	4.90
14	Loy Yang 5	7	2	60.9375	50	50	24.38		
15	Loy Yang 5	7	3	56.3594	50	50	22.54		
16	Loy Yang 6	7	1	80.8438	50	50	32.34	27.17	6.52
17	Loy Yang 6	7	2	49.6094	50	50	19.84		
18	Loy Yang 6	7	3	73.3125	50	50	29.33		
19	Loy Yang 7	7	1	62.5938	50	50	25.04	32.72	11.80
20	Loy Yang 7	7	2	67.0156	50	50	26.81		
21	Loy Yang 7	7	3	115.7730	50	50	46.31		
22	Loy Yang 1	28	1	62.5547	50	50	25.02	22.65	3.43
23	Loy Yang 1	28	2	60.5391	50	50	24.22		
24	Loy Yang 1	28	3	46.8047	50	50	18.72		
25	Loy Yang 2	28	1	46.3047	50	50	18.52	20.16	4.55
26	Loy Yang 2	28	2	63.2734	50	50	25.31		
27	Loy Yang 2	28	3	41.6563	50	50	16.66		
28	Loy Yang 3	28	1	104.8050	50	50	41.92	43.16	6.36
29	Loy Yang 3	28	2	93.7969	50	50	37.52		
30	Loy Yang 3	28	3	125.1330	50	50	50.05		
31	Loy Yang 4	28	1	29.9375	50	50	11.98	12.66	0.60
32	Loy Yang 4	28	2	32.8047	50	50	13.12		
33	Loy Yang 4	28	3	32.1953	50	50	12.88		
34	Loy Yang 5	28	1	53.3125	50	50	21.33	25.27	3.44
35	Loy Yang 5	28	2	68.9844	50	50	27.59		
36	Loy Yang 5	28	3	67.2344	50	50	26.89		
37	Loy Yang 6	28	1	56.6406	50	50	22.66	26.44	4.20
38	Loy Yang 6	28	2	64.2422	50	50	25.70		
39	Loy Yang 6	28	3	77.4063	50	50	30.96		
40	Loy Yang 7	28	1	81.8438	50	50	32.74	28.77	4.13
41	Loy Yang 7	28	2	61.2578	50	50	24.50		
42	Loy Yang 7	28	3	72.6719	50	50	29.07		

Table A.3 Hazelwood and Yallourn Brown Coal Fly Ash Geopolymer Mortars Testing Results

No.	Mixture	Days Test	No.	Result					
				Max Force (kN)	Area(mm^2)		Compressive Strength (MPa)		
					L(mm)	W(mm)	Sample	Average	Std Dev
1	Hazelwood 1	7	1	23.4844	50	50	9.39	9.08	0.28
2	Hazelwood 1	7	2	22.1641	50	50	8.87		
3	Hazelwood 1	7	3	22.4766	50	50	8.99		
4	Hazelwood 2	7	1	Not set	50	50	NA	NA	NA
5	Hazelwood 2	7	2	Not set	50	50	NA		
6	Hazelwood 2	7	3	Not set	50	50	NA		
7	Hazelwood 3	7	1	19.0000	50	50	7.60	8.81	1.10
8	Hazelwood 3	7	2	24.4063	50	50	9.76		
9	Hazelwood 3	7	3	22.6328	50	50	9.05		
10	Hazelwood 4	7	1	Not set	50	50	NA	NA	NA
11	Hazelwood 4	7	2	Not set	50	50	NA		
12	Hazelwood 4	7	3	Not set	50	50	NA		
13	Hazelwood 5	7	1	11.7500	50	50	4.70	5.80	0.99
14	Hazelwood 5	7	2	15.1953	50	50	6.08		
15	Hazelwood 5	7	3	16.5313	50	50	6.61		
16	Yallourn 1	7	1	24.2813	50	50	9.71	9.79	1.00
17	Yallourn 1	7	2	27.0703	50	50	10.83		
18	Yallourn 1	7	3	22.0938	50	50	8.84		
19	Yallourn 2	7	1	21.2500	50	50	8.50	6.56	2.51
20	Yallourn 2	7	2	9.3047	50	50	3.72		
21	Yallourn 2	7	3	18.6250	50	50	7.45		
22	Yallourn 3	7	1	26.6016	50	50	10.64	9.37	1.58
23	Yallourn 3	7	2	24.6641	50	50	9.87		
24	Yallourn 3	7	3	18.9922	50	50	7.60		
25	Yallourn 4	7	1	14.2580	50	50	5.70	5.03	0.91
26	Yallourn 4	7	2	9.9766	50	50	3.99		
27	Yallourn 4	7	3	13.5078	50	50	5.40		
28	Yallourn 5	7	1	17.9609	50	50	7.18	7.95	0.72
29	Yallourn 5	7	2	20.1406	50	50	8.06		
30	Yallourn 5	7	3	21.5313	50	50	8.61		

Table A.4 Loy Yang Brown Coal Fly Ash Geopolymer Concrete Testing Results

No.	Mixture	Days Test	No.	Result					
				Max Force (kN)	Area(mm^2)		Compressive Strength (MPa)		
					L(mm)	W(mm)	Sample	Average	Std Dev
1	Loy Yang	7	1	557.9370	100	99.8	55.91	59.59	3.49
2	Loy Yang	7	2	631.5360	100	100.5	62.84		
3	Loy Yang	7	3	598.3900	99.7	100	60.02		
4	Loy Yang	56	1	512.3690	99.5	100	51.49	52.08	3.88
5	Loy Yang	56	2	561.0730	100	99.8	56.22		
6	Loy Yang	56	3	485.3130	100	100	48.53		
7	Loy Yang	91	1	606.0840	100.5	100	60.31	60.38	0.46
8	Loy Yang	91	2	599.6490	98.5	100	60.88		
9	Loy Yang	91	3	599.6790	100	100	59.97		
10	Loy Yang Batch 1	7	1	472.9910	100.3	101.5	46.46	44.95	1.98
11	Loy Yang Batch 1	7	2	466.3990	100.1	102	45.68		
12	Loy Yang Batch 1	7	3	436.3770	99.7	102.5	42.70		
13	Loy Yang Batch 1	28	1	392.6810	100	101	38.88	43.81	4.31
14	Loy Yang Batch 1	28	2	466.2770	100	102	45.71		
15	Loy Yang Batch 1	28	3	473.0890	100	101	46.84		
16	Loy Yang Batch 1	91	1	502.8370	100	101	49.79	42.62	6.25
17	Loy Yang Batch 1	91	2	392.3900	100	102.5	38.28		
18	Loy Yang Batch 1	91	3	395.7640	99	100.5	39.78		
19	Loy Yang Batch 2 – A	28	1	339.5430	102	100	33.29	29.38	6.62
20	Loy Yang Batch 2 – A	28	2	226.0550	103	101	21.73		
21	Loy Yang Batch 2 – A	28	3	339.4300	102	100.5	33.11		
22	Loy Yang Batch 2 – B	28	1	234.5320	100	101	23.22	23.76	2.73
23	Loy Yang Batch 2 – B	28	2	265.7810	99.5	100	26.71		
24	Loy Yang Batch 2 – B	28	3	215.5200	101	100	21.34		
25	Loy Yang Batch 2 – C	28	1	250.9940	100	101	24.85	31.41	7.72
26	Loy Yang Batch 2 – C	28	2	403.0920	101.5	99.5	39.91		
27	Loy Yang Batch 2 – C	28	3	293.1230	99	100.5	29.46		
28	Loy Yang Batch 2 – D	28	1	114.7760	99.5	100	11.54	13.29	4.43
29	Loy Yang Batch 2 – D	28	2	101.6040	102	99.5	10.01		
30	Loy Yang Batch 2 – D	28	3	186.0210	100.5	101	18.33		
31	Loy Yang Carbonation	28	1	289.4870	101	101	28.38	29.70	1.74
32	Loy Yang Carbonation	28	2	296.4410	102	100	29.06		
33	Loy Yang Carbonation	28	3	326.2590	102	101	31.67		
34	OPC Block	28	1	549.5350	99	98	56.64	53.38	5.85
35	OPC Block	28	2	466.3310	100	100	46.63		
36	OPC Block	28	3	568.7190	100	100	56.87		
37	Loy Yang ETM	28	1	240.5020	99	101	24.05	24.61	0.49
38	Loy Yang ETM	28	2	250.8270	100.5	100	24.96		
39	Loy Yang ETM	28	3	245.7210	99	100	24.82		

Appendix B The Durability Properties

Table B.1 Schmidt Rebound Hammer Test

Equipment : Schmidt Type N

Rebound index at 28 days

Loy Yang Brown Coal Fly Ash Geopolymer Concrete

Test	Schmidt Hammer	
	Batch 1-(i)	Batch 1-(ii)
1	12	12
2	11	16
3	12	17
4	11	13
5	14	13
6	11	22
7	13	20
8	10	14
9	11	17
10	10	22
11	11	19
12	10	16
13	11	17
14	11	17
15	11	19
16	12	14
Mean	**11.3**	**16.8**
Std. Dev	1.04	2.99

Rebound index at 90 days

Test	Schmidt Hammer	
	Batch 1-(i)	Batch 1-(ii)
1	11	13
2	11	16
3	10	15
4	12	12
5	11	18
6	12	19
7	10	21
8	10	18
9	11	17
10	10	18
11	10	20
12	13	16
13	10	15
14	11	18
15	10	17
16	11	14
Mean	**10.8**	**16.7**
Std. Dev	0.88	2.39

OPC Control

Test	Schmidt Hammer	
	A	B
1	21	20
2	21	30
3	24	23
4	23	20
5	27	22
6	27	29
7	27	30
8	22	22
9	21	26
10	29	26
11	27	24
12	21	20
13	20	21
14	23	26
15	27	29
16	20	20
Mean	**23.8**	**24.3**
Std. Dev	2.99	3.67

Test	Schmidt Hammer	
	A	B
1	24	29
2	23	22
3	21	27
4	27	26
5	25	23
6	29	28
7	24	22
8	25	31
9	24	29
10	27	28
11	25	23
12	20	26
13	23	27
14	25	20
15	24	27
16	24	23
Mean	**24.4**	**25.7**
Std. Dev	2.12	3.04

Table B.2 Resistivity Test Results

Equipment : Wenner RESIPOD Proceq

Resistivity at 28 days

Loy Yang Brown Coal Fly Ash Geopolymer Concrete

Test	Resistivity (kΩcm)	
	Batch 1-(i)	**Batch 1-(ii)**
1	54.8	64.1
2	25.6	32.8
3	14.7	17.6
4	17.2	17.5
5	10.0	11.3
6	5.3	5.4
7	5.2	5.8
8	7.9	9.7
9	6.0	8.6
10	4.2	5.8
11	6.1	6.9
12	11.3	20.3
13	6.0	26.0
14	6.2	22.2
15	10.4	39.0
16	56.9	60.0
Mean	**15.5**	**22.1**
Std. Dev	16.18	17.95

OPC Control

Test	Resistivity (kΩcm)	
	A	**B**
1	11.0	11.5
2	7.2	7.8
3	6.7	6.5
4	6.4	7.0
5	5.9	5.9
6	4.7	5.3
7	5.0	6.0
8	5.8	6.9
9	5.8	5.8
10	5.4	5.0
11	5.3	6.0
12	6.5	6.0
13	6.9	7.0
14	7.1	6.3
15	8.0	8.7
16	13.7	12.0
Mean	**7.0**	**7.1**
Std. Dev	2.26	1.97

Resistivity at 90 days

Test	Resistivity (kΩcm)	
	Batch 1-(i)	**Batch 1-(ii)**
1	45.1	43.4
2	18.1	29.1
3	11.2	15.0
4	12.0	15.0
5	11.5	15.2
6	5.5	6.6
7	5.2	6.0
8	7.4	9.7
9	7.4	9.8
10	4.3	6.5
11	4.8	6.8
12	9.4	12.7
13	15.0	19.6
14	12.6	14.6
15	17.5	24.1
16	29.6	30.1
Mean	**13.5**	**16.5**
Std. Dev	10.29	10.16

Test	Resistivity (kΩcm)	
	A	**B**
1	10.9	12.2
2	7.3	7.5
3	6.8	6.3
4	6.7	6.8
5	5.8	6.3
6	5.0	5.6
7	5.0	5.3
8	6.0	6.3
9	6.0	5.9
10	5.5	5.4
11	6.0	5.6
12	6.8	7.1
13	6.0	7.3
14	5.3	6.7
15	6.0	9.2
16	14.3	12.6
Mean	**6.8**	**7.3**
Std. Dev	2.34	2.16

Table B.3 UPV Test Results

Equipment : TICO Ultrasonic Instrument Proceq; Specimen length : 30cm

Velocity at 28 days

Loy Yang Brown Coal Fly Ash Geopolymer Concrete

Test	Batch 1-(i)		Batch 1-(ii)	
	Time (µs)	Velocity (m/s)	Time (µs)	Velocity (m/s)
1	97.4	3080	88.3	3398
2	107.6	2788	121.5	2469
3	362.0	829	144.8	2072
4	326.0	920	332.0	904
5	321.0	935	348.0	862
6	360.0	833	338.0	888
7	109.5	2740	117.6	2551
8	96.6	3106	133.5	2247
9	89.1	3367	103.6	2896
10	129.5	2317	107.6	2788
11	362.0	829	306.0	980
12	335.0	896	334.0	898
13	379.0	792	338.0	888
14	343.0	875	117.6	2551
15	181.7	1651	85.1	3525
16	185.0	1622	102.7	2921
Mean	**236.5**	**1723.6**	**194.9**	**2052.3**
Std. Dev	119.37	997.36	111.47	987.48

Velocity at 90 days

Test	Batch 1-(i)		Batch 1-(ii)	
	Time (µs)	Velocity (m/s)	Time (µs)	Velocity (m/s)
1	99.2	3024	96.5	3109
2	112.4	2669	130.5	2299
3	130.4	2301	133.7	2244
4	330.2	909	145.8	2058
5	340.5	881	340.2	882
6	331.6	905	333.7	899
7	124.5	2410	105.6	2841
8	105.2	2852	128.6	2333
9	107.6	2788	105.4	2846
10	130.5	2299	290.5	1033
11	333.6	899	320.6	936
12	363.5	825	300.7	998
13	375.0	800	323.5	927
14	334.2	898	123.7	2425
15	190.2	1577	111.4	2693
16	170.8	1756	93.8	3198
Mean	**223.7**	**1737.0**	**192.8**	**1982.5**
Std. Dev	112.52	864.55	101.85	882.94

OPC Control

Test	A		B	
	Time (µs)	Velocity (m/s)	Time (µs)	Velocity (m/s)
1	66.9	4484	67.3	4458
2	66.8	4491	68.2	4399
3	66.4	4518	68.0	4412
4	66.5	4511	68.1	4405
5	67.5	4444	68.2	4399
6	66.4	4518	69.1	4342
7	66.6	4505	72.4	4144
8	67.2	4464	72.3	4149
9	66.1	4539	66.7	4498
10	67.6	4438	66.1	4539
11	68.0	4412	67.5	4444
12	68.2	4399	68.0	4412
13	72.1	4161	67.6	4438
14	69.6	4310	69.0	4348
15	67.6	4438	68.4	4386
16	69.1	4342	69.4	4323
Mean	**67.7**	**4435.9**	**68.5**	**4380.9**
Std. Dev	1.54	97.63	1.72	106.70

Test	A		B	
	Time (µs)	Velocity (m/s)	Time (µs)	Velocity (m/s)
1	70.1	4280	68.1	4405
2	68.4	4386	68.0	4412
3	67.5	4444	67.5	4444
4	67.2	4464	69.8	4298
5	69.5	4317	68.4	4386
6	69.3	4329	71.5	4196
7	68.5	4380	66.9	4484
8	68.0	4412	70.3	4267
9	67.8	4425	68.3	4392
10	66.4	4518	68.3	4392
11	68.0	4412	67.8	4425
12	68.0	4412	69.5	4317
13	66.8	4491	66.4	4518
14	68.6	4373	72.5	4138
15	69.1	4342	70.9	4231
16	67.5	4444	70.0	4286
Mean	**68.2**	**4401.7**	**69.0**	**4349.5**
Std. Dev	1.00	64.57	1.71	106.51

Table B.4 Water Absorption (Sorptivity) Test Results (Autoclam Sorptivity Index)

Equipment : Autoclam Permeability System / Amphora

Water Absorption at 28 days Water Absorption at 90 days

Loy Yang Brown Coal Fly Ash Geopolymer Concrete

Time (min)	√time (√min)	Batch 1-(i) Volume (µL)	Batch 1-(i) ASI ($\mu^3/\sqrt{min}$)
0	0.00	4	---
1	1.00	2500	25.000
2	1.41	4746	33.559
3	1.73	6844	39.514
4	2.00	8790	43.950
5	2.24	10640	47.584
6	2.45	12378	50.533
7	2.65	14080	53.217
8	2.83	15696	55.494
9	3.00	17250	57.500
10	3.16	19000	60.083
11	3.32	21170	63.830
12	3.46	23320	67.319
13	3.61	25496	70.713
14	3.74	27644	73.882
15	3.87	29786	76.907
Average	**5-15 min**		**61.551**

Test failed for Batch 1-(i) at 90 days

Time (min)	√time (√min)	Batch 1-(ii) Volume (µL)	Batch 1-(ii) ASI ($\mu^3/\sqrt{min}$)
0	0.00	2	---
1	1.00	2250	22.500
2	1.41	4220	29.840
3	1.73	5870	33.890
4	2.00	7246	36.230
5	2.24	8396	37.548
6	2.45	9458	38.612
7	2.65	10458	39.528
8	2.83	11532	40.772
9	3.00	12476	41.587
10	3.16	13304	42.071
11	3.32	14090	42.483
12	3.46	15000	43.301
13	3.61	16310	45.236
14	3.74	17894	47.824
15	3.87	19426	50.158
Average	**5-15 min**		**42.647**

Time (min)	√time (√min)	Batch 1-(ii) Volume (µL)	Batch 1-(ii) ASI ($\mu^3/\sqrt{min}$)
0	0.00	2	---
1	1.00	2512	25.120
2	1.41	5086	35.963
3	1.73	7676	44.317
4	2.00	10250	51.250
5	2.24	12758	57.056
6	2.45	15336	62.609
7	2.65	17936	67.792
8	2.83	20500	72.478
9	3.00	23006	76.687
10	3.16	25588	80.916
11	3.32	28162	84.912
12	3.46	30750	88.768
13	3.61	33274	92.285
14	3.74	35870	95.867
15	3.87	38470	99.329
Average	**5-15 min**		**79.882**

OPC Control

Time (min)	√time (√min)	A	
		Volume (µL)	WPI ($\mu^3/\sqrt{min}$)
0	0.00	0	---
1	1.00	78	0.780
2	1.41	118	0.834
3	1.73	146	0.843
4	2.00	168	0.840
5	2.24	188	0.841
6	2.45	204	0.833
7	2.65	220	0.832
8	2.83	234	0.827
9	3.00	248	0.827
10	3.16	256	0.810
11	3.32	268	0.808
12	3.46	278	0.803
13	3.61	288	0.799
14	3.74	298	0.796
15	3.87	308	0.795
Average	**5-15 min**	**8.0**	**0.815**

Table B.5 Air Permeability

Equipment : Autoclam Permeability System / Amphora

Air Permeability at 28 days

Air Permeability at 90 days

Loy Yang Brown Coal Fly Ash Geopolymer Concrete

Test failed for Batch 1-(i) at 28 days

Test failed for Batch 1-(i) at 90 days

Test failed for Batch 1-(ii) at 28 days

Test failed for Batch 1-(ii) at 90 days

OPC Control

Time (min)	**A**
	Pressure mBar
0	524
1	519
2	499
3	478
4	457
5	437
6	418
7	399
8	381
9	365
10	348
11	333
12	318
13	304
14	291
15	278

No test for OPC A at 90 days